BIT ERROR RATE PERFORMANCE ANALYSIS AND OPTIMIZATION

OF SUBOPTIMUM DETECTION PROCEDURES

By

NORMAN CHARLES BEAULIEU

B.A.Sc., The University of British Columbia, 1980

M.A.Sc., The University of British Columbia, 1983

A THESIS SUBMITTED IN PARTIAL FULFILLMENT OF

THE REQUIREMENTS FOR THE DEGREE OF

DOCTOR OF PHILOSOPHY

in

THE FACULTY OF GRADUATE STUDIES

DEPARTMENT OF ELECTRICAL ENGINEERING

We accept this thesis as conforming

to the required standard

THE UNIVERSITY OF BRITISH COLUMBIA

January 1986

In presenting this thesis in partial fulfilment of the
requirements for an advanced degree at the University
of British Columbia, I agree that the Library shall make
it freely available for reference and study. I further
agree that permission for extensive copying of this thesis
for scholarly purposes may be granted by the head of my
department or by his or her representatives. It is
understood that copying or publication of this thesis
for financial gain shall not be allowed without my written
permission.

Department of __Electrical Engineering__

The University of British Columbia
1956 Main Mall
Vancouver, Canada
V6T 1Y3

Date _August 19, 1986_

ABSTRACT

Three suboptimum detection schemes are examined. The deterioration in performance, measured in the probability of error sense, of weighted partial decision, binary partial decision, and sample-and-sum detectors are analyzed. Even though these schemes are inferior to the digital matched filter, they can be used in systems with more modest computational capabilities. Analytic expressions are obtained for the penalties. The effects on the penalties of the signalling waveform employed, the number of samples processed, and the signal-to-noise ratio are considered in detail. Included are the penalties for the optimum weighted partial decision detector.

The effects of dependence among the samples on the detector losses are investigated. It is shown that, in some cases, the losses of the suboptimum procedures can be reduced by processing more, dependent, samples. The amount of the loss that can be recovered depends on the prefilter characteristic and the sampling rate, as well as the detection algorithm.

The structure of the optimum detector for hard-limited data signals is presented and its performance is compared with those of some commonly used schemes. Performance in impulsive as well as Gaussian noise environments is considered. The optimum receiver for M-ary signalling based on received signal samples quantized to an arbitrary number of levels is derived and compared to another common detector.

The fundamental loss in signal detectability due to hard-limiting in a sampled system operating in Gaussian noise is investigated. The relation of the loss to the signal-to-noise ratio and the number of samples is analyzed.

TABLE OF CONTENTS

LIST OF TABLES

LIST OF FIGURES

ACKNOWLEDGEMENT

I wish to thank my advisor Dr. C.S.K. Leung for suggesting the topic and for rendering assistance during the course of the work.

Finally, I wish to express my appreciation to the office staff for their willing assistance, encouragement and cheerfulness.

I INTRODUCTION

1.1. Motivation

A fundamental problem in communication theory and design is how to best detect information signals in noise. Optimal detection methods are known but may be expensive or difficult to implement. Suboptimum detection procedures are employed in a number of diverse areas. Data recovery circuits in modems are frequently based on suboptimal procedures where cost-effective implementations trade off complexity against performance. In underwater sound detection systems, arrays of receivers that may be quite large are used to detect weak signals. For large arrays, the processing required can be reduced significantly by employing suboptimal procedures that have more modest computational requirements than the optimal processing. Digital receivers for systems employing time or frequency spreading techniques have large time-bandwidth products and must process a large number of samples. Simplified versions of digital matched filters offer flexibility, reliability, speed, compactness and cost efficiency.

In order to assess, compare and choose alternative detection procedures for a given application, the communications engineer requires knowledge of the performance of the schemes. This is one of the principal objectives of this research. The performances of a number of ad hoc detectors are analysed. The results are useful for performance evaluation of existing designs as well as for initiating new designs in data recovery and signal detection systems.

Another principal objective is to investigate the optimality of the schemes employed. In particular, given certain processing constraints, what are the optimum detection schemes? The results of this investigation will provide theoretical limits for the performance that can be achieved by systems operating with particular hardware or processing limitations.

The thesis research has industrial as well as academic significance. In the short term, the results will provide answers that will enable product designers to construct improved receiver subsystems. In the long term, the development of theory of suboptimal detection procedures entails dealing with some fundamental issues regarding the properties and the components of the losses incurred by these processes. A better understanding of signal detection will come from the theory developed.

1.2. Scope of the Thesis

This thesis considers suboptimum detection procedures. Both theoretical and numerical results are presented. With the exception of section 4.6, the work deals with binary systems. The emphasis is on evaluating the performance of the detectors with the performance measured in the signal detectability sense. That is, the probability of error is used as the performance criterion.

The thesis is concerned throughout with the processing of sets of signal samples. The analysis and results are cast in the context of data recovery in digital communication receivers. The mathematical techniques and the results, however, are quite general and apply to a wide range of problems. The signal samples may, for example, be from a diversity digital communication system, or a radar or sonar signal detection system.

The effects of hard-limiting on signal detectability are investigated in detail. The relations of the detector losses to the number of samples processed, the signal-to-noise ratio, and the processing algorithm are of central interest.

In order to gain insight into the principal mechanisms and relations of the detector losses, some simplifying assumptions have been made. In particular, it has been assumed that there is negligible intersymbol interference (ISI) and that bit synchronization is available.

ISI is not present in pulse detection systems. Furthermore, many communication systems operate with little or no ISI. Low speed modems for telephone channels and radio modems are two examples. The present results also apply to ISI channels when the received signal has been equalized.

The method used to obtain bit synchronization is not of particular interest here. Timing recovery circuits can provide bit synchronization with less than a few percent jitter. The effects of this jitter on the penalties of the detectors is of minor importance as consideration of the binary eye indicates.

Some of the results of this thesis have been reported earlier in the journal papers, "On the Performance of Three Suboptimum Detection Schemes for Binary Signalling" [7], "Optimal Detection of Hard-Limited Data Signals in Different Noise Environments" [8], "Penalties of Sample-and-Sum and Weighted Partial Decision Detectors in Gaussian Noise" [9], and the conference papers, "A Comparison of Three Suboptimum Detectors for Binary Signalling" [32], "On Hard-Limiting in Sampled Binary Data Systems" [33], "The Optimal Hard-Limiting Detector for Data Signals in Different Noise Environments" [10], and "Penalties of Weighted Partial Decision Detectors in Gaussian Noise" [34].

1.3. Review of Relevant Work

A review of work relevant to this thesis is given in this section. Brief comments on the methods used and the results obtained are given for each reference. The reader may find it helpful to refer to the glossary for explanation of some of the terms.

Tozer and Kollerstrom [1] have considered the penalties of hard decision in the detection of binary antipodal signals in additive white Gaussian noise. In this analysis, short subsections of the signal are detected, giving a number of hard binary decisions. The subsections of the signal are constrained to be of equal energy and are detected by appropriate matched filters. The data polarity is recovered by using majority rule on the subsection decisions. This detection scheme is compared to the optimum detection achieved by using an analogue matched filter over the entire signal duration. It is shown that for a large number of independent subsections and small signal-to-noise ratios a penalty of 1.96 dB is incurred.

Milutinovic [2,3,35,36] has described a suboptimum detection procedure based on weighting partial decisions. This work considers binary signals in additive white Gaussian noise. The detection algorithm is based on two counters, B_o and B_1. The received signal is sampled M times in the duration of one signalling element. Each sample is compared with a threshold value and, depending on the outcome, counter B_o or B_1 is incremented by a weight which depends on the sample index. After M partial decisions, the transmitted signal is determined by a comparison of the two counters. The weights are chosen to be proportional to the distance between the two transmitted signals at the sampling

instant. Also considered is an algorithm based on binary partial decisions. In this scheme, all samples are weighted equally.

The performance of the two suboptimum detectors is compared to that of a digital matched filter. The penalty is computed for a particular set of antipodal signals for three values of sample size M. The results are example specific. It is found that the penalty of the weighted partial decision detector is about 2 dB for all three values of M and increases slightly with increasing signal-to-noise ratio. The penalty of the binary partial decision detector is about 3 dB for low signal-to-noise ratios and increases sharply as the signal-to-noise ratio becomes large.

Lockhart [4] has considered replacing analogue filter and analogue detector circuits in data receivers by digital networks designed from truth table specifications. A method of compiling the truth tables from received signal probabilities is presented. The technique is illustrated by an example. The detection of binary antipodal raised cosine signals in the presence of Gaussian noise is examined. The received signal samples are assumed to be independent. The performance of the digital network is compared to that achieved by using a single sample detector. An error probability versus signal-to-noise ratio curve is presented for each scheme. It is noted that the proposed scheme performs better. It is also noted that the truth table is valid for all values of signal-to-noise ratio and can be derived more directly by considering a hard-limited received signal filtered by a nonrecursive matched filter.

The algorithm presented by Lockhart is an application of the maximum aposteriori probability (MAP) rule to the situation where there are a number of independent hard-limited received signal samples and the transmitter signal set, as well as the noise statistics are known. The independence assumption will require that the noise be white or that appropriate filtering of the received signal be done. The computationally direct method of considering the hard-limited, nonrecursively matched filtered signal samples is the weighted partial decision algorithm described by Milutinovic [2,3]. For the signalling waveform and the number of samples considered the MAP rule and the weighted partial decision algorithm yield the same truth table. In general, however, the MAP rule truth table will depend on the signal-to-noise ratio and the two procedures will not be truth table equivalent.

Chie [5] has investigated a simplified digital detector which performs only additions on the noisy signal samples. In this analysis, the signalling waveforms are antipodal nonreturn-to-zero (NRZ) pulses and the additive noise is white and Gaussian. The detector prefilter is assumed to pass the signal without distortion. Hence, all the signal samples have the same magnitude and there is no ISI. It is also assumed that perfect synchronization is available.

Numerical results are presented for a typical implementation example configured with sixteen samples and a four bit analogue-to-digital converter (ADC). The sensitivity of the detector performance to the number of samples processed, the number of ADC bits, and the ADC loading is examined each individually. For this example, it appears that four bit quantization performs almost as well as quantization with an

infinite number of bits and that very little can be gained in performance by using more than sixteen samples.

Chang [6] has also investigated the sample-and-sum detector examined by Chie [5]. Again, antipodal NRZ signals in white Gaussian noise are considered. The performance degradation of the detector is related to the bandwidth of the prefilter, the sampling rate, and the number of quantization levels. The distortion of a single pulse resulting from the prefilter is dealt with in the analysis, but the effects of ISI are assumed to be negligible. Perfect synchronization is assumed throughout. It is concluded that, for the examples investigated, a prefilter bandwidth on the order of twice the bit rate is adequate and that three or four bit quantization is almost as good as infinite quantization.

1.4. Outline of the Thesis

In this section, an outline of the thesis is given. The principal results of each chapter are described in turn.

Chapter two introduces three suboptimum detection procedures: the Sample-and-Sum (SAS), the Weighted Partial Decision (WPD) and the Binary Partial Decision (BPD) algorithms. The bit error rate performances of these detectors are analysed for large time-bandwidth product conditions. This is first done for binary antipodal signals and it is then shown that the results may be generalized to arbitrary binary signals. The relation among the losses of the three schemes is presented.

In chapter three, the performances of the three detectors for large time-bandwidth systems with dependent samples are considered. It is shown that, in some cases, the losses of the suboptimum schemes can

be reduced by processing more, dependent, samples. The amount of the loss recoverable is related to the prefilter shape and the sampling rate.

The structure of the optimum, minimum probability of error, detector for hard-limited samples is presented in chapter four. Whereas previous chapters have dealt with large time-bandwidth product conditions and Gaussian noise, the results of this chapter are general and apply to an arbitrary number of samples and most common noise environments. The optimum detector for M-ary signalling with each received sample quantized to an arbitrary number of levels is also derived. Again, the result is valid for most noise distributions.

In chapter five, the penalty associated with the use of the WPD detector in Gaussian noise is examined in detail. The effects on the penalty of the signalling waveform employed, the number of samples processed, and the signal-to-noise ratio are examined. Two common ad hoc choices of weights are considered as well as the optimum weights.

The performance degradations of the SAS and BPD detectors are analysed for arbitrary SNR's in chapter six. The effects on the penalties of the signalling waveform employed and the number of samples processed are also considered in detail. The relationship among the losses of the SAS, BPD and WPD detectors for low SNR and finite sample sizes is derived.

Finally, chapter seven gives a more detailed summary of the results of the thesis research and suggests some topics for further research.

II PERFORMANCE COMPARISON OF THREE SUBOPTIMUM DETECTION SCHEMES
FOR BINARY SIGNALLING

2.1. Introduction

In this chapter, the problem of detecting one of two equally likely
signals using digital techniques is addressed. The case of antipodal signals
is first considered and it is then shown that the results are readily gener-
alized to arbitrary signals. The model considered is shown in figure 2.1.
Depending on the message $m \epsilon \{0,1\}$ to be transmitted, a signal $+s(t)$ or $-s(t)$
is sent over the additive white Gaussian noise (AWGN) channel. The two-sided
power spectral density of the noise process $n(t)$ is assumed to be $N_o/2$. The
signal $s(t)$ is assumed to be non-zero only in the time interval $[0,T]$ sec.
and bandlimited to B Hz†. The received signal $r(t)$ is filtered to remove
excess out-of-band noise producing the signal $v(t)$ which is then processed
by the detector.

The detector samples the signal $v(t)$ at a rate of 2B samples per
second, yielding a total of $M = 2BT$ noisy samples of the transmitted signal.
A consequence of this sampling rate is that the (Gaussian) noise samples in
$v(t)$ will be independent [11]. Furthermore, in order to ensure that the
transmitted signal $s(t)$ is essentially undistorted by the receiver filter, we
require that

$$M = 2BT \gg 1. \tag{2.1}$$

Exactly how large M should be depends in part on the shape of $s(t)$. If $s(t)$
is fairly smooth (e.g. a sinusoidal wave) then a value of 10 would suffice.

† Strictly speaking, a time-limited signal cannot be completely bandlimited.
However, for practical purposes, all the signal energy will lie within a
frequency range of $B \gg \frac{1}{T}$.
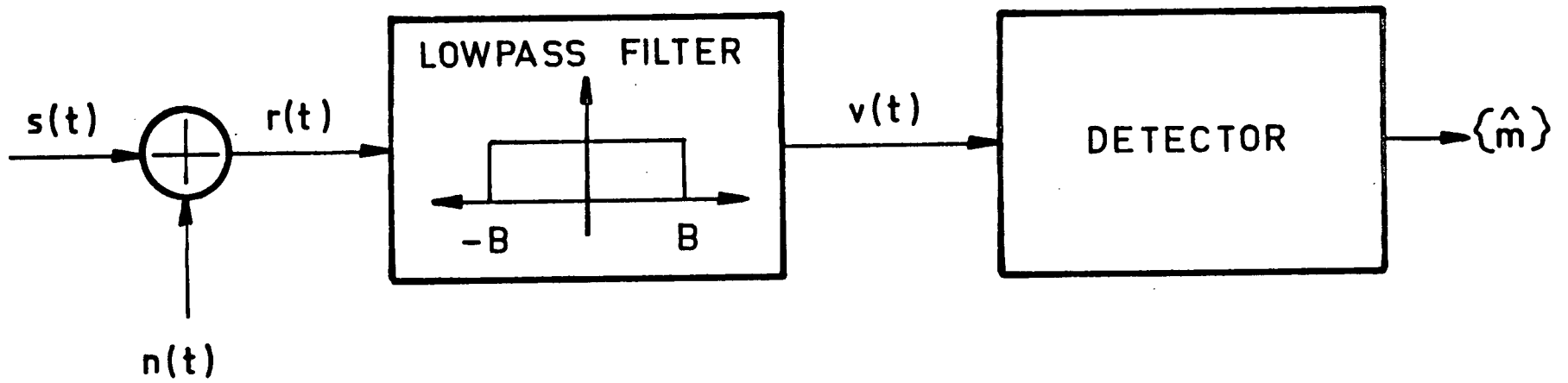
Figure 2.1. Block diagram of the data receiver.

On the other hand if s(t) has sharp transitions (e.g. a square wave), then a larger value of about 100 is required. These values of M are sufficient to

keep $\rho \overset{\Delta}{=} \dfrac{\displaystyle\int_0^T |s(t)-\tilde{s}(t)|dt}{\displaystyle\int_0^T |s(t)|dt}$, where $\tilde{s}(t)$ denotes the output of the filter, to

less than 1.5%.

It is well-known [11] that the optimum detector for minimizing the probability of error $P(e) \overset{\Delta}{=} \text{Pr}\{\hat{m} \neq m\}$ in the above problem is the digital matched filter (DMF). Its operation can be described as follows: Let

$$v_i = s_i + n_i \quad , \quad i = 1,2,\ldots,M \tag{2.2}$$

denote the M samples of $v(t)$, i.e. $v_i = v\left(\dfrac{iT}{M}\right)$, which are to be processed. The values $\{s_i\}_{i=1}^{M}$ denote the samples of $s(t)$, i.e. $s_i = s\left(\dfrac{iT}{M}\right)$ and the $\{n_i\}_{i=1}^{M}$ are independent Gaussian noise random variables with means 0 and variances $\sigma_n^2 = BN_o$. The DMF computes

$$D_{OPT} \overset{\Delta}{=} \sum_{i=1}^{M} v_i s_i \tag{2.3}$$

and decides $\hat{m} = 0$ if $D_{OPT} > 0$; otherwise it declares $\hat{m} = 1$. The resulting probability of error is given by [11]

$$P(e) = Q\left(\sqrt{\dfrac{2E_s}{N_o}}\right) \tag{2.4}$$

where $E_s \triangleq \int_0^T s^2(t)dt$ is the energy of $s(t)$ and $Q(\alpha) \triangleq \frac{1}{\sqrt{2\pi}} \int_\alpha^\infty e^{-x^2/2}dx$.

Equation (2.4) gives the error probability for an analogue matched filter. It is also valid for the DMF when M is large.

We note that the DMF requires M multiplications and (M-1) additions. A number of suboptimal schemes [1-10,12,13] have been proposed which have more modest computational requirements. These include the Sample-and-Sum (SAS), the Weighted Partial Decision (WPD) and the Binary Partial Decision (BPD) detectors. Previous analyses of these suboptimal schemes have been confined to specific signalling waveforms s(t) and specific (small) values of M. In the following sections, an analysis of the penalty incurred by each of these schemes for an arbitrary signalling waveform and large values of M is given. The penalty is defined as the increase in signal energy required by a suboptimum detector in order to achieve the same error probability as a digital matched filter (in the large sample case, this is the same as the error probability of the analogue matched filter). Examples illustrating how the penalties vary with M are also included. Note that the model used implies a small signal-to-noise ratio condition. The results, therefore, are valid for small signal-to-noise ratios. This restriction is removed in chapters 5 and 6.

(2.5)

2.2. The Sample-and-Sum (SAS) Detector

The SAS detector [5,6,13] computes the quantity

$$D_{SAS} \triangleq \sum_{i=1}^{M} v_i \, sgn(s_i) \qquad (2.5)$$

where $sgn(x) = \begin{cases} +1 & \text{if } x>0 \\ 0 & \text{if } x=0 \\ -1 & \text{if } x<0 \end{cases}$, and declares $\hat{s} = 0$ if $D_{SAS} > 0$. Otherwise, $\hat{s} = 1$

is decided. Comparison of (2.3) and (2.5) shows that the SAS detector avoids multiplication by not weighting the samples of the received signal. The resulting penalty is now analyzed.

Given $m = 0$, i.e. $+s(t)$ is transmitted, the mean of D_{SAS} is given by

$$\overline{D}_{SAS} = \sum_{i=1}^{M} |s_i| \tag{2.6}$$

and the variance of D_{SAS} is given by

$$\sigma_{D_{SAS}}^2 = M\sigma_n^2$$
$$= MBN_o$$
$$= \frac{M^2 N_o}{2T} . \tag{2.7}$$

An error will be made if $D_{SAS} < 0$. We note that since D_{SAS} is the sum of Gaussian random variables, it is itself a Gaussian random variable. Thus,

$$P(e|m=0) = Q\left(\frac{\sum_{i=1}^{M} |s_i|}{\sigma_{D_{SAS}}}\right)$$

$$= Q\left(\frac{\frac{1}{T}\sum_{i=1}^{M} |s_i| \frac{T}{M}}{\sqrt{N_o/2T}}\right) . \tag{2.8}$$

By symmetry,

$$P(e) = P(e|m=0) = P(e|m=1).$$

Note also that

$$\lim_{M \to \infty} \sum_{i=1}^{M} |s_i| \frac{T}{M} = \int_0^T |s(t)| dt. \quad \text{Therefore, as } M \to \infty,$$

$$P(e) = Q\left(\sqrt{\frac{2T}{N_o}} \langle |s(t)| \rangle\right), \tag{2.9}$$

where $\langle |s(t)| \rangle = \frac{1}{T} \int_0^T |s(t)| dt$ represents the average magnitude of the signalling waveform $s(t)$. If we define

$$\alpha = \frac{E_s}{T \{\langle |s(t)| \rangle\}^2}, \tag{2.10}$$

equation (2.9) can be rewritten as

$$P(e) = Q\left(\sqrt{\frac{2E_s}{\alpha N_o}}\right). \tag{2.11}$$

By comparison of (2.11) with (2.4), it can be seen that to achieve the same value of P(e), the SAS detector uses α times the energy required by the DMF detector. For a constant $s(t)$, $\alpha = 1$ as might be expected. (It can be shown using Schwarz's Inequality [11] that the minimum value of α is 1.) However, for a sinusoidal signalling waveform, $\alpha = \pi^2/8$ or 0.912 dB.

2.3. The Weighted Partial Decision (WPD) Detector

In the WPD detector [2], the necessity for multiplication is avoided by ignoring the magnitudes of the received signal samples and using only their polarities. The decision is based on

$$D_{WPD} \triangleq \sum_{i=1}^{M} \text{sgn}(v_i) \cdot s_i . \qquad (2.12)$$

If $D_{WPD} > 0$, $\hat{m} = 0$ is declared; otherwise $\hat{m} = 1$ is declared. In an actual implementation, two accumulators A_0 and A_1 could be used. If $v_i > 0$, A_0 is incremented by s_i and if $v_i < 0$, then A_1 is incremented by s_i. In the (unlikely) event that $v_i = 0$, neither accumulator is incremented. After all M samples have been processed, the contents of A_0 and A_1 are compared to determine $\hat{m}$.

We now proceed to calculate $P(e)$ for the WPD detector. Since by symmetry, $P(e|m=0) = P(e|m=1)$, we assume with no loss of generality that $m = 0$, i.e. $+s(t)$ is sent. In this case, we can rewrite (2.12) as

$$D_{WPD} = \sum_{i=1}^{M} D_i |s_i| , \qquad (2.13)$$

where the partial decision random variable D_i is defined by

$$D_i = \begin{cases} +1 & \text{if } \text{sgn}(v_i) = \text{sgn}(s_i) \neq 0 \\ 0 & \text{if either } \text{sgn}(v_i)=0 \text{ or } \text{sgn}(s_i)=0 . \\ -1 & \text{otherwise} \end{cases} \qquad (2.14)$$

It follows that $P(D_i=1) = 1-p_i$ and $P(D_i=-1) = p_i$ where

$$P_i = P(n_i > |s_i|)$$
$$= Q\left(\sqrt{\frac{2T}{MN_o}} |s_i|\right) . \qquad (2.15)$$

The mean and variance of $D_i|s_i|$ are given by $(1-2p_i)|s_i|$ and $4p_i(1-p_i)|s_i|^2$ respectively. Under certain conditions which are satisfied in this case, it can be shown [14] that as $M\to\infty$, D_{WPD} has the asymptotically Gaussian distribution

$$n\left(\sum_{i=1}^{M} (1-2p_i)|s_i|, \sum_{i=1}^{M} 4p_i(1-p_i)|s_i|^2\right).$$

Using this result, it is shown in Appendix A for small signal-to-noise ratios that the probability of error for the WPD detector as $M\to\infty$ is given by

$$P(e) = Q\left(\sqrt{\frac{4E_s}{\pi N_o}}\right). \qquad (2.16)$$

It is interesting to note that for large values of M, the WPD detector uses $\frac{\pi}{2}$ times the energy required by the DMF detector to achieve the same value of $P(e)$. This penalty of 1.96 dB is independent of the specific signalling waveform used, in contrast to the SAS detector in which the penalty does depend on the shape of $s(t)$.

2.4. The Binary Partial Decision (BPD) Detector

The BPD detector can be considered as a special case of the WPD detector in which the information regarding the magnitude of the sample values $\{s_i\}_{i=1}^{M}$ is not used. This results in a simple implementation in which a counter (initially reset to 0) is incremented or decremented by 1 depending on the polarities of v_i and s_i. Specifically, define

$$D_{BPD} \triangleq \sum_{i=1}^{M} D_i \qquad (2.17)$$

where $D_i = \text{sgn}(v_i) \cdot \text{sgn}(s_i)$, as in (2.14). Then if $D_{BPD} > 0$, $\hat{m} = 0$ is declared; otherwise $\hat{m} = 1$ is decided. It can easily be seen that the detector will make an error if and only if a majority of the M samples have had their polarities reversed by the channel noise. Proceeding as in section 2.3, it can be shown that as $M \to \infty$, D_{BPD} has the asymptotically Gaussian distribution

$$n\left(\sum_{i=1}^{M} (1-2p_i) \, , \sum_{i=1}^{M} 4p_i(1-p_i) \right).$$

Using this result, it is shown in Appendix B that the probability of error for the BPD detector as $M \to \infty$ is given by

$$P(e) = Q\left(\sqrt{\frac{4E_s}{\pi N_o \alpha}} \right), \qquad (2.18)$$

where α is as defined in (2.10). Compared with the DMF detector, we see that the BPD detector is $10 \log_{10}\left(\frac{\pi\alpha}{2}\right) = 1.96 + 10 \log_{10}\alpha$ dB less efficient. We note that the penalty can be interpreted as consisting of 2 components: 1.96 dB is lost because decisions are based only on the polarities of the received signal samples (not on their magnitudes) and $10 \log_{10}\alpha$ dB is lost because equal weights are being given to received signal samples even though the sample corresponding to a large $|s_i|$ is less likely to be in error than the sample corresponding to a small $|s_i|$. These 2 components correspond to the losses resulting from the WPD and the SAS detectors respectively.

2.5. Generalization to Arbitrary Signalling Waveforms

The results of the three preceeding sections can be easily generalized to arbitrary signalling waveforms. Let $s_0(t)$ and $s_1(t)$ denote any two finite-energy waveforms defined on $[0,T]$. This set of signals can be transformed into a set of binary antipodal signals by defining

$$s_0'(t) = s_0(t) - \frac{s_0(t) + s_1(t)}{2} \tag{2.19a}$$

and

$$s_1'(t) = s_1(t) - \frac{s_0(t) + s_1(t)}{2} . \tag{2.19b}$$

This transformation subtracts the arithmetic mean of the two signals from each signal. The results derived in the previous sections then apply directly to $\{s_0'(t), s_1'(t)\}$, where E_s is to be interpreted as the energy in $s_0'(t)$ or $s_1'(t)$. The energy E_s of (2.4), (2.11), (2.16) and (2.18) can be related

to the signals $s_0(t)$ and $s_1(t)$ by noting that

$$E_s = \int_0^T [s_0'(t)]^2 \, dt$$

$$= \frac{1}{4} \left[E_{s_0} + E_{s_1} - 2 \int_0^T s_0(t) \, s_1(t) \, dt \right], \tag{2.20}$$

where E_{s_i}, $i=0,1$, is the energy of $s_i(t)$. Of course, if $s_1(t) = -s_0(t)$,

$E_s = E_{s_0} = E_{s_1}$. On the other hand, if $E_{s_0} = E_{s_1}$ and $\int_0^T s_0(t) \, s_1(t) \, dt = 0$

corresponding to binary orthogonal signalling, $E_s = \dfrac{E_{s_0}}{2}$ leading as expected

to a loss of 3 dB relative to binary antipodal signalling.

2.6. Discussion

The asymptotic losses associated with the use of three suboptimum

detection schemes have been analyzed. Table I gives a summary of the results

as applied to three specific signalling waveforms.

	Losses relative to DMF detector (dB)		
Waveform	SAS	WPD	BPD
Square	0	1.96	1.96
Sinusoid	0.912	1.96	2.87
Raised Cosine	1.76	1.96	3.72

Table I - Asymptotic losses for suboptimum schemes.

As indicated below, these asymptotic values are reached quite rapidly. The losses for the SAS, WPD and BPD detectors are plotted against the sample size M in figures 2.2 - 2.5. In figures 2.2 and 2.3, a sinusoidal signalling waveform is assumed, whereas a square signalling waveform is used in figures 2.4 and 2.5. For each figure, a target value of P(e) is used. In figures 2.2 and 2.4, this value is 10^{-3} and in figures 2.3 and 2.5, it is 10^{-7}. The losses represent the increase in E_s required to achieve the same target value of P(e) using the suboptimum detector and equation (2.4) respectively.

The plots in these figures were obtained numerically using a VAX-11/750. Losses were calculated for each suboptimum scheme for different (odd) values of M. It should be noted that the distortion of the signalling waveform which would result for small values of M was taken into account in these calculations. Details concerning the computation of P(e) are given in Appendix C. Recall that the samples are spaced $\frac{T}{M}$ sec. apart. The first
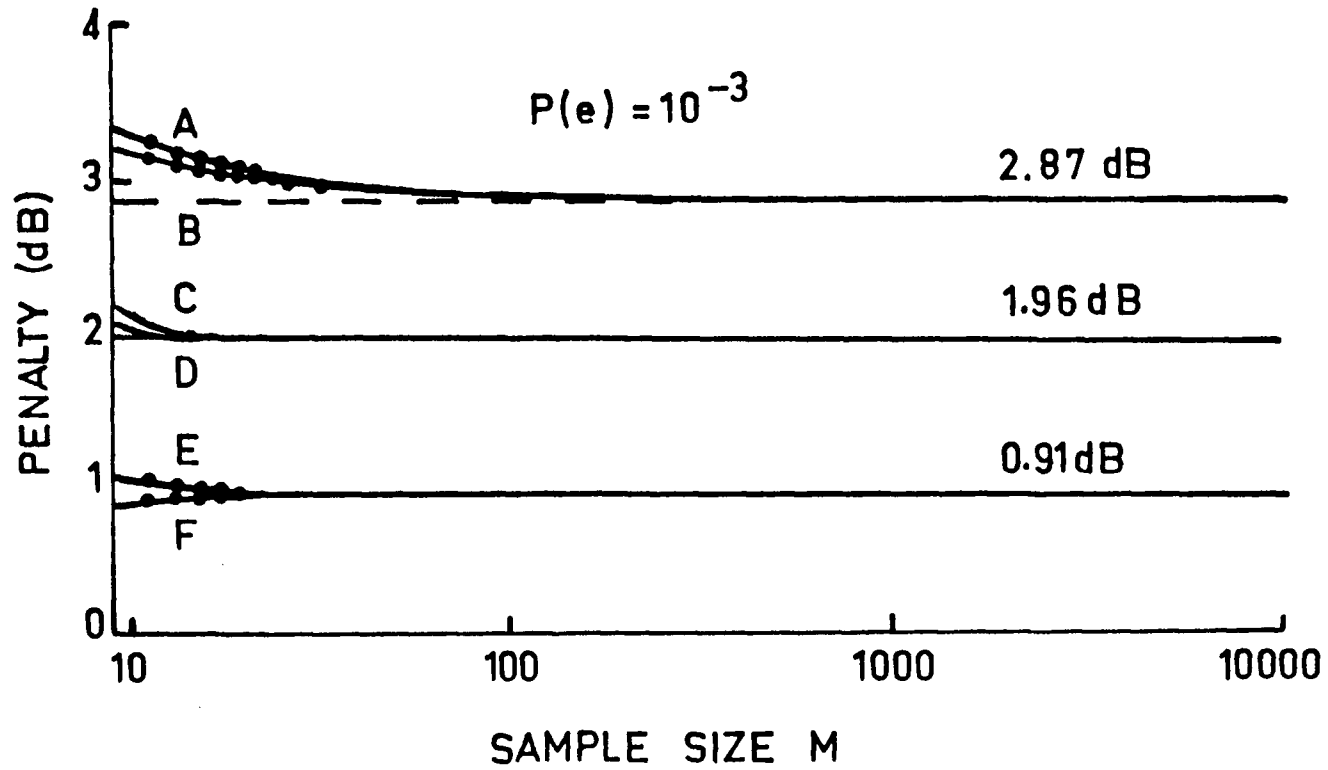
Figure 2.2. The penalty as a function of the (odd) sample size M. The signalling waveform is a single sinusoid. Curves B, D and F (A, C, E) are for the best (worst) choice of sampling starting time for the BPD, WPD and SAS detectors respectively.
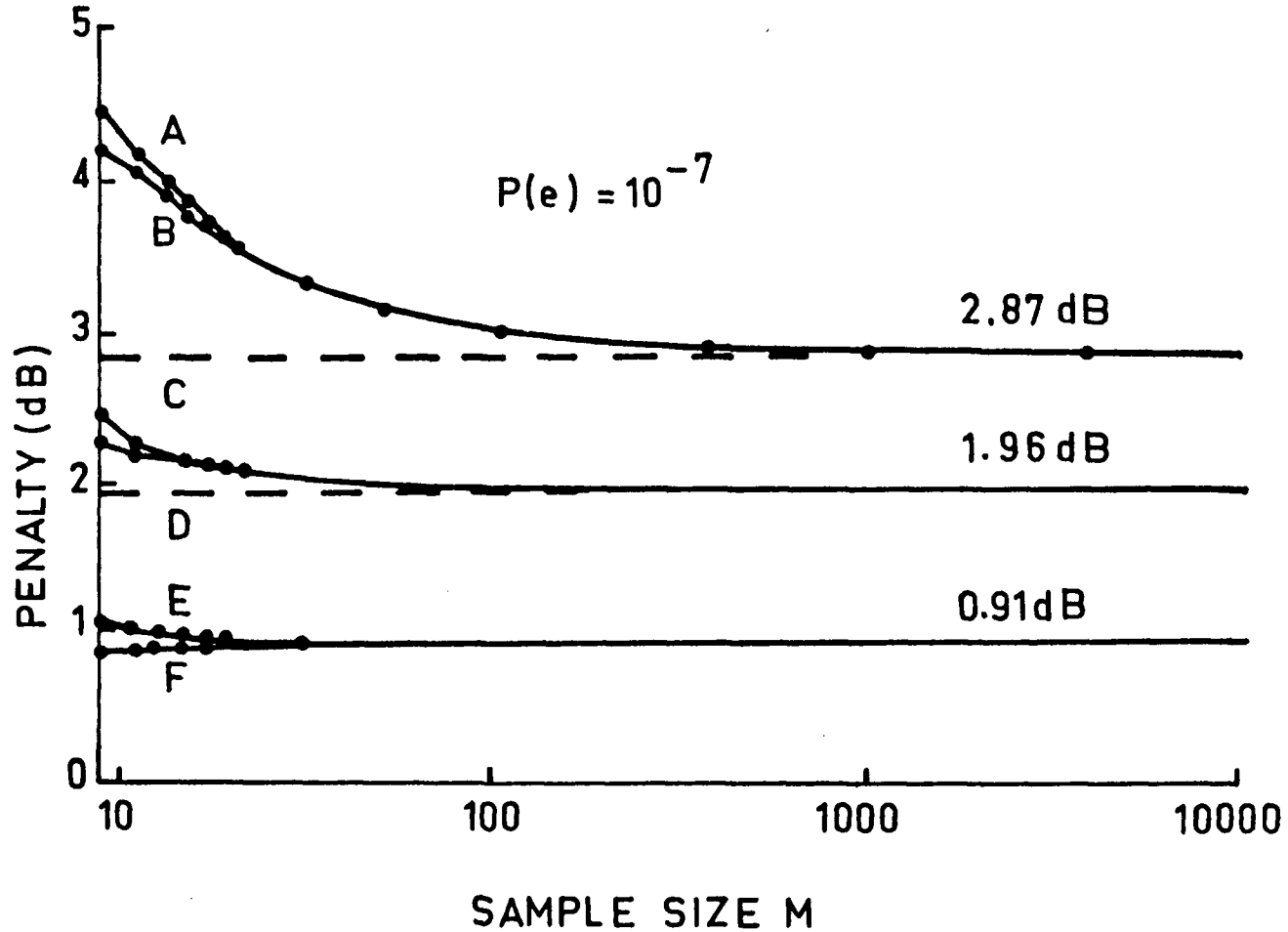
Figure 2.3. The penalty as a function of the (odd) sample size M. The signalling waveform is a single sinusoid. Curves B, D and F (A, C, E) are for the best (worst) choice of sampling starting time for the BPD, WPD and SAS detectors respectively.
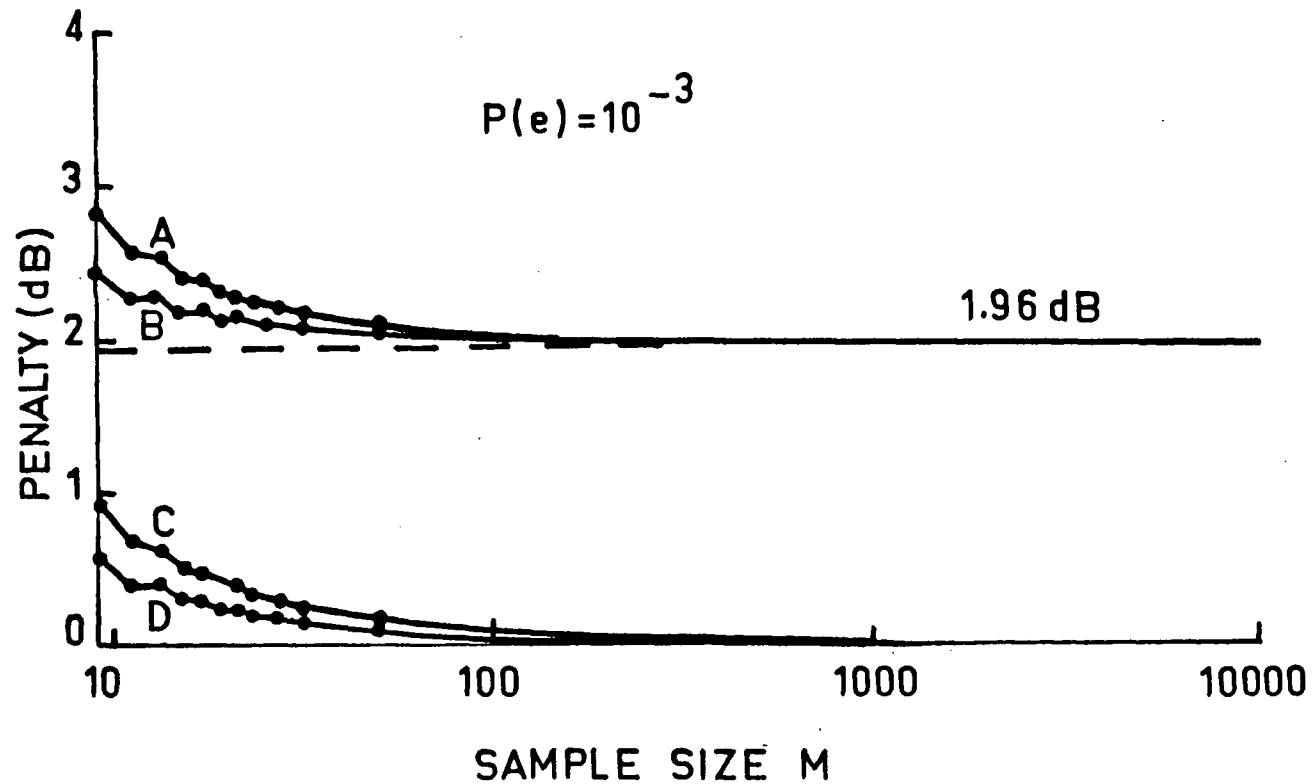
Figure 2.4. The penalty as a function of the (odd) sample size M. The signalling waveform is a square-wave. Curves A and B are for the worst and best choice of sampling starting time respectively for the BPD and WPD detectors. Curves C and D represent the worst and best choice of sampling starting time respectively for the SAS detector.
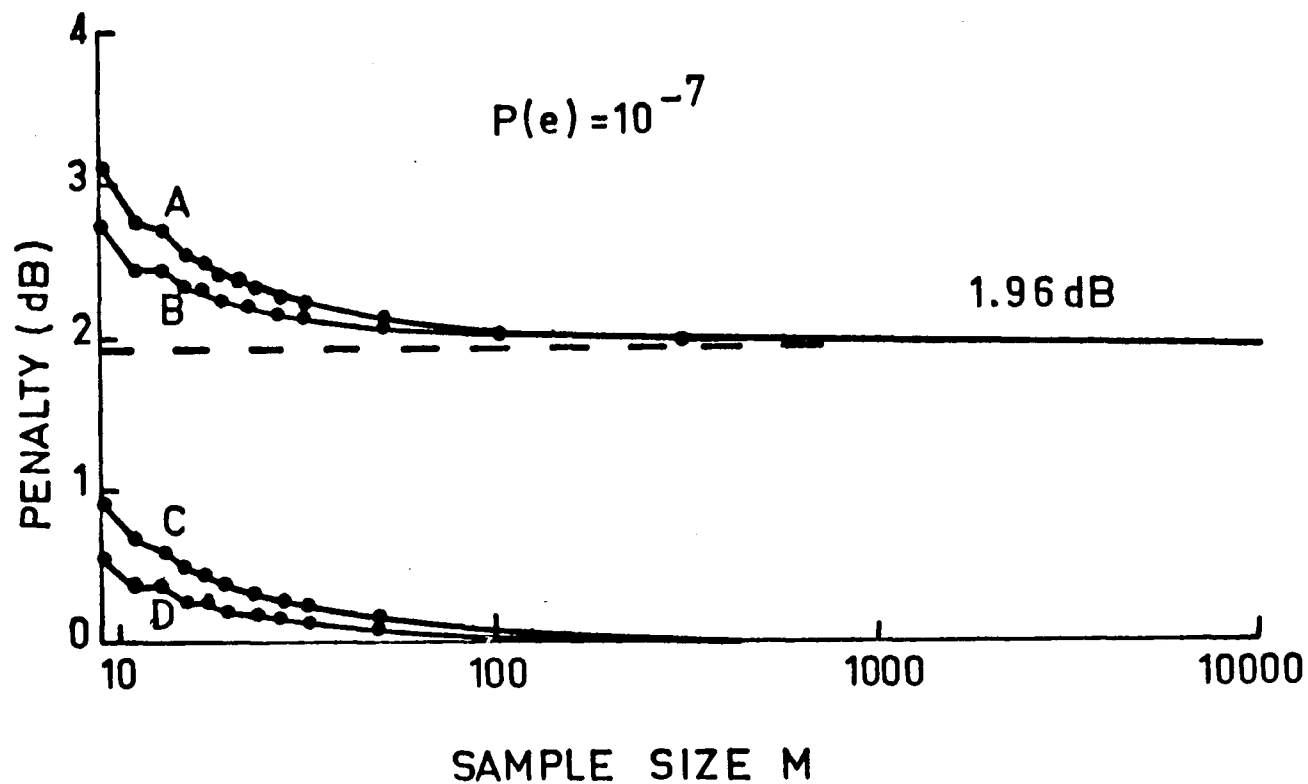
Figure 2.5. The penalty as a function of the (odd) sample size M. The signalling waveform is a square-wave. Curves A and B are for the worst and best choice of sampling starting time respectively for the BPD and WPD detectors. Curves C and D represent the worst and best choice of sampling starting time respectively for the SAS detector.

sample can be chosen anywhere in the interval $\left(0, \frac{T}{M}\right)$. The difference in losses obtained by selecting the best and the worst times for the first sample is also indicated in the figures. As would be expected, the time of the first sample has little effect on the losses for large values of M.

Figure 2.2 shows that with the sinusoidal signalling waveform and $P(e)=10^{-3}$, for M greater than about 15, the SAS, WPD and BPD detector losses are within 0.05, 0.03 and 0.25 dB of their asymptotic values. For $P(e)=10^{-7}$, figure 2.3 shows that the corresponding figures are 0.1, 0.2 and 1 dB respectively. For square wave signalling, the WPD and BPD detectors are equivalent. From figure 2.4, it can be seen that for $P(e)=10^{-3}$, and M greater than about 15, the SAS and WPD detector losses are within 0.5 dB of their asymptotic values. For a smaller value of $P(e)=10^{-7}$, figure 2.5 indicates roughly the same behaviour.

III EFFECTS OF OVERSAMPLING ON THE PERFORMANCE OF THREE

SUBOPTIMUM DETECTION SCHEMES

3.1. Introduction

In chapter 2, the penalty incurred in the use of three suboptimum detectors was analysed. The filter characteristics and the sampling rates used in the analysis guaranteed the independence of the received signal samples. In this chapter, the effects of sample dependence on the penalties are examined. The effects of oversampling are analysed for Butterworth, Gaussian and ideal lowpass filters as well as for a cascade of N identical poles.

The receiver model is shown in figure 3.1. The case of antipodal signals will be analysed but the results can be generalized to arbitrary binary signals by using the transformation of section 2.5. Depending on the message $m \varepsilon \{0,1\}$ to be transmitted, a signal $+s(t)$ or $-s(t)$ is sent over an additive white Gaussian noise (AWGN) channel. The two-sided power spectral density of the noise process is $N_o/2$. The signal $s(t)$ is assumed to be non-zero only in the time interval $[0,T]$ sec. and bandlimited to B Hz. The received signal $r(t)$ is filtered to remove excess out of band noise to produce the signal $v(t)$ which is then processed by the detector. The lowpass filter has 3dB cutoff frequency B.

The detector samples the signal $v(t)$ at a rate of 2cB samples per second yielding a total of $M = 2cBT$ noisy samples $v_i = s_i + n_i$ of the transmitted signal where $f_i = f\left(\frac{[i - 0.5]T}{M}\right)$ and the $\{n_i\}_{i=1}^{M}$ are Gaussian (not necessarily independent) noise random variables with means 0 and variances σ_n^2. The parameter c may be thought of as the oversampling factor. Increasing c gives more, dependent, samples for processing. There are a
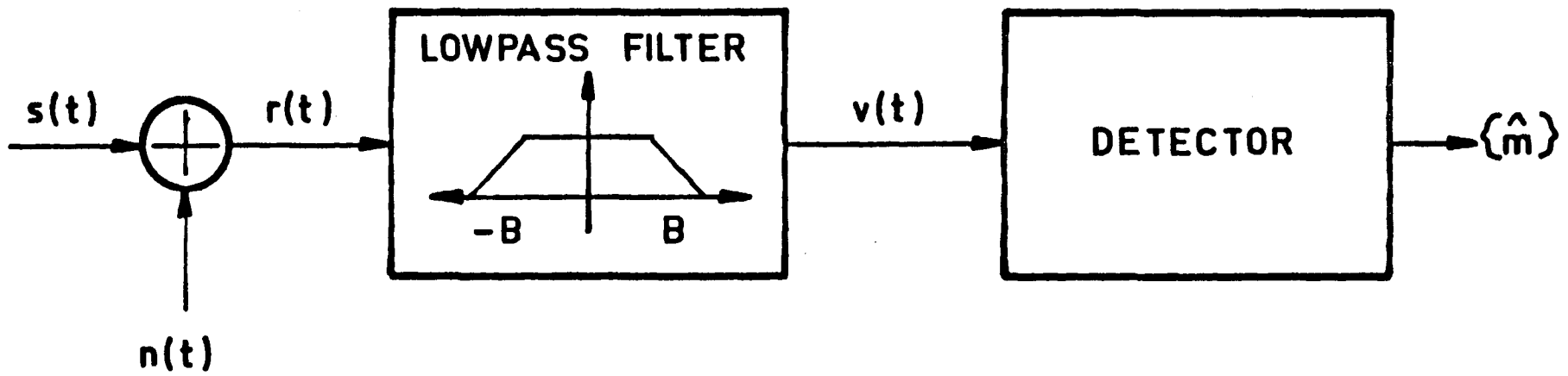
Figure 3.1. Block diagram of the data receiver.

maximum of M = 2BT independent samples available from an ideal lowpass filter corresponding to c = 1 and sampling frequency f_s = 2B [11]. The normalized sampling rate is c = f_s/2B. In order to ensure that the transmitted signal is essentially undistorted by the receiver filter, we require that

$$M = 2BT \gg 1. \qquad (3.1)$$

The ideal lowpass filter admits noise power $\sigma_n^2 = N_o B$. In general,

$$\sigma_n^2 = \gamma_n N_o B \qquad (3.2)$$

where

$$\gamma_n = \frac{1}{2B} \int_{-\infty}^{\infty} |H(f)|^2 df \qquad (3.3)$$

is the normalized noise bandwidth of the filter and H(f) is the amplitude response of the filter. One has [18,19]

$$|H(f)|^2 = [1 + (f/B)^{2N}]^{-1} \qquad (3.4a)$$
$$\text{N-th order Butterworth}$$

$$|H(f)|^2 = [1 + (f/B)^2(2^{1/N} - 1)]^{-N} \qquad (3.4b)$$
$$\text{cascade of N identical poles}$$

$$|H(f)|^2 = e^{-(f/B)^2 \ln 2} \qquad (3.4c)$$
$$\text{Gaussian}$$

for the N-th order Butterworth, the cascade of N identical poles and the Gaussian filter respectively. Using (3.4a) - (3.4c) and (3.3) gives

$$\gamma_n = \frac{\pi}{2N \, \sin[\pi/2N]}$$ (3.5a)

N-th order Butterworth

$$\gamma_n = \frac{1 \cdot 3 \cdot 5 \cdot \, \cdots \, (2N - 3)\pi}{\sqrt{2^{1/N} - 1} \, 2^N \, (N-1)!}$$ (3.5b)

cascade of N identical poles

$$\gamma_n = \sqrt{\frac{\pi}{4\ell n 2}}$$ (3.5c)

Gaussian

for the N-th order Butterworth, the N-pole cascaded and the Gaussian filter respectively.

3.2. The Sample-and-Sum (SAS) Detector with Dependent Samples

The SAS detector with dependent samples computes the quantity $D_{SAS} = \sum_{i=1}^{M} v_i \, sgn(s_i)$ as described previously in section 2.2. The penalty may be determined by proceeding as was done there.

Given that $m = 0$ is transmitted, the mean of D_{SAS} is given by $\overline{D}_{SAS} = \sum_{i=1}^{M} |s_i|$ and the variance of D_{SAS} is given by

$$\sigma^2_{D_{SAS}} = E[(D_{SAS} - \overline{D}_{SAS})^2] = E[(\sum_{i=1}^{M} v_i sgn(s_i) - \sum_{i=1}^{M} |s_i|)^2] \qquad (3.6)$$

where $E[x]$ denotes the expected value of x. The square in (3.6) may be expanded and the terms rearranged to give

$$\sigma^2_{D_{SAS}} = \sigma^2_n M\{1 + \frac{2}{M} \sum_{i=1}^{M-1} \sum_{j=i+1}^{M} sgn(s_i s_j) r_n(j-i)\} \qquad (3.7)$$

where $r_n(j-i) = E[n_j n_i]/E[(n_i)^2]$ is the normalized autocorrelation of the noise which is assumed stationary.

If the signalling waveform $s(t)$ is continuous on $0 < t < T$ and single-phase, i.e. $s(t) > 0$ for $0 < t < T$, then (3.7) gives

$$\sigma^2_{D_{SAS}} = \sigma^2_n M\{1 + \frac{2}{M} \sum_{i=1}^{M-1} \sum_{j=1}^{i} r_n(j)\} . \qquad (3.8)$$

Using the result [20] that

$$\lim_{M \to \infty} \frac{1}{M} \sum_{i=1}^{M-1} \sum_{j=1}^{i} r_n(j) = \sum_{j=1}^{\infty} r_n(j)$$

whenever the series

$$\sum_{j=1}^{\infty} r_n(j) = \lim_{i \to \infty} \sum_{j=1}^{i} r_n(j) \qquad (3.9)$$

is convergent with (3.8) gives for large values of M

$$\sigma^2_{D_{SAS}} \approx \sigma_n^2 M\{1 + 2 \sum_{i=1}^{\infty} r_n(i)\}$$ (3.10)

when the series (3.9) converges.

Let the term split-phase refer to a signal s(t) which is continuous on the interval $0 < t < T$ and which satisfies the conditions $signum\{s(t_A)\} \cdot signum\{s(t_B)\} = -1$ for $(0 < t_A < T/2, T/2 < t_B < T)$ and $s(T/2) = 0$. Then result (3.10) is valid for split-phase signals. This is proven from (3.7) by proceeding as in the single-phase case. The following analysis applies to all signalling waveforms which satisfy (3.10).

The random variable D_{SAS} is Gaussian since it is the sum of jointly Gaussian random variables. Therefore, (3.1), (3.2), (3.10) and (2.10) give

$$P(e) = P(e|m=0) = P(e|m=1)$$

$$= Pr(D_{SAS}<0) = Q\{\bar{D}_{SAS}/\sigma_{D_{SAS}}\}$$

$$= Q\{ \frac{\sqrt{2cT} \sum_{i=1}^{M} |s_i|}{M\sqrt{\gamma_n N_o[1 + 2 \sum_{i=1}^{\infty} r_n(i)]}} \}$$

$$= Q \{ \sqrt{\frac{2cE_s}{\gamma_n \alpha N_o[1 + 2 \sum_{i=1}^{\infty} r_n(i)]}} \} .$$ (3.11)

Comparison of (3.11) with (2.4) shows that to achieve the same error

probability as the optimum detector, the SAS detector with dependent samples

requires $\alpha \Gamma_n$ more energy where

$$\Gamma_n = \gamma_n \{1 + 2 \sum_{i=1}^{\infty} r_n(i)\}/c \ . \tag{3.12}$$

The loss represented by Γ_n is in addition to the α loss described in section

2.2. One observes from (3.12) that Γ_n has two components. The factor γ_n

arises because a filter with finite roll-off admits more noise than an

ideal filter with infinitely sharp cut-off. The sum $\sum_{i=1}^{\infty} r_n(i)$ results from

the dependence of the samples.

It is interesting to consider Γ_n for the ideal lowpass filter. In

this case, $\gamma_n = 1$ and $r_n(i) = \dfrac{\sin(\pi i/c)}{(\pi i/c)}$. Using the fact that the Fourier

sine series representation for the function $f(x) = \pi - x$, $0 < x < \pi$, is [21]

$$f(x) \sim 2 \sum_{i=1}^{\infty} \frac{\sin ix}{i}$$

gives for $x = \pi/c$ with $c > 1$,

$$2 \sum_{i=1}^{\infty} \frac{\sin (\pi i/c)}{(\pi i/c)} = c - 1 \ ,$$

where convergence is guaranteed by a Fourier Theorem. Hence, $\Gamma_n = 1$ for all values of c > 1 for the ideal lowpass filter. That is, processing more than the maximum number of independent samples neither improves nor deteriorates the performance when (3.1) is satisfied. Note also that the loss, α, incurred by not weighting the samples is not retrievable in whole or in part by oversampling.

In the general case, the normalized autocorrelation $r_n(\tau)$ of filtered white noise is related to the filter characteristic by the Wiener-Khintchine theorem [22]. That is, $r_n(\tau)$ is the normalized inverse Fourier transform of the squared magnitude frequency response of the filter. Starting from (3.4a) – (3.4c) one may derive

$$r_n(\tau) = \sin(\pi/2N) \sum_{\ell=1}^{N} \exp[-2\pi B|\tau|\sin\left(\frac{2\ell-1}{2N}\pi\right)] \sin\{\frac{2\ell-1}{2N}\pi + 2\pi B|\tau|\cos\left(\frac{2\ell-1}{2N}\pi\right)\}$$

Nth order Butterworth   (3.13a)

$$r_n(\tau) = \frac{(N-1)!}{(2N-2)!} e^{-b|\tau|} \sum_{k=0}^{N-1} \frac{(2N-k-2)!(2b|\tau|)^k}{k!(N-k-1)!}, \quad b = 2\pi B/\sqrt{2^{1/N}-1}$$

cascade of N identical poles   (3.13b)

$$r_n(\tau) = e^{-\tau^2\pi^2B^2/\ln2}$$

Gaussian   (3.13c)

for the N-th order Butterworth, the cascade of N identical poles and the Gaussian filter respectively. Figure 3.2 presents $r_n(\tau)$ as a function of
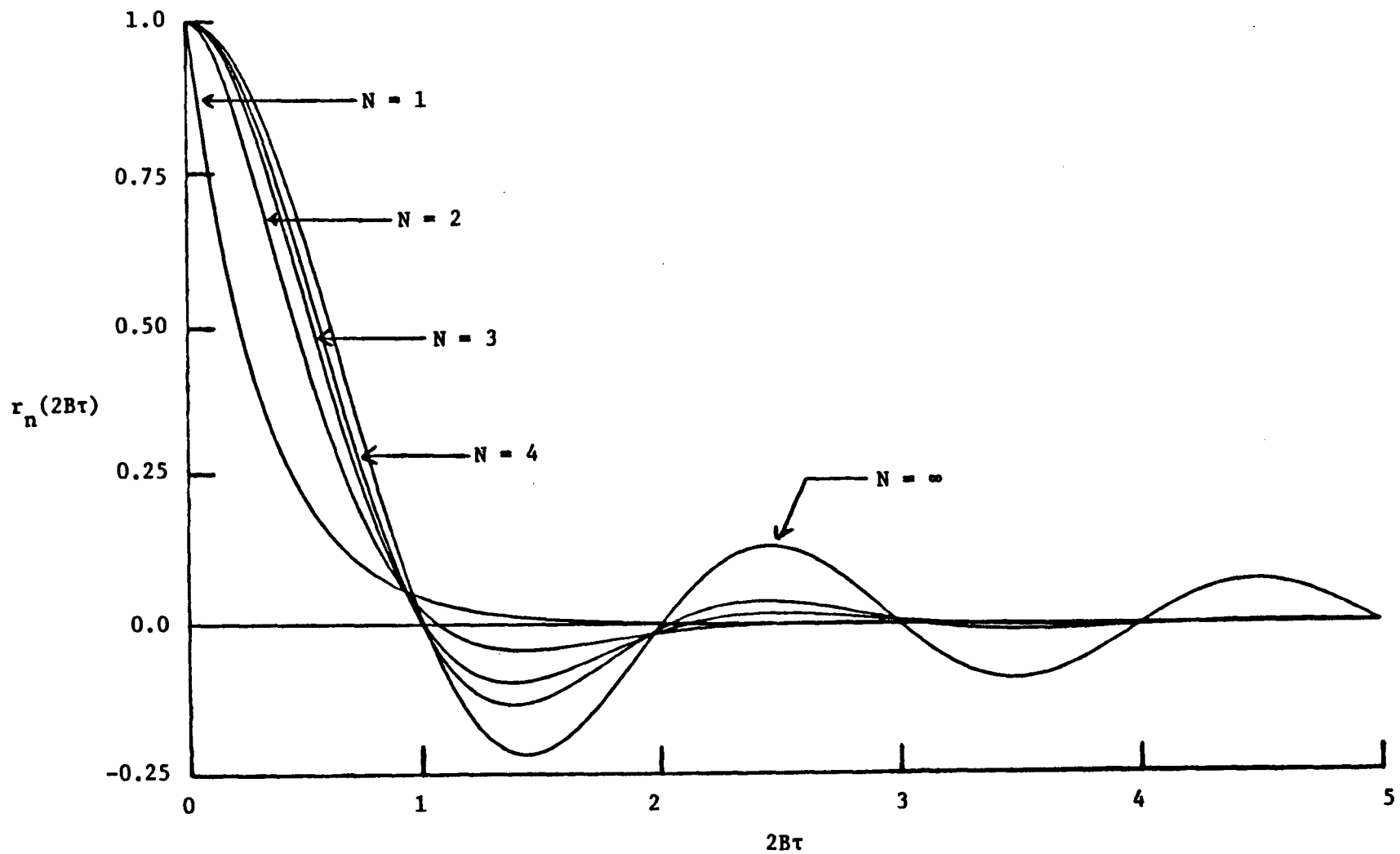
Figure 3.2. The normalized autocorrelation function $r_n(\tau)$ of white noise filtered by a Butterworth lowpass filter of order N. The ideal lowpass filter corresponds to $N = \infty$.

$B\tau$ for the Butterworth ($N = 1-4$) and ideal lowpass filters. Figure 3.3 shows $r_n(\tau)$ for the cascaded pole ($N = 1, 2, 4, 6$) and Gaussian filters.

The terms in the sum of (3.12) occur at time instants $t_i = i/2cB$. Therefore, equations (3.13a)-(3.13c) combined with (3.12) and (3.5a)-(3.5c) yield, after some manipulations,

$$\Gamma_n = \frac{\pi}{2cN\sin(\pi/2N)} \left\{ 1 + \sin\left(\frac{\pi}{2N}\right) \sum_{\ell=1}^{N} \frac{\sin\left(a_\ell + \frac{\pi}{c}\cos a_\ell\right) - e^{-\frac{\pi}{c}\sin a_\ell} \sin a_\ell}{\cosh\left(\frac{\pi}{c}\sin a_\ell\right) - \cos\left(\frac{\pi}{c}\cos a_\ell\right)} \right\},$$

$$a_\ell = \frac{2\ell-1}{2N}\pi \qquad\qquad \text{N-th order Butterworth} \qquad (3.14a)$$

$$\Gamma_n = \frac{1\cdot3\cdot5\cdot\ \cdots\ (2N-3)\pi}{\sqrt{2^{1/N}-1}\ 2^N(N-1)!c} \left\{ 1 + \frac{2(N-1)!}{(2N-2)!} \sum_{i=1}^{\infty} e^{-ih} \right.$$

$$\left. \sum_{k=0}^{N-1} \frac{(2N-k-2)!(2ih)^k}{k!(N-k-1)!} \right\}, \qquad h = \frac{\pi}{c\sqrt{2^{1/N}-1}} \qquad (3.14b)$$

$$\text{cascade of N identical poles}$$

$$\Gamma_n = \frac{1}{c}\sqrt{\frac{\pi}{4\ln2}} \left\{ 1 + 2 \sum_{i=1}^{\infty} e^{-i^2\pi^2/4c^2\ln2} \right\}.$$

$$\text{Gaussian} \qquad (3.14c)$$

The quantity Γ_n is plotted as a function of the normalized sampling rate $f_s/2B = c$ in figures 3.4 and 3.5 for Butterworth and cascaded pole filters respectively. Also shown in figure 3.5 is the curve for the Gaussian filter
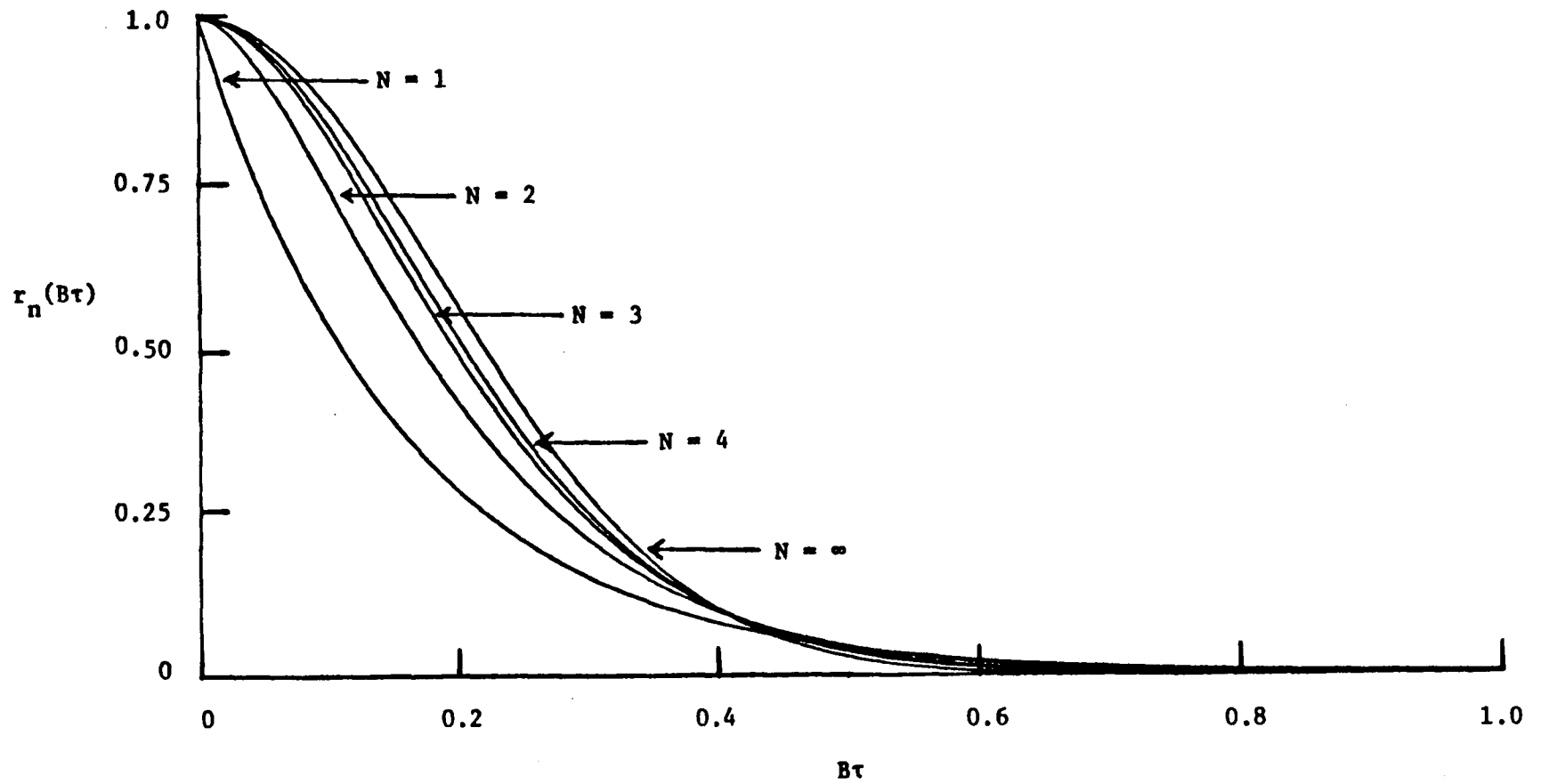
Figure 3.3. The normalized autocorrelation function $r_n(\tau)$ of white noise filtered by a cascade of N identical poles. The Gaussian filter corresponds to N = ∞.
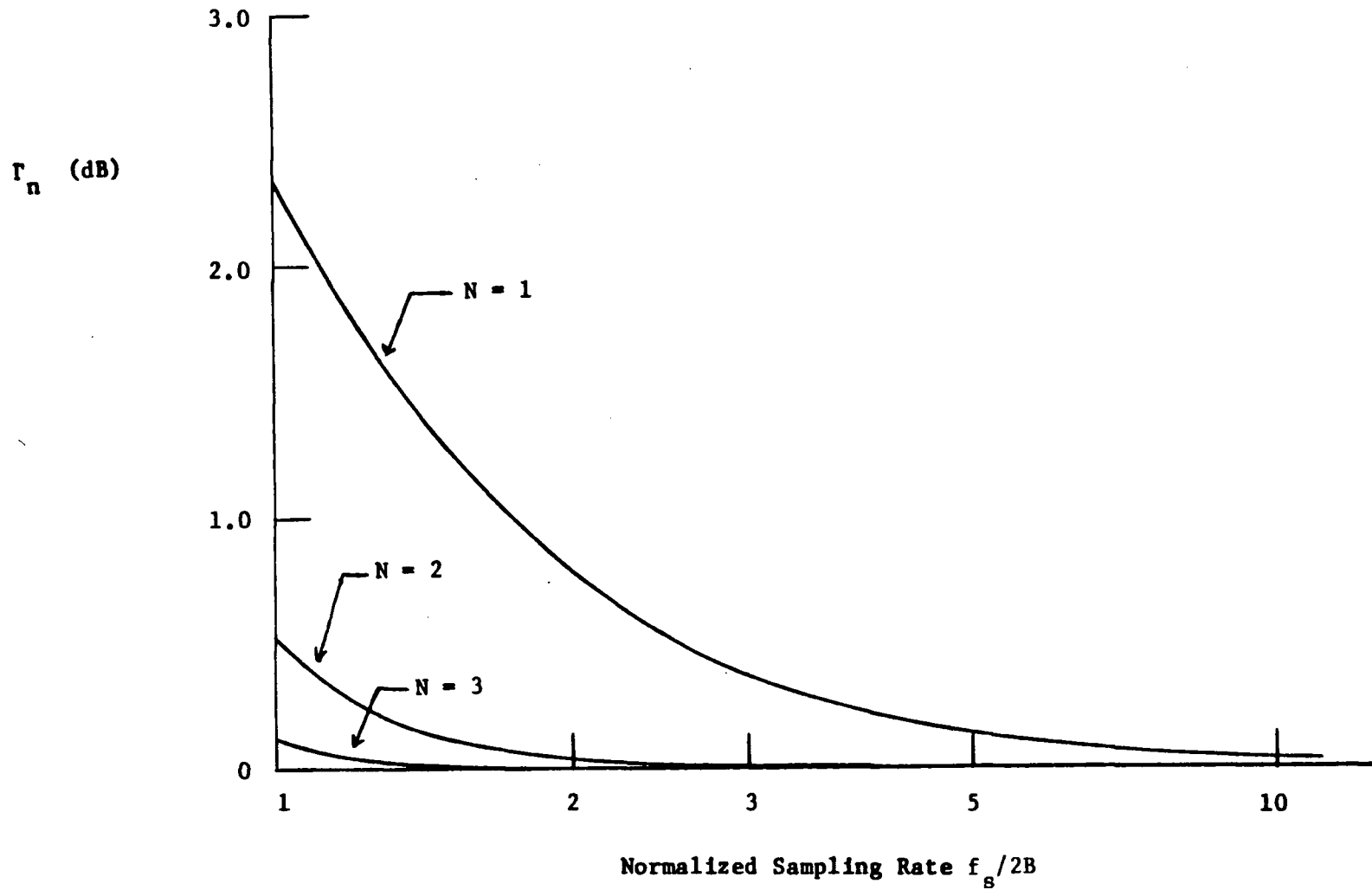
Figure 3.4. The additional penalty Γ_n for the SAS detector with a Butterworth prefilter of order N.
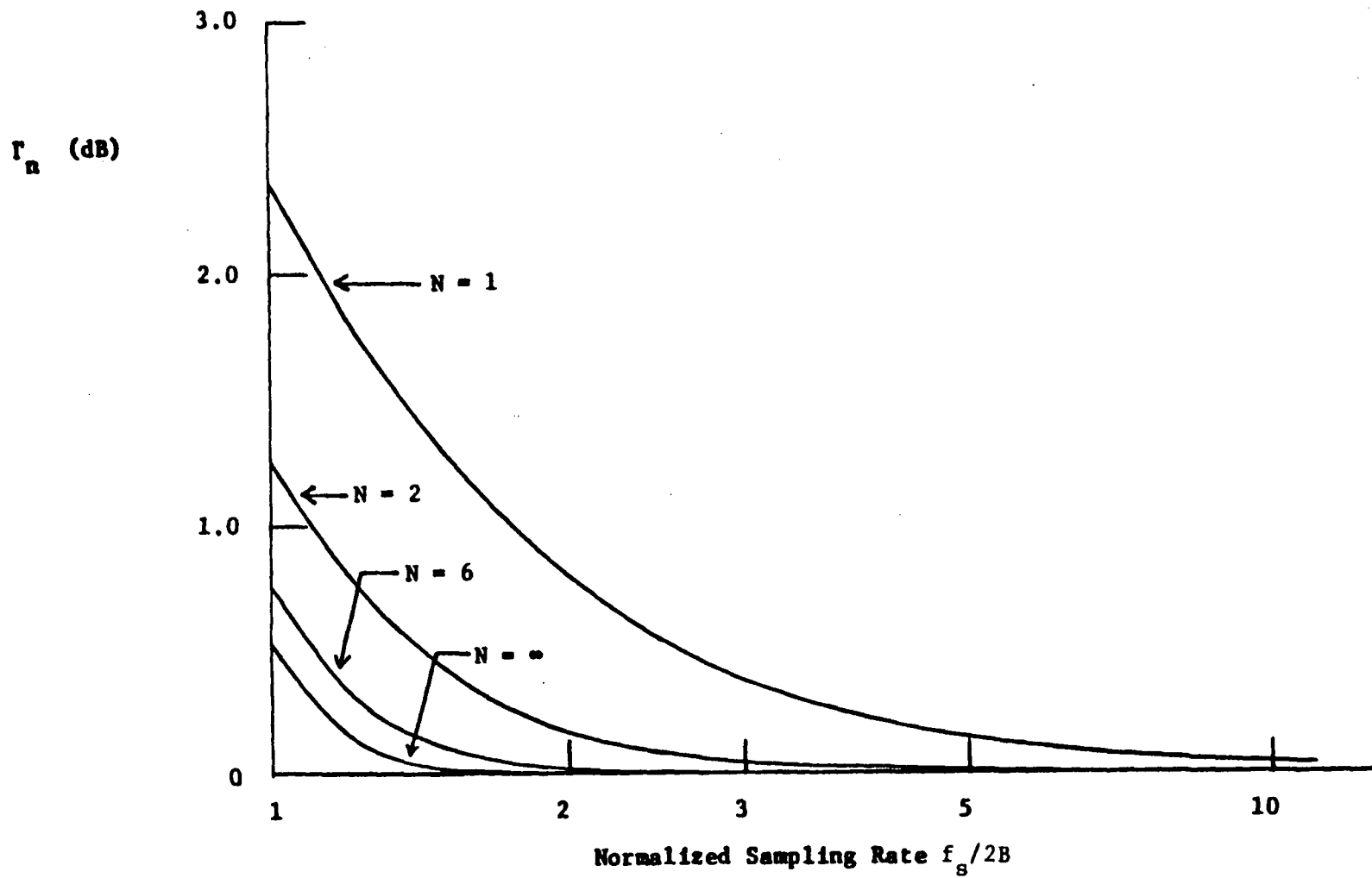
Figure 3.5. The additional penalty Γ_n for the SAS detector with prefilter consisting of a cascade of N identical poles. The Gaussian prefilter corresponds to N = ∞.

which corresponds to a cascaded-pole filter with $N = \infty$. In all cases, Γ_n decreases with c and $\lim_{c \to \infty} \Gamma_n = 1$. Using the Wiener-Khintchine theorem, it can be shown that $\lim_{c \to \infty} \Gamma_n = 1$ for any filter provided that $r_n(\tau)$ is integrable.

3.3. The Weighted Partial Decision (WPD) Detector with Dependent Samples

The WPD detector with dependent samples bases its decision on

$$D_{WPD} = \sum_{i=1}^{M} \text{sgn}(v_i) \cdot s_i = \sum_{i=1}^{M} D_i |s_i| \qquad (3.15)$$

as described in section 2.3. The error probability is found by proceeding as previously. That is, the mean and variance of D_{WPD} are derived and a central limit theorem is used to approximate the error probability for large values of M. The partial decision random variables D_i are now permitted to be dependent. In order to proceed, we postulate that a central limit theorem holds for certain sums of dependent random variables. Many central limit theorems for dependent random variables formalize in some sense a heuristic notion that one expects a central limit theorem to hold if the random variables behave more like independent random variables the further they are separated [23]. The dependent random variables considered here behave in this fashion. Computer simulations are used to test the validity of the postulate and to illustrate how the penalty varies with M.

When a general filter and dependent samples, as described by (3.1) and (3.2), are considered equation (2.15) must be replaced by

$$p_i = Pr(n_i > |s_i|) = Q\{\sqrt{\frac{2cT}{\gamma_n N_o M}} |s_i|\} \quad . \tag{3.16}$$

The mean and variance of $D_i |s_i|$ are again given by $(1-2p_i)|s_i|$ and $4p_i(1-p_i)|s_i|^2$ respectively. The mean of D_{WPD} is found from (3.15)

$$\overline{D}_{WPD} = \sum_{i=1}^{M} (1-2p_i)|s_i| \tag{3.17}$$

and the variance of D_{WPD} is

$$\sigma^2_{D_{WPD}} = E[(D_{WPD} - \overline{D}_{WPD})^2] = E[(\sum_{i=1}^{M} D_i|s_i| - \sum_{i=1}^{M} \overline{D}_i|s_i|)^2]$$

$$= \sum_{i=1}^{M} \sigma^2_{D_i}|s_i|^2 + \sum_{i=1}^{M} \sum_{\substack{j=1 \\ i \neq j}}^{M} |s_i||s_j| \{E[D_i D_j - \overline{D}_i \overline{D}_j]\} \quad . \tag{3.18}$$

It is shown in Appendix D that for large values of M

$$E[D_i D_j] - \overline{D}_i \overline{D}_j \approx \frac{2}{\pi} \arcsin \{r_n(j-i)\} \tag{3.19}$$

where the noise process is assumed to be stationary. Then (3.18) can be rewritten as

$$\sigma^2_{D_{WPD}} = \sum_{i=1}^{M} \sigma^2_{D_i} |s_i|^2 + \frac{2}{\pi} \sum_{\substack{i=1 \\ i \neq j}}^{M} \sum_{j=1}^{M} |s_i||s_j| \arcsin\{r_n(j-i)\} \quad . \qquad (3.20)$$

By proceeding as in Appendix A with p_i given by (3.16), it may be shown that for large values of M

$$\sum_{i=1}^{M} \sigma^2_{D_i} |s_i|^2 \approx \frac{ME_s}{T} \qquad (3.21)$$

and

$$\bar{D}_{WPD} \approx \sqrt{\frac{4cM}{\pi N_o \gamma_n T}} E_s \quad . \qquad (3.22)$$

Furthermore, it is proven in Appendix E that as $M \rightarrow \infty$

$$\frac{T}{M E_s} \sum_{\substack{i=1 \\ i \neq j}}^{M} \sum_{j=1}^{M} |s_i||s_j| \arcsin\{r_n(j-i)\} \approx 2 \sum_{i=1}^{\infty} \arcsin\{r_n(i)\} \quad . \qquad (3.23)$$

Combining (3.21) and (3.23) with (3.20) and (3.22) gives

$$\frac{\bar{D}_{WPD}}{\sigma_{D_{WPD}}} \approx \sqrt{\frac{4E_s c}{\pi N_o \gamma_n \left(1 + \frac{4}{\pi} \sum_{i=1}^{\infty} \arcsin\{r_n(i)\}\right)}} \quad . \qquad (3.24)$$

Applying a central limit theorem to the sum of (3.15) and using (3.24) gives the error probability

$$P(e) \approx Q\left\{ \sqrt{\frac{4E_s c}{\pi N_0 \gamma_n \left(1 + \frac{4}{\pi} \sum_{i=1}^{\infty} \arcsin\{r_n(i)\}\right)}} \right\}. \qquad (3.25)$$

Comparison of (3.25) with (2.4) shows that the penalty of the WPD detector with dependent samples is $\pi/2 \; \Gamma_n$ where

$$\Gamma_n = \gamma_n \left[1 + \frac{4}{\pi} \sum_{i=1}^{\infty} \arcsin\{r_n(i)\} \right]/c \quad . \qquad (3.26)$$

The loss represented by Γ_n is in addition to the $\pi/2$ or 1.96 dB loss of the WPD detector with independent samples. Note that $2/\pi \; \arcsin\{r_n(i)\}$ is the normalized autocorrelation function after hard-limiting of a random variable possessing normalized autocorrelation function $r_n(i)$ [24]. Equation (3.26) is, therefore, analagous to equation (3.12). The function $2/\pi \; \arcsin\{r_n(B\tau)\}$ is shown in figures 3.6 and 3.7 for Butterworth and cascaded pole filters respectively.

The additional penalty Γ_n is plotted as a function of the normalized sampling rate in figures 3.8 and 3.9 for Butterworth and cascaded pole filters respectively. The values $r_n(i)$ are determined from equations (3.13a) - (3.13c) with $r_n(i) = r_n(i/2cB)$. Observe that for high sampling rates, the penalty for a low order filter is less than that for a high order filter. For example, in figure 3.8 at $f_s/2B = 15$, $\Gamma_n = -1.5$ dB for $N = 1$ while $\Gamma_n = -0.9$ dB for $N = \infty$. A similar observation was made in [25], in the
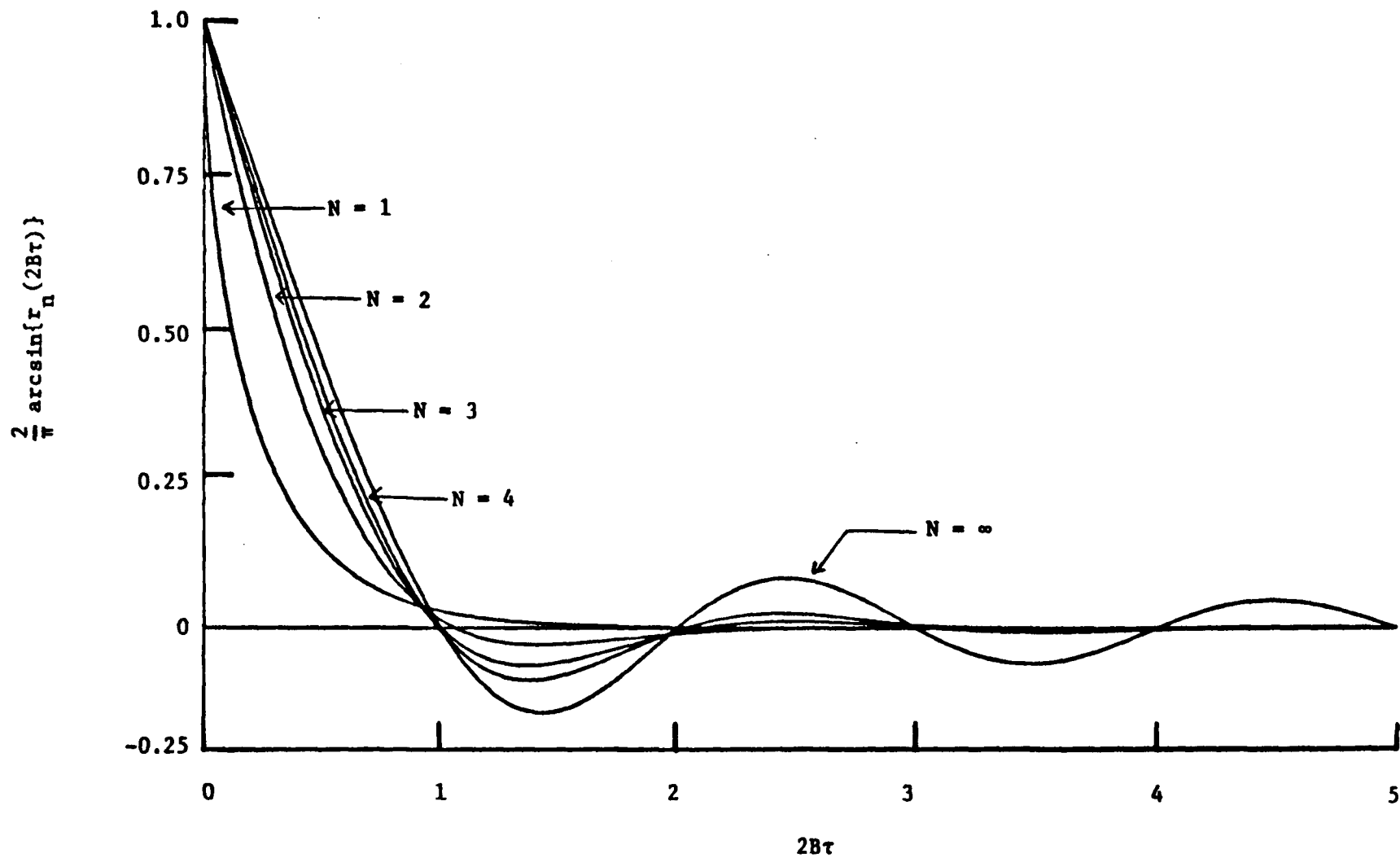
Figure 3.6. The normalized autocorrelation function of white noise after lowpass filtering and hard-limiting. The filter used is N-th order Butterworth. The ideal lowpass filter corresponds to N = ∞.
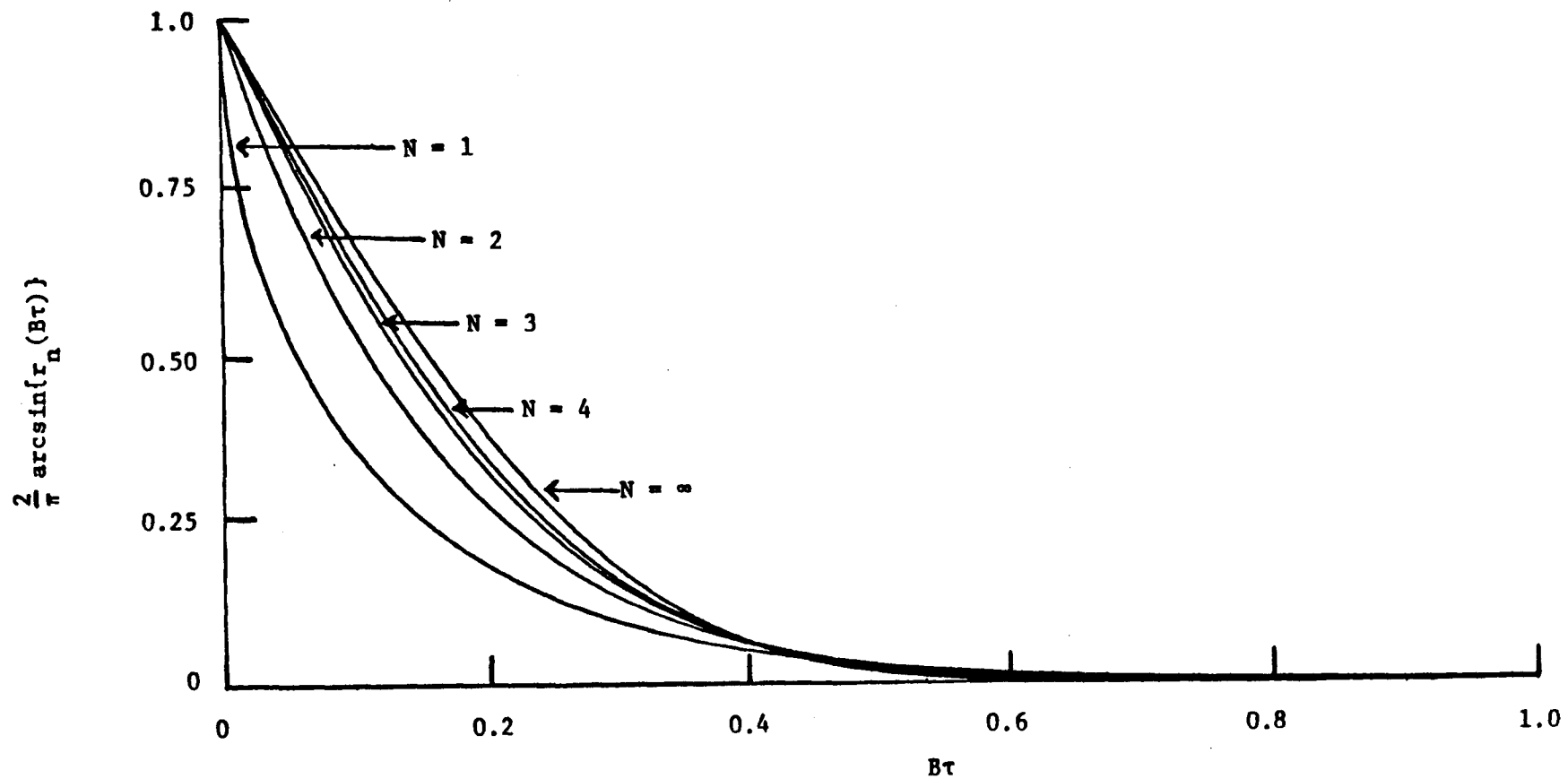
Figure 3.7. The normalized autocorrelation function of white noise after lowpass filtering and hard-limiting. The filter used is a cascade of N identical poles. The Gaussian lowpass filter corresponds to N = ∞.
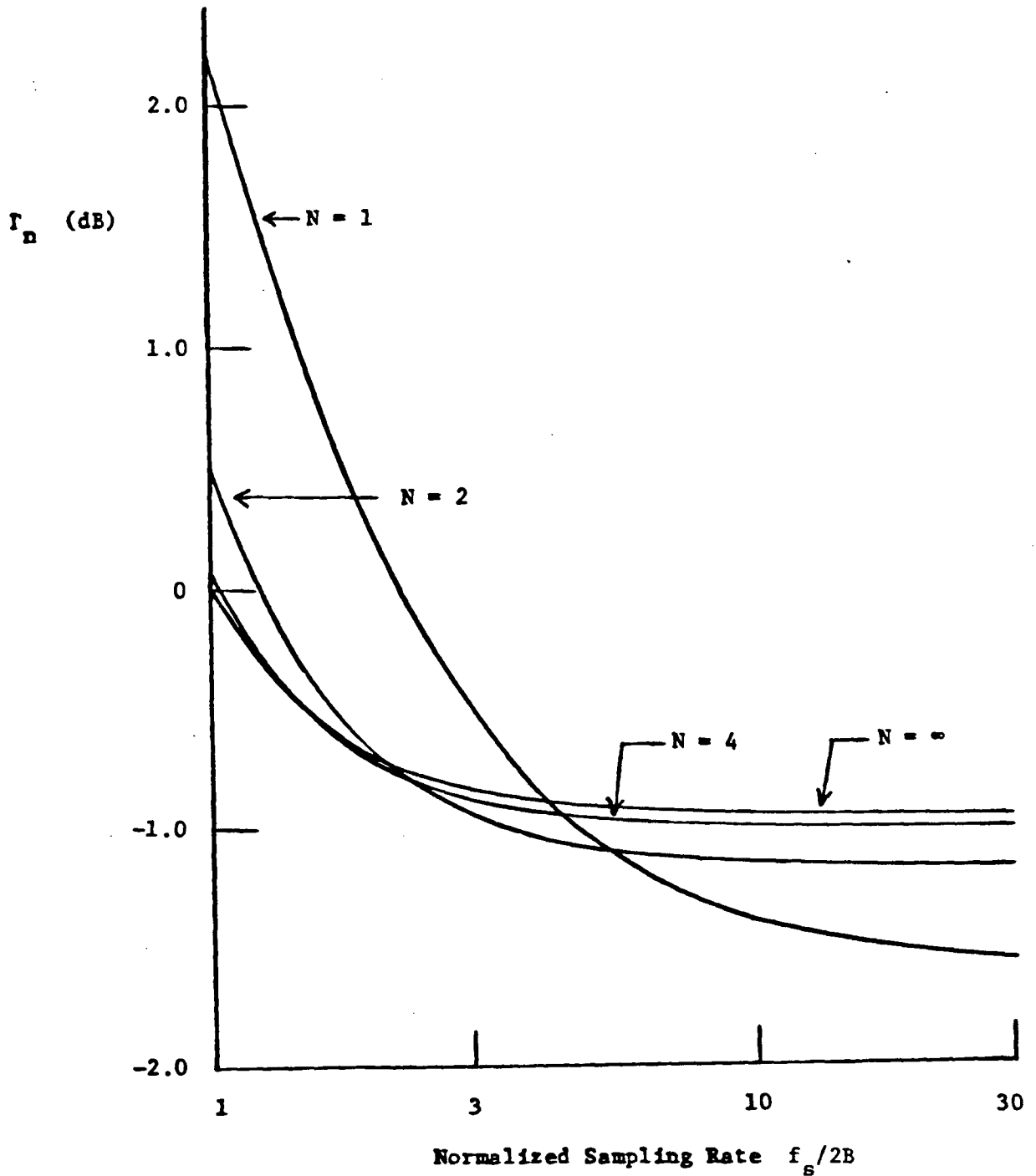
Figure 3.8. The additional penalty Γ_n of the WPD and BPD detectors. The prefilter is N-th order Butterworth lowpass. The ideal lowpass filter corresponds to $N = \infty$.
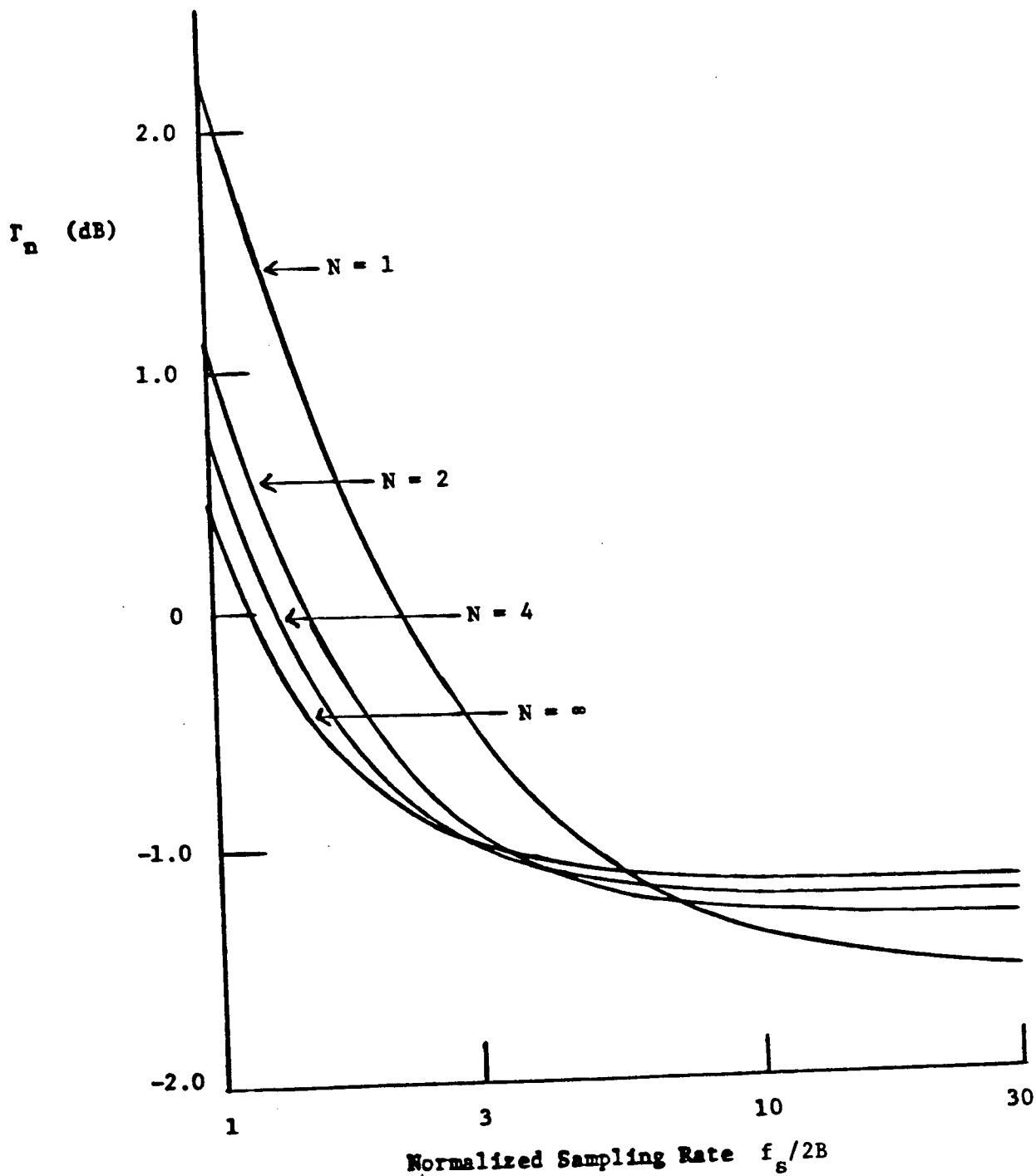
Figure 3.9. The additional penalty Γ_n of the WPD and BPD detectors. The prefilter is a cascade of N identical lowpass poles. The Gaussian lowpass corresponds to N = ∞.

context of polarity coincidence array detectors.

3.4. The Binary Partial Decision (BPD) Detector with Dependent Samples

The BPD detector with dependent samples computes

$$D_{BPD} \overset{\Delta}{=} \sum_{i=1}^{M} D_i \quad .$$ (3.27)

The probability of error is determined by proceeding as in section 2.4. For large M,

$$\frac{\bar{D}_{BPD}}{\sigma_{BPD}} \approx \sqrt{\frac{4cT\{<|s(t)|>\}^2}{\pi N_o \gamma_n [1 + \frac{4}{\pi} \sum_{i=1}^{\infty} \arcsin\{r_n(i)\}]}} = \sqrt{\frac{4cEs}{\pi N_o \gamma_n \alpha [1 + \frac{4}{\pi} \sum_{i=1}^{\infty} \arcsin\{r_n(i)\}]}}$$ (3.28)

where α has been previously defined in (2.10). Assuming a central limit theorem holds for the sum in equation (3.27) and using (3.28) gives for the error probability

$$P_{BPD}(e) \approx Q\left\{ \sqrt{\frac{4cEs}{\pi N_o \gamma_n \alpha [1 + \frac{4}{\pi} \sum_{i=1}^{\infty} \arcsin\{r_n(i)\}]}} \right\}$$ (3.29)

The penalty of the BPD detector with dependent samples is found by comparing (3.29) with (2.4). It is $\alpha \pi/2 \Gamma_n$ where Γ_n is given by (3.26). That is, the

additional penalty Γ_n is the same for the BPD and WPD detectors and is independent of the signalling waveform.

3.5. Conclusions

The asymptotic losses of three suboptimum detection schemes with dependent sampling have been analyzed. In order to verify the central limit theorem postulated in section 3.3 and to illustrate how quickly the asymptotic values are reached, we have simulated the WPD detector with dependent samples. Coloured Gaussian noise samples were generated using the method of reference [26]. The signal-to-noise ratio required to attain $P(e) = 1.00 \times 10^{-3}$ is determined from figure 3.8 and equations (3.25) and (2.4). Using a first order Butterworth prefilter, the simulated error probabilities for $f_s/2B = 1$ were 1.13×10^{-3} and 1.01×10^{-3} for $M = 9$ and $M = 31$ respectively. For $f_s/2B = 3$ and $M = 27$, 93 and 303 the $P(e)$ values were 1.77×10^{-3}, 1.14×10^{-3} and 1.05×10^{-3} respectively.

It was noted earlier that better performance can be achieved by using a first order lowpass filter rather than a fourth order filter. This has also been verified by simulation. Again, the SNR required to achieve $P(e) = 1.00 \times 10^{-3}$ is determined from the present results and used in the simulator. The analysis indicates that 0.48 dB greater SNR is required for the fourth order filter when both filters are Butterworth and $f_s/2B = 15$ for $M = 1515$. The simulated error probabilities were 1.09×10^{-3} and 1.04×10^{-3} for the first and fourth order filters respectively. Note that an increase of 0.48 dB decreases $P(e)$ from 1.00×10^{-3} to 5.46×10^{-4}.

IV OPTIMAL DETECTION OF HARD-LIMITED DATA SIGNALS IN DIFFERENT

NOISE ENVIRONMENTS

4.1. Introduction

A number of digital techniques for detecting binary antipodal signals are based on examining the polarities of the received signal samples and ignoring their amplitudes. The weighted partial decision (WPD) and binary partial decision (BPD) detectors analyzed in chapters 2 and 3 are two examples. In this chapter, the structure of the optimum detector $D_{OPT,HL}$ for the hard-limited samples is derived. Its performance is compared with those of some commonly used ad hoc detectors in both impulsive and Gaussian noise environments. For the Gaussian case, the performance is also compared with that of the optimum detector D_{OPT} which operates directly on the unquantized received samples.

The generalization of the $D_{OPT,HL}$ detector to M-ary signalling with each received sample quantized to an arbitrary number of levels is also examined. The optimum, minimum probability of error, receiver for this case is derived.

4.2. Derivation of the Optimum Detector for Hard-Limited Samples

In this section, we derive the optimum processing for a number of hard-limited samples. For ease of discussion, it is assumed that the samples come from one of two antipodal signals that have been corrupted by additive channel noise.[†] Depending on the message

---

[†]The analysis is extended to arbitrary signalling schemes in section 4.6.

$m\varepsilon\{0,1\}$ to be transmitted, a signal $+s(t)$ or $-s(t)$ is sent over a noisy channel. The detector decides which message $\hat{m}$, $\hat{m}\varepsilon\{0,1\}$ was sent on the basis of the hard-limited samples. The optimum detector $D_{OPT,HL}$ minimizes the probability of error $P(e) \triangleq Pr(\hat{m} \neq m)$.

Assume that the transmitted signals $\pm s(t)$ are time-limited to the interval $[0,T]$. If $s(t)$ is sent (corresponding to message $m=0$), then

$$v_i = + s_i + n_i , \qquad i = 1,2,\ldots,N_s \qquad (4.1)$$

where $\{v_i\}_{i=1}^{N_s}$ denote the N_s samples of $v(t)$, i.e. $v_i = v\left(\frac{[i-0.5]T}{N_s}\right)$, to be processed. The values $\{s_i\}_{i=1}^{N_s}$ denote the samples of $+s(t)$ and $\{n_i\}_{i=1}^{N_s}$ represent outcomes of independent noise random variables (r.v.'s). The noise is assumed to possess an even probability density function. If the message is $m=1$, then $-s(t)$ is sent, and $v_i = -s_i + n_i$, $i=1,2,\ldots,N_s$. Each sample v_i is hard-limited by the detector according to

$$D_i = \begin{cases} +1 & \text{if } sgn(v_i) = sgn(s_i) \neq 0 \\ 0 & \text{if } sgn(v_i) = 0 \text{ or } sgn(s_i) = 0 \\ -1 & \text{otherwise} \end{cases} \qquad (4.2)$$

$$\text{where } sgn(x) = \begin{cases} +1 & \text{if } x > 0 \\ 0 & \text{if } x = 0 . \\ -1 & \text{if } x < 0 \end{cases}$$

The probability that sample v_i is of opposite polarity to the transmitted sample $+s_i$ or $-s_i$ ($s_i \neq 0$, $v_i \neq 0$) is given by

$$p_i = Pr(D_i = -1 | m=0) = Pr(D_i = 1 | m=1) = Pr(N_i > |s_i|) . \qquad (4.3)$$

The minimum P(e) detector corresponds to the maximum a posteriori (MAP) decision rule which states that $\hat{m}=0$ is chosen if

$$\Pr\left(\{d_i\}_{i=1}^{N_s} \mid m=0\right) \Pr\left(m=0\right) > \Pr\left(\{d_i\}_{i=1}^{N_s} \mid m=1\right) \Pr\left(m=1\right) \qquad (4.4)$$

where d_i denotes a particular outcome of the random variable D_i. In the case of equally likely messages, inequality (4.4) reduces to

$$\Pr\left(\{d_i\}_{i=1}^{N_s} \mid m=0\right) > \Pr\left(\{d_i\}_{i=1}^{N_s} \mid m=1\right) . \qquad (4.5)$$

Let A_1 denote the set of all i's such that $d_i=1$ and A_{-1} denote the set of all i's such that $d_i=-1$. Then, the optimum decision rule is to choose $\hat{m}=0$ if

$$\prod_{i \epsilon A_1} (1-p_i) \prod_{i \epsilon A_{-1}} p_i > \prod_{i \epsilon A_1} p_i \prod_{i \epsilon A_{-1}} (1-p_i). \qquad (4.6)$$

From (4.6), the optimum decision rule can be stated as follows: form the statistic

$$d_{OPT,HL} \triangleq \sum_{i=1}^{N_s} d_i \ln \left(\frac{1-p_i}{p_i}\right) ; \qquad (4.7)$$

if $d_{OPT,HL} > 0$, $\hat{m}=0$ is declared; otherwise, $\hat{m}=1$ is declared.

Various weighted partial decision (WPD) detectors for hard-limited signals have been proposed [2] which have the following general form. The test statistic is $d_{WPD} \triangleq \sum_{i=1}^{N_s} d_i \omega_i$, where $\{\omega_i\}_{i=1}^{N_s}$ are weights assigned to the different samples. The WPD detector chooses $\hat{m}=0$ if $d_{WPD} > 0$ and $\hat{m}=1$ if $d_{WPD} < 0$. The weights $\omega_i=1$, $\omega_i=|s_i|$ and $\omega_i=s_i^2$ are often used. It can be seen

from equation (4.7) that the optimum weights are given by

$$\omega_i^* = \ln \left(\frac{1-P_i}{P_i} \right) .$$

(4.8)

In the next three sections, the detector $D_{OPT,HL}$ is compared to these schemes and, in the case of Gaussian noise, to the optimum detector based on the unquantized samples $\{v_i\}_{i=1}^{N_s}$.

4.3. Optimum Weights for Low Signal-to-Noise Ratios

In this section it is shown that, for most common noise models, the optimum weights as given by equation (4.8) are well approximated by $\omega_i = |s_i|$ when the signal-to-noise ratio (SNR) is low. Assume that the noise variables $\{N_i\}_{i=1}^{N_s}$ have an identical probability density function (pdf) which is even. This holds for most commonly used noise models such as the Gaussian, Laplace or Cauchy pdf's. Let the cumulative distribution function (CDF) be denoted by $F_n(\cdot)$. Suppose that $F_n(\cdot)$ can be represented by a Maclaurin series expansion, i.e.

$$F_n(\alpha) = \sum_{k=0}^{\infty} F_n^k(0) \frac{\alpha^k}{k!}$$

(4.9)

where $F_n^k(0)$ denotes the k-th derivative of $F_n(\alpha)$ evaluated at $\alpha=0$. One may combine (4.3), (4.8) and (4.9) to obtain

$$\omega_i^* = \ln \left(\frac{F_n(|s_i|/\sigma)}{1-F_n(|s_i|/\sigma)} \right)$$

(4.10a)

$$\bullet \ \ell n \left(\frac{\frac{1}{2} + \sum_{k=1}^{\infty} F_n^k(0) \frac{(|s_i|/\sigma)^k}{k!}}{\frac{1}{2} - \sum_{k=1}^{\infty} F_n^k(0) \frac{(|s_i|/\sigma)^k}{k!}} \right) \qquad (4.10b)$$

$$\bullet \ \ell n \left(1 + \frac{2 \sum_{k=1}^{\infty} F_n^k(0) \frac{(|s_i|/\sigma)^k}{k!}}{\frac{1}{2} - \sum_{k=1}^{\infty} F_n^k(0) \frac{(|s_i|/\sigma)^k}{k!}} \right) \qquad (4.10c)$$

In (4.10b) the fact that the noise pdf is an even function has been used and σ is the noise scale parameter. For low signal-to-noise ratios, i.e. $|s_i|/\sigma \ll 1$, one has

$$\omega_i^* \bullet 4F_n^1(0) \ |s_i|/\sigma, \qquad (4.11)$$

since $\ell n(1 + x) \bullet x - \frac{1}{2} x^2 + \frac{1}{3} x^3 + \ldots$, for $-1 < x < 1$. In (4.11) it has also been assumed that $F_n^1(0) \neq 0$, as is the case for a Gaussian, Laplace or Cauchy pdf. Finally, one notes that scaling of the weights by a constant does not affect the decision rule. Hence, ω_i^* may be chosen to be approximately equal to $|s_i|$.

4.4. Optimum Weights for High SNR's

In the case of high SNR's the optimum weights depend on the noise pdf. The Gaussian, Laplace and Cauchy distributions will be considered in turn.

4.4.1. Gaussian Noise Distribution

For a Gaussian noise r.v. of variance σ_n^2, it follows from equation (4.3) that $p_i = Q(\frac{|s_i|}{\sigma_n})$ where $Q(\alpha) = \frac{1}{\sqrt{2\pi}} \int_\alpha^\infty e^{-x^2/2} \, dx$. When the SNR is high, $\frac{|s_i|}{\sigma_n} \gg 1$, p_i is well approximated [31] by $\frac{1}{\sqrt{2\pi} \frac{|s_i|}{\sigma_n}} \exp(-\frac{s_i^2}{2\sigma_n^2})$. From (4.8), the optimum weights are approximated by

$$\omega_i^* \approx \frac{s_i^2}{2\sigma_n^2} . \tag{4.12}$$

Since scaling the weights by a constant does not affect the decision rule defined by (4.7), ω_i^* can be chosen to be approximately equal to s_i^2.

4.4.2. Laplace Noise Distribution

This distribution is sometimes used as a model for impulsive noise [11]. The Laplace pdf is defined by $f(\alpha) = \frac{1}{2c} e^{-|\alpha|/c}$, $-\infty < \alpha < \infty$, with variance $2c^2$. In this case, $p_i = \frac{1}{2} e^{-|s_i|/c}$. For high SNR's, from (4.9), the optimum weights can be approximated by

$$\omega_i^* \approx \frac{|s_i|}{c} . \tag{4.13}$$

Since the decision rule is unchanged by scaling $\{\omega_i^*\}_{i=1}^{N_s}$, ω_i^* can be chosen as $|s_i|$.

4.4.3. Cauchy Noise Distribution

The Cauchy distribution defined by the pdf $f(\alpha) = \dfrac{b/\pi}{b^2 + \alpha^2}$, $-\infty < \alpha < \infty$, is used to model severe impulsive noise [27]. In this case for high SNR's, the optimum weights are approximately given by $\omega_i^* = 1$ as shown in Appendix F.

4.5. Some Numerical Examples

In this section a number of examples are presented. These examples illustrate some of the issues involved in the selection of the weights and compare the detector performances for different choices. In all of the examples the signal-to-noise ratio is defined as $20 \log_{10} \left(\dfrac{A}{\sigma_n}\right)$, $20 \log_{10} \left(\dfrac{A}{c}\right)$ and $20 \log_{10} \left(\dfrac{A}{b}\right)$ for the Gaussian, Laplace and Cauchy distributions respectively, where A is the pulse amplitude.

As a first example, we consider the detection of a raised cosine pulse, sampled $N_s = 11$ times according to (4.1), in Gaussian noise. The optimum detector for the unquantized samples in Gaussian noise is the digital matched filter (DMF) for which $P(e) = Q\left(\sqrt{\sum_{i=1}^{N_s} s_i^2 / \sigma_n}\right)$. Figure 4.1 shows the probability of error obtained using the DMF and the WPD detector with weights $\ln\left(\dfrac{1-P_i}{P_i}\right)$, $|s_i|$, s_i^2 and 1. The $\ln\left(\dfrac{1-P_i}{P_i}\right)$ and s_i^2 curves, though indistinguishable, are not identical. It can be seen that the use of the s_i^2 weights instead of the optimum weights results in little loss. However, the use of
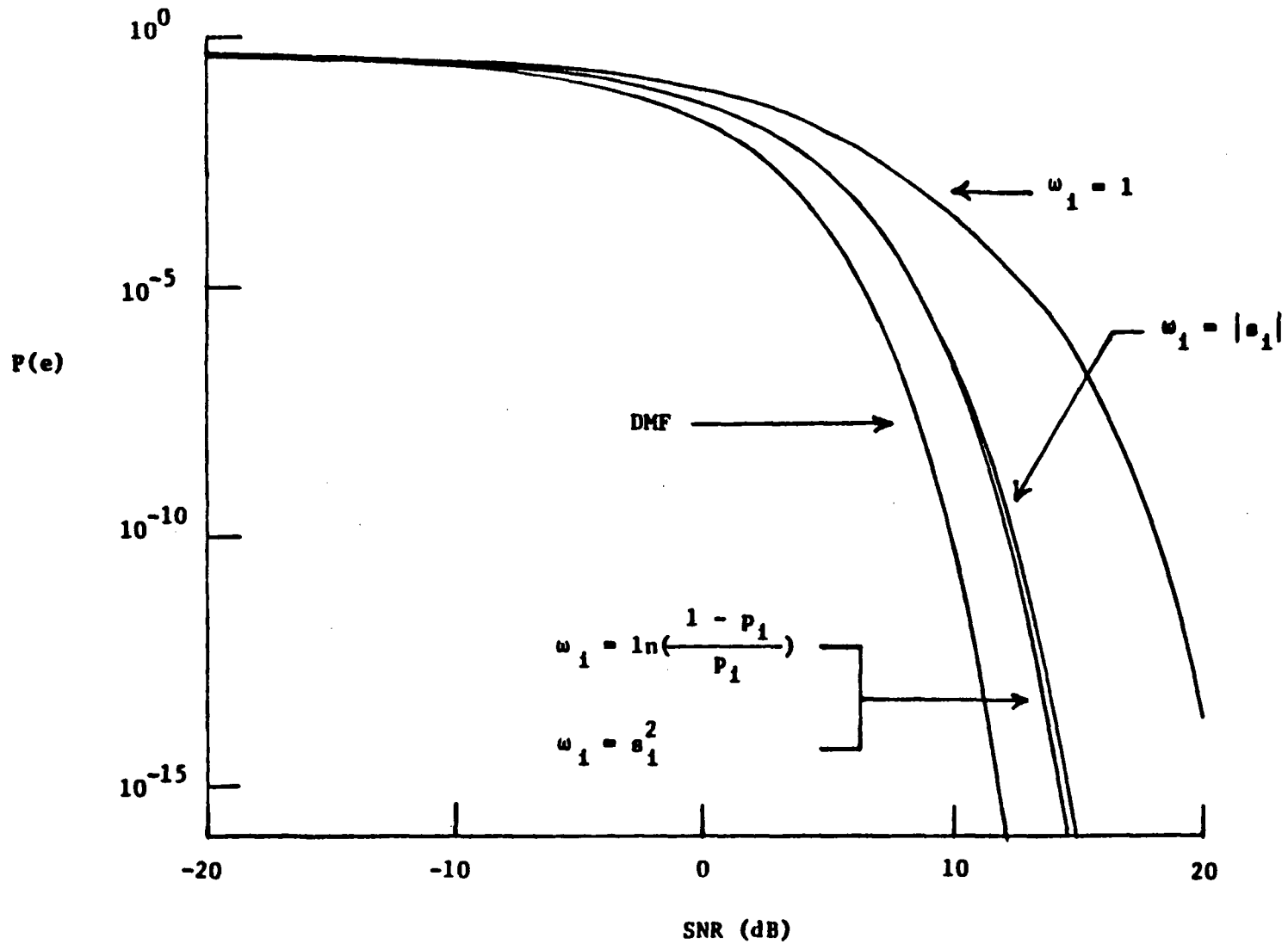
Figure 4.1. Error probabilities for the DMF detector and four different WPD detectors. A raised cosine pulse in additive white Gaussian noise is sampled 11 times.

$\omega_i = 1$ results in a substantial loss, e.g. a penalty of about 3.7 dB is incurred at $P(e) = 10^{-4}$ relative to $D_{OPT, HL}$. For the same error probability an inherent penalty of about 2 dB results from hard-limiting the samples. It is interesting to note that in certain cases, the WPD detectors with weights $\ln\left(\frac{1-P_i}{P_i}\right)$, $|s_i|$ and s_i^2 are equivalent. Examples include the case of a raised cosine in Gaussian noise sampled $N_s = 3$, 4 or 6 times.

For a second example, the detection of a half sinusoid pulse sampled $N_s = 3$ times is investigated. This example shows that caution should be exercised when dealing with ties. A tie occurs when $d_{WPD} = \sum_{i=1}^{N_s} d_i \, \omega_i = 0$. If the weights $|s_i|$ are used, a tie will occur if the first and third samples have opposite polarity to the second sample. One option in this case is to choose message $\hat{m}$ based on the outcome of a fair coin toss. This may, however, lead to poorer performance than that obtained by using the optimum MAP decision rule. This is illustrated in figure 4.2 which shows the error probability as a function of the SNR for the WPD detector with weights $\omega_i = \ln\left(\frac{1-P_i}{P_i}\right)$, $|s_i|$, and s_i^2. In this case, the $\ln\left(\frac{1-P_i}{P_i}\right)$ and s_i^2 weights are equivalent. The $|s_i|$ weights detector with random tie resolution performs poorer at high SNR's, e.g., an increase of about 1.5 dB in SNR is required to maintain a target value of $P(e) = 10^{-4}$. In this case if the decisions corresponding to ties are properly chosen, the $|s_i|$ weights detector is equivalent to $D_{OPT, HL}$.

Also shown in figure 4.2 are the error performances of the DMF detector
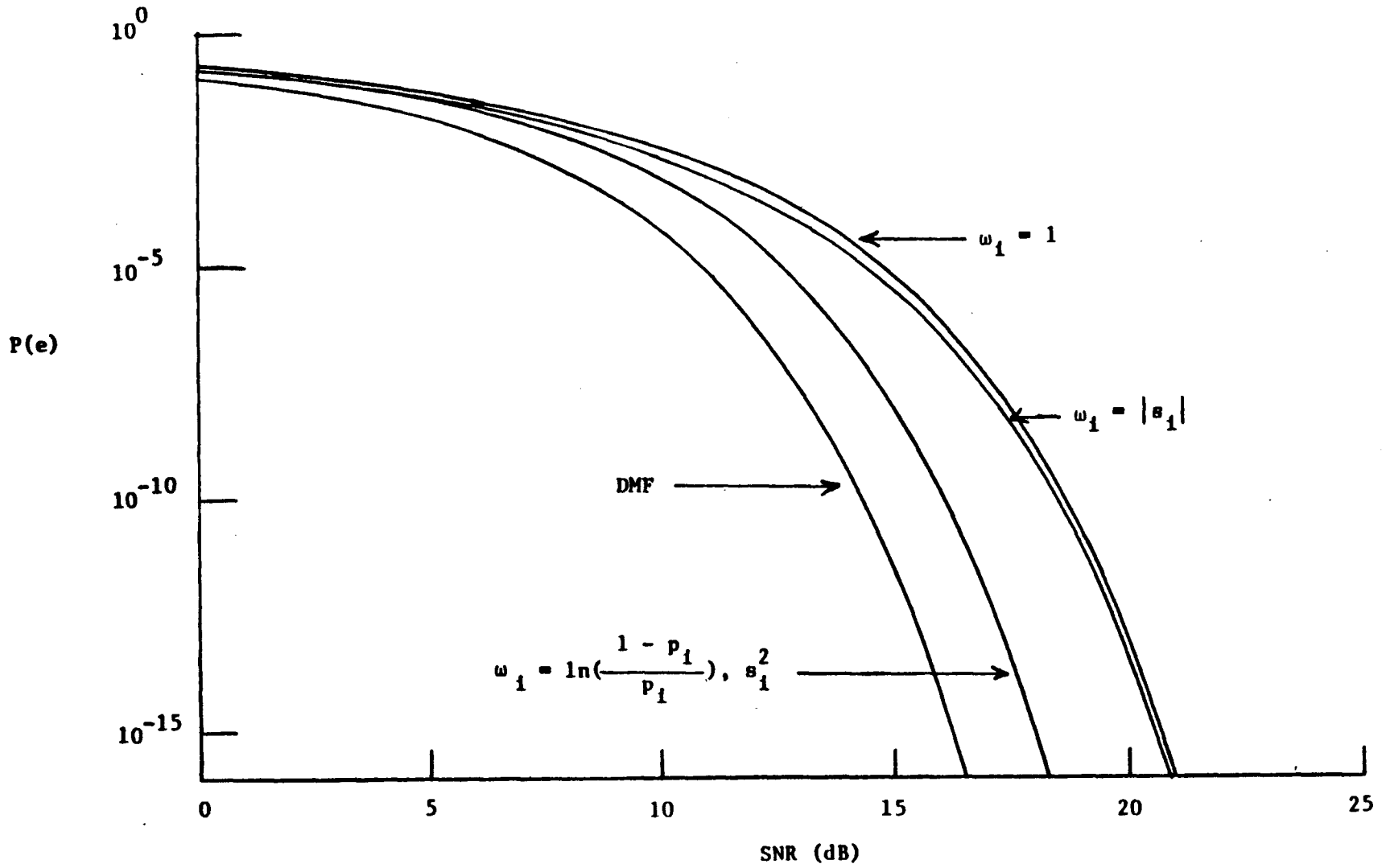
Figure 4.2. Error probabilities for the DMF detector and four different WPD detectors. A half sinusoid in additive white Gaussian noise is sampled 3 times.

and the WPD detector with $\omega_i=1$. It is seen that the WPD detector with optimum weights (or s_i^2 weights) performs poorer than the DMF detector by about 1.8 dB (actually a factor of 1.5). It performs, nonetheless, appreciably better than the equal weights detector; e.g., to achieve $P(e)=10^{-4}$, an additional 2.0 dB is required.

An example involving the detection of a raised cosine pulse sampled $N_s=7$ times in Laplace noise is now considered. As discussed in sections 4.3 and 4.4, the weights $|s_i|$ are nearly optimum for very low and very high SNR environments. This can be observed in figure 4.3. The only noticeable difference between the $\ln\left(\frac{1-p_i}{p_i}\right)$ and $|s_i|$ curves occur for SNR's between -3 dB and 21 dB. The weights $\omega_i=1$ detector is significantly poorer, the difference being about 4 dB at $P(e)=10^{-5}$. The $\omega_i = s_i^2$ detector performs almost as well as the optimum weights detector. The difference is less than 0.6 dB for $P(e) < \sim 10^{-6}$.

The last example of this section involves the detection of a raised cosine pulse sampled $N_s=3$ times in Cauchy noise. The error probabilities for $\omega_i = \ln\left(\frac{1-p_i}{p_i}\right)$, $|s_i|$ and 1 are plotted in figure 4.4. The weights $|s_i|$ detector outperforms the equal weights detector when the SNR is less than 15.1 dB. For higher SNR values, the unity weights detector has a significantly better performance. In Appendix G it is shown that in this example with $N_s = 3$ samples the $P(e)$ of the optimum weights detector is equal to the smaller of the $P(e)$'s for the weights $|s_i|$ and 1 detectors. For this example, it can easily be seen that the weights $|s_i|$ and s_i^2 detectors are equivalent.
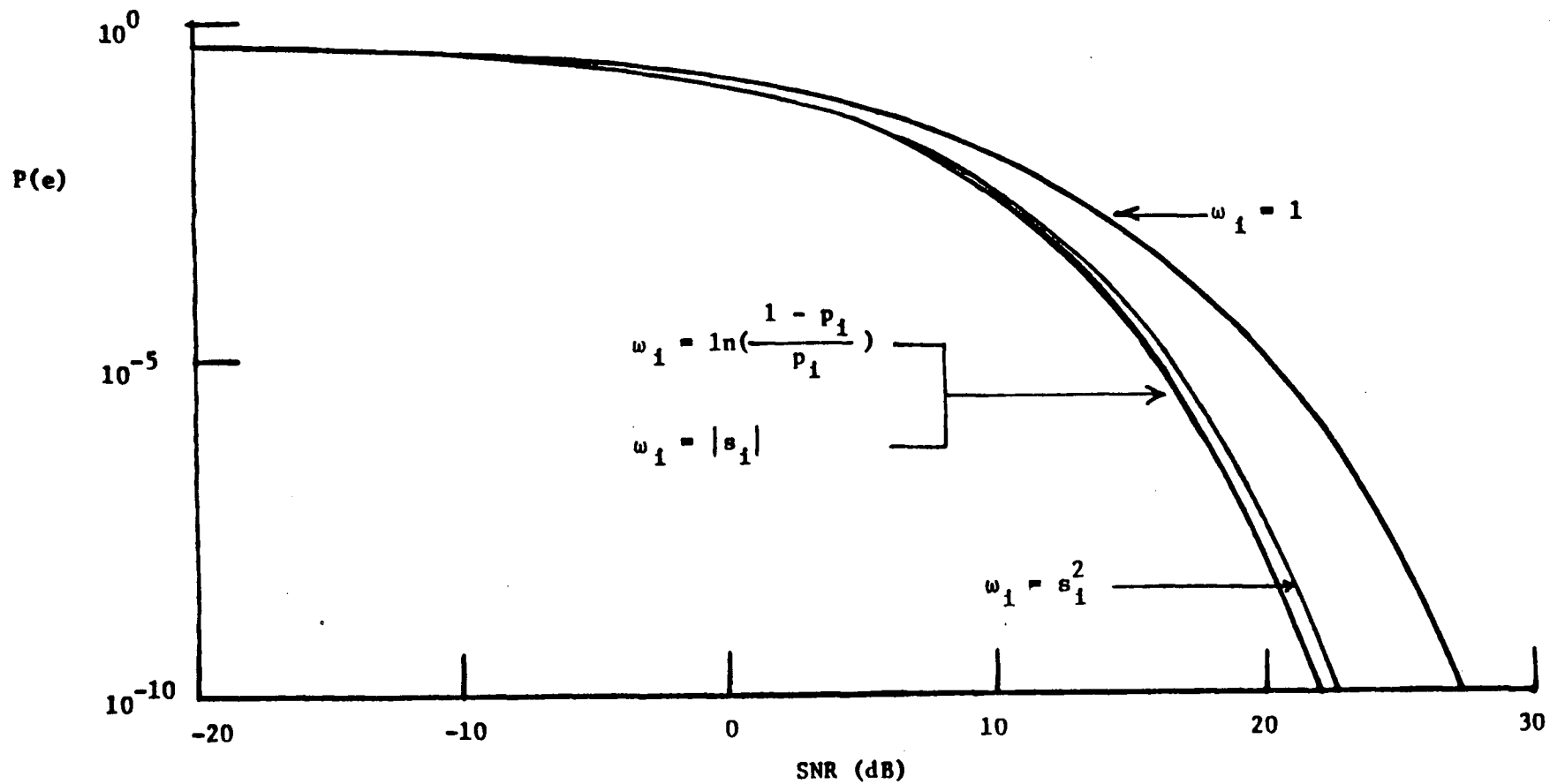
Figure 4.3. Error probabilities for the detection of a raised cosine pulse in Laplace noise sampled 7 times. Three different WPD detectors are illustrated.
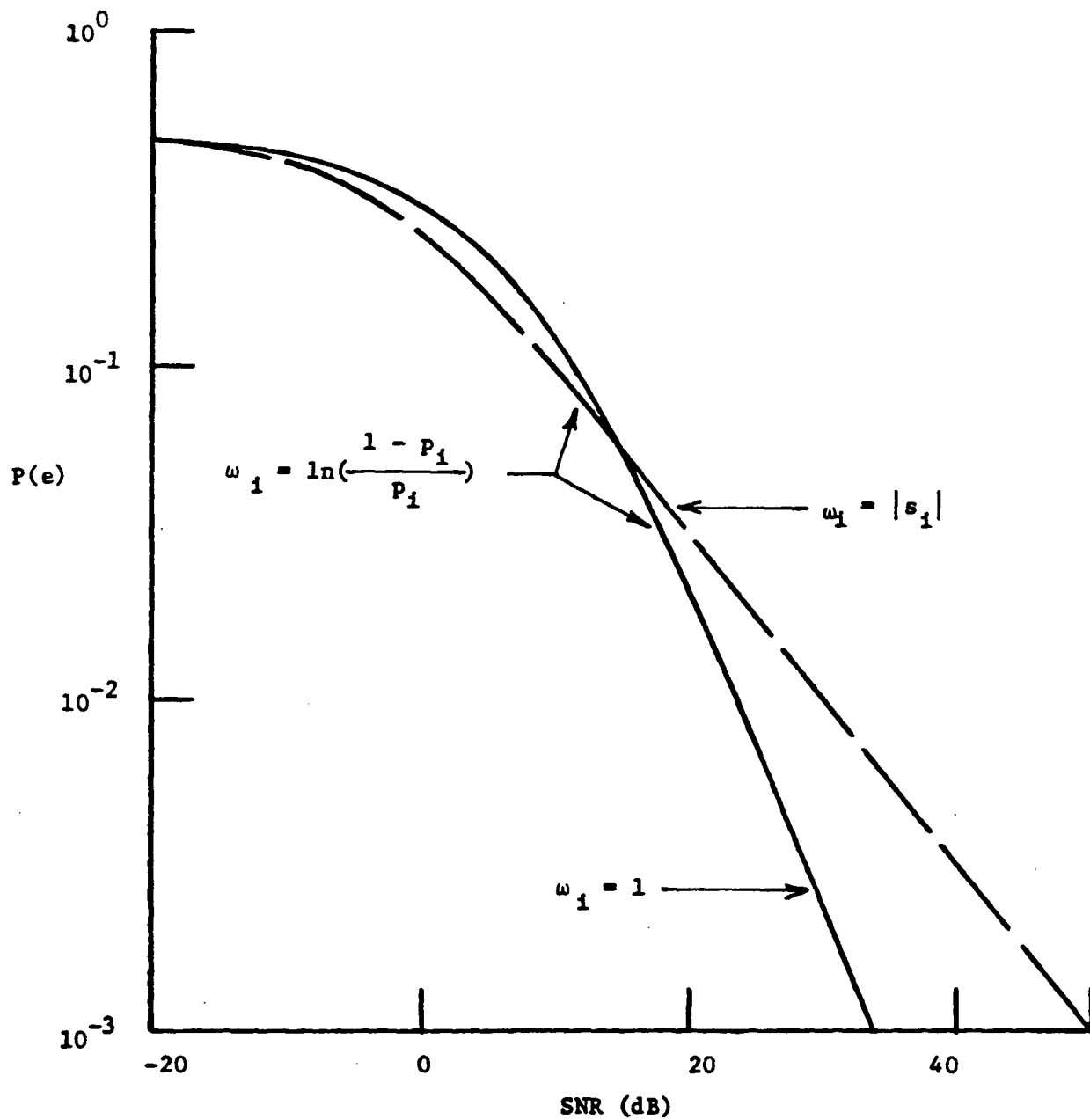
Figure 4.4. Error probabilities for the detection of a raised cosine pulse in Cauchy noise sampled 3 times. Three different WPD detectors are illustrated.

However, there are signalling waveforms for which the weights $|s_i|$ detector performs much better than the weights s_i^2 detector.

4.6. Generalization to M-ary Signalling and Multilevel Quantization

In this section, the WPD detectors for M-ary signalling with each received sample quantized to an arbitrary number of levels are examined. These detectors can be viewed as generalizations of the binary signalling detectors of section 4.2. Thus, consider that the message m can now take on one of M values, $m \in \{1,\ldots,M\}$. Corresponding to $m = j$, the signal $s_j(t)$ is sent and the N_s received samples are $v_i = s_{j,i} + n_i$, $i = 1,2,\ldots N_s$, $j \in \{1,2,\ldots M\}$ where $s_{j,i} = s_j(\frac{(i-0.5)T}{N_s})$ and $\{n_i\}_{i=1}^{N_s}$ are independent noise samples.

Let $\underline{v} = (v_1, v_2, \ldots v_{N_s})$ denote the vector of received samples. In the case of M equally likely messages, the minimum P(e) detector corresponds to the maximum likelihood decision rule, i.e., choose $\hat{m} = j$ if

$$P_r(\underline{v}|m=j) > Pr(\underline{v}|m=k) \quad \text{for all } k \neq j . \quad (4.14)$$

Let each received sample v_i, $i=1,2,\ldots,N_s$ be quantized to one of q regions $\{R_{i,\ell}\}_{\ell=1}^q$ and define the function $d_i = \ell$ if $v_i \in R_{i,\ell}$. On the basis of $\underline{d} = (d_1, d_2, \ldots, d_{N_s})$, the WPD detector decides on the transmitted message m.

The minimum P(e) detector will decide $\hat{m} = j$ if

$$Pr(\underline{d}|m=j) > Pr(\underline{d}|m=k) \quad \text{for all } k \neq j . \quad (4.15)$$

Since the samples are independent, inequality (4.15) becomes

$$\prod_{i=1}^{N_s} \Pr\left(d_i \mid m=j\right) > \prod_{i=1}^{N_s} \Pr\left(d_i \mid m=k\right) , \quad \text{all } k \ne j \; . \tag{4.16}$$

Let A_ℓ denote the set of all i's such that $d_i=\ell$. Then (4.16) can be rewritten as

$$\prod_{i \in A_1} \Pr\left(d_i=1 \mid m=j\right) \prod_{i \in A_2} \Pr\left(d_i=2 \mid m=j\right)\cdots \prod_{i \in A_q} \Pr\left(d_i=q \mid m=j\right) >$$

$$\prod_{i \in A_1} \Pr\left(d_i=1 \mid m=k\right) \prod_{i \in A_2} \Pr\left(d_i=2 \mid m=k\right)\cdots \prod_{i \in A_q} \Pr\left(d_i=q \mid m=k\right) \quad \text{all } k \ne j \; . \tag{4.17}$$

Defining

$$P_{i,\ell \mid n} = \Pr\left(d_i=\ell \mid m=n\right), \quad i = 1,2,\ldots N_s, \quad \ell = 1,2,\ldots,q, \quad n = 1,2,\ldots M$$

and taking logarithms, (4.17) becomes

$$\sum_{i \in A_1} \ell n\, P_{i,1 \mid j} + \sum_{i \in A_2} \ell n\, P_{i,2 \mid j} + \cdots + \sum_{i \in A_q} \ell n\, P_{i,q \mid j} >$$

$$\sum_{i \in A_1} \ell n\, P_{i,1 \mid k} + \sum_{i \in A_2} \ell n\, P_{i,2 \mid k} + \cdots + \sum_{i \in A_q} \ell n\, P_{i,q \mid k}, \quad \text{all } k \ne j \; . \tag{4.18}$$

From (4.18) it is seen that one way of implementing the optimum WPD detector

is as follows: Associate with each message an accumulator C_n, $n=1,2,\ldots,M$.

Step 1. Initialize all M accumulators to zero.

Step 2. For each i, $i=1,2,\ldots,N_s$ increment C_n by $\ell n\, P_{i,\ell \mid n}$ if and only if

$v_i \in R_{i,\ell}$.

Step 3. Determine the accumulator C_j with the largest value, i.e.,

$C_j = \max_n \{C_n\}$; declare $\hat{m}=j$.

It can be verified that the above procedure when M=q=2 and $s_{1,i}=-s_{2,i}$

reduces to that of section 4.2. We conclude this section by looking at an example. Figure 4.5 shows the error probabilities for 2, 4 and 8 level pulse amplitude modulation (PAM) for the DMF and the WPD detectors with optimum and unity weights. In this example q=M and the term "unity weights" refers to incrementing accumulator C_n by 1 if and only if $v_i \in R_{i,n}$. In this example, the signalling waveforms are raised cosines and the noise is Gaussian. The M amplitude values are $\pm B$, $\pm 3B, \ldots, \pm(M-1)B$ where B is the amplitude of the smallest energy pulse. The M-1 decision thresholds for any sampling instant are located at the midpoints of the intervals between adjacent signals. In all cases the receiver processes 5 samples. The SNR is defined as the average value of $20 \log_{10}(A/\sigma_n)$ where A is the amplitude of the pulse and the M messages are assumed equiprobable. The optimum detector for the N_s unquantized samples makes its decision according to (4.14). Furthermore, $\Pr(\underline{v}|m=j) = P_{\underline{N}}(\underline{v}-\underline{s}_j)$ where $\underline{s}_j$ denotes the vector of signal samples $\{s_{j,i}\}$ and $P_{\underline{N}}(\cdot)$ denotes the N-fold Gaussian density of the noise samples. Equivalently, the optimum decision is to pick the signal j that lies closest in terms of Euclidean distance to the received vector. By making use of the fact that the signal vectors are collinear the probability of error for the DMF in this case can be shown to be

$$P_{OPT}(e) = 2(1 - \frac{1}{M})Q(\sqrt{\sum_{i=1}^{N_s} s_{u,i}^2 / \sigma_n}) \qquad (4.19)$$

where $\underline{s}_u$ denotes the signal with amplitude B.

One sees in figure 4.5 that the WPD detector with optimum weights suffers some loss relative to the optimum detection of the unquantized

The graph shows curves with labels:

$M = 2$

$\omega_i = 1$

$\omega_i = \ln(\dfrac{1 - p_i}{p_i})$

DMF

Axes: $P(e)$ (vertical, from 10^0 to 10^{-10}, with 10^{-5} marked), SNR (dB) (horizontal, from 0 to 30).
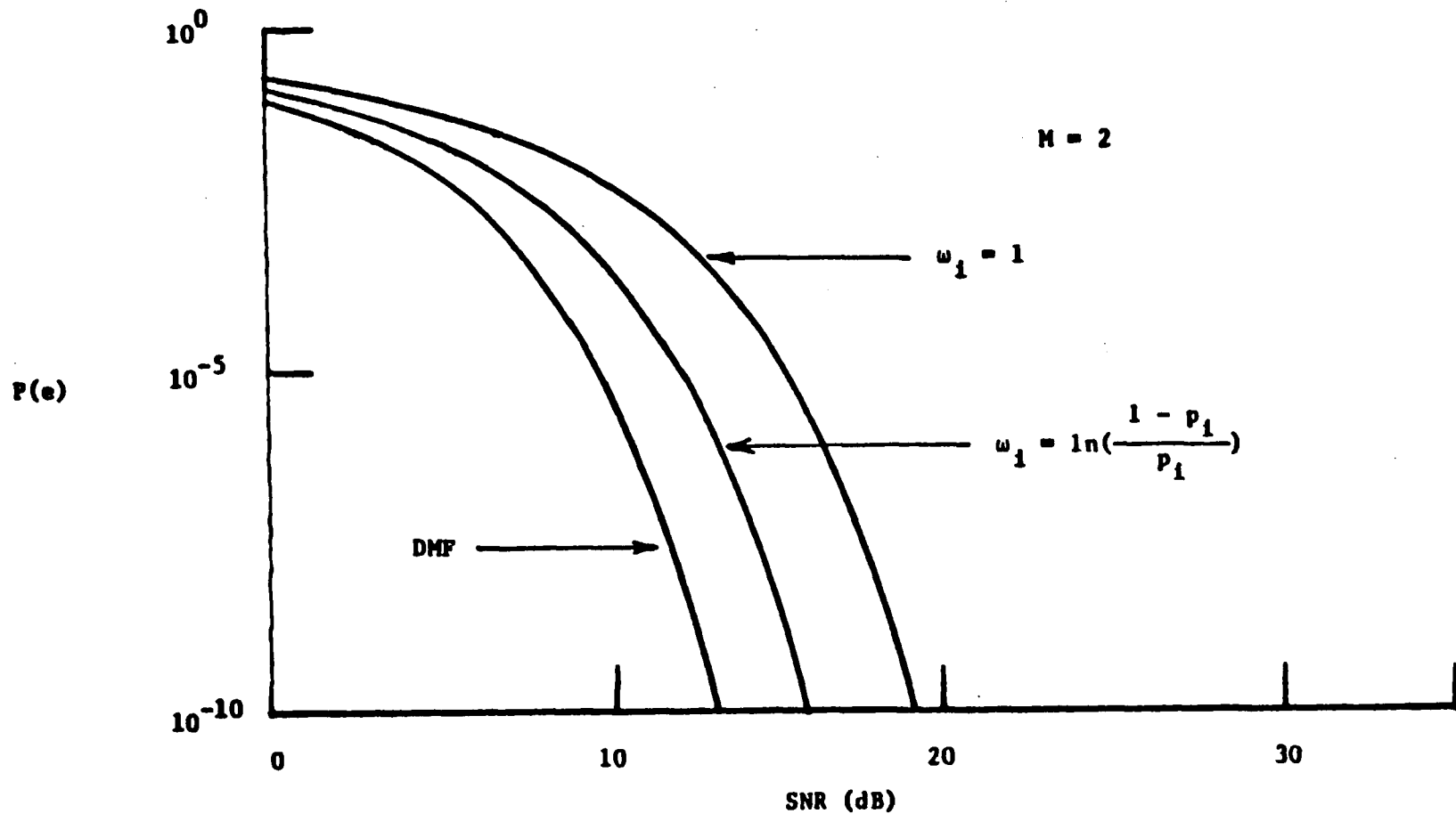
(a)

Figure 4.5. PAM error probabilities for the DMF and the WPD detectors with optimum and unity weights. The received signals are raised cosines in Gaussian noise sampled 5 times. The number of signalling levels is 2, 4 and 8 for figures (a), (b) and (c) respectively.
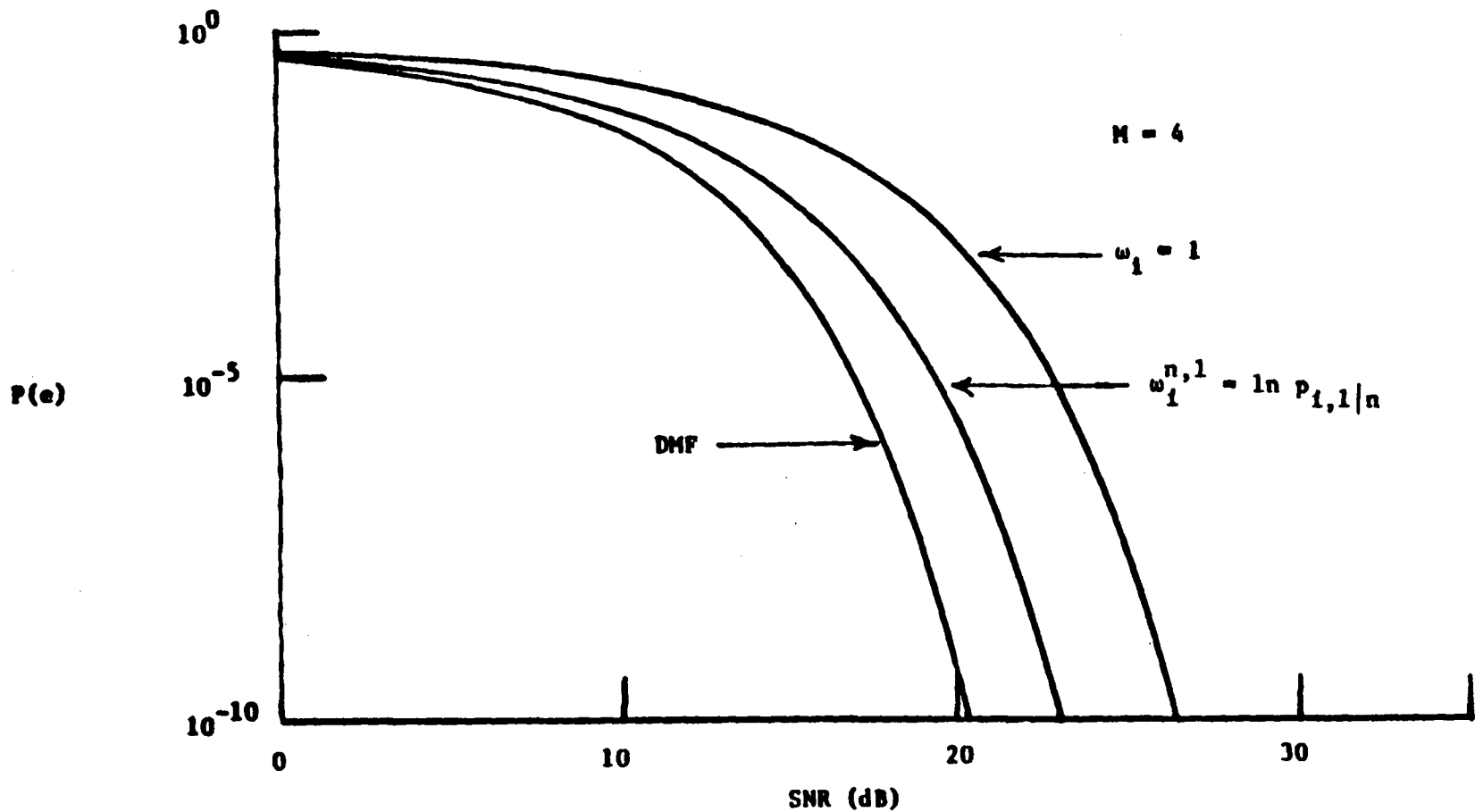
(b)

Figure 4.5. PAM error probabilities for the DMF and the WPD detectors with optimum and unity weights. The received signals are raised cosines in Gaussian noise sampled 5 times. The number of signalling levels is 2, 4 and 8 for figures (a), (b) and (c) respectively.
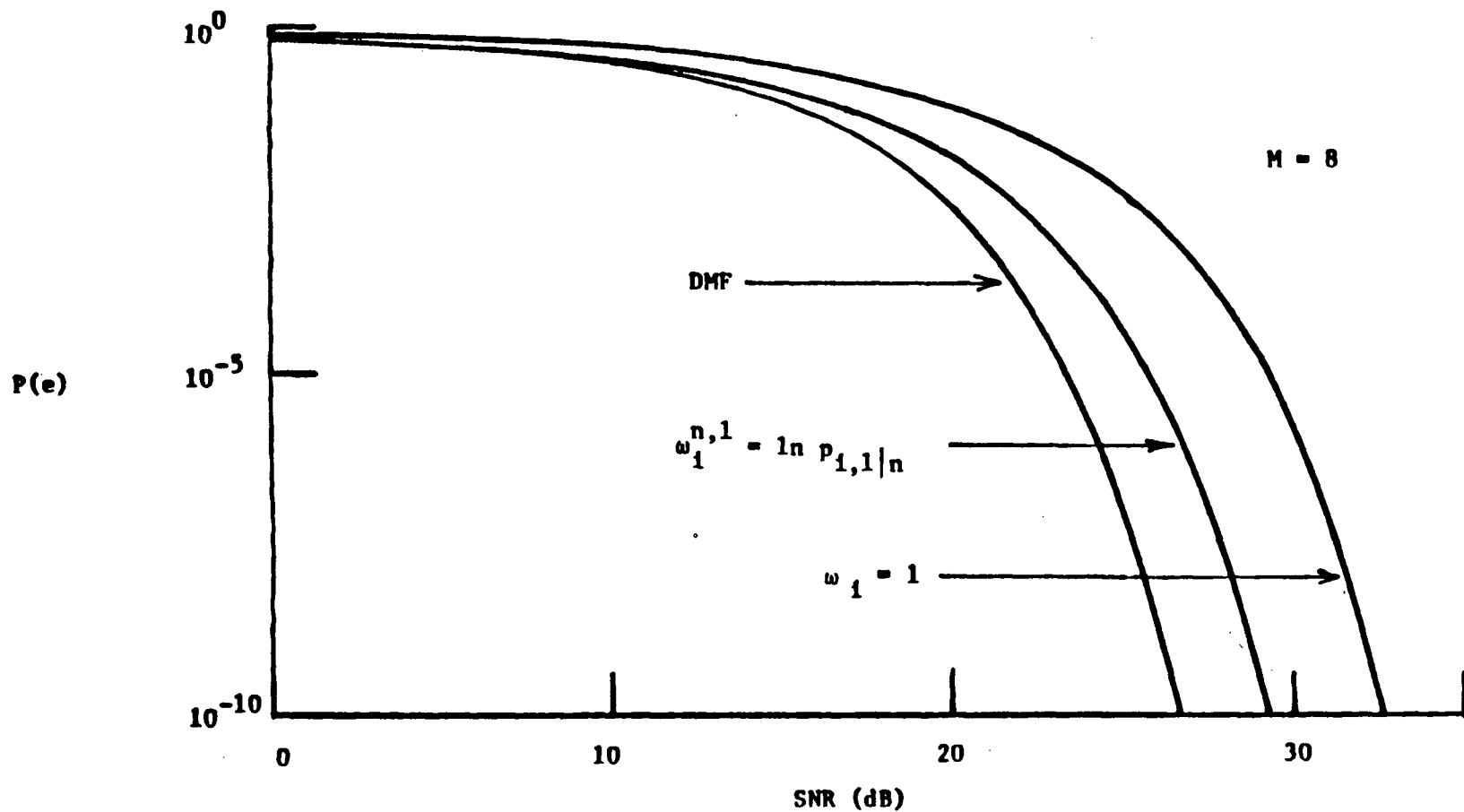
Figure 4.5. PAM error probabilities for the DMF and the WPD detectors with optimum and unity weights. The received signals are raised cosines in Gaussian noise sampled 5 times. The number of signalling levels is 2, 4 and 8 for figures (a), (b) and (c) respectively.

samples. For $P(e)=10^{-4}$ there is a penalty of about 2.2 dB for all 3 cases. The performance is, however, significantly better than when equal weights are used. The differences are about 3.2, 3.4 and 3.5 dB for signalling with 2, 4 and 8 levels, respectively, for the same $P(e)=10^{-4}$ value.

4.7. Conclusions

The problem of detecting binary antipodal data signals based on a number of hard-limited samples has been analyzed and the optimum detector has been derived for an arbitrary noise environment. The optimal processing is characterized by a set of weights. In general, the values of the weights depend on the signal-to-noise ratio as well as on the shape of the signals and the probability distribution of the channel noise. The optimal weights are approximately $|s_i|$ for low SNR's for most noise environments. For high SNR's the weights s_i^2, $|s_i|$ and 1 are nearly optimum for Gaussian, Laplace and Cauchy noise respectively.

In some instances, a set of weights which is independent of the signal-to-noise ratio performs almost as well as the optimum weights for practical ranges of SNR. It is interesting to note that in these cases, nearly optimum processing of the hard-limited samples can be performed using only threshold decisions and additions.

The optimum detector for M-ary data signals based on samples quantized to an arbitrary number of levels has also been derived. The processing requires forming sums of optimized weights, analogous to the binary antipodal case.

V PENALTIES OF WEIGHTED PARTIAL DECISION DETECTORS IN GAUSSIAN NOISE

5.1. Introduction

The performance of the WPD detector with weights $\omega_i = |s_i|$ has been analyzed for low SNR conditions in chapters 2 and 3. The optimum WPD detector for arbitrary SNR was derived in chapter 4. In this chapter, the penalties of WPD detectors are analyzed for arbitrary signal-to-noise ratios. The weights $\omega_i = |s_i|$ and $\omega_i = s_i^2$ detectors as well as the optimum weights detector are considered. The effects on the penalties of the signalling waveform employed, the number of samples processed, and the SNR are considered in detail.

The optimum WPD detector is the optimum detector for hard-limited samples and the digital matched filter is the optimum detector for the continuous amplitude samples. Hence, the penalty of the optimum WPD detector relative to the DMF detector represents the fundamental loss in signal detectability due to hard-limiting in a sampled system.

5.2. Problem Statement

We consider the model of a data communication system shown in figure 5.1. Depending on the message $m\epsilon\{0,1\}$ to be transmitted, a signal $+A\,s(t)$ or $-A\,s(t)$ is sent over the additive white Gaussian noise (AWGN) channel. The positive constant A is a scaling factor. The received signal $r(t)$ is filtered to remove out of band noise and the resulting signal $v(t)$ is sampled at some appropriate rate.
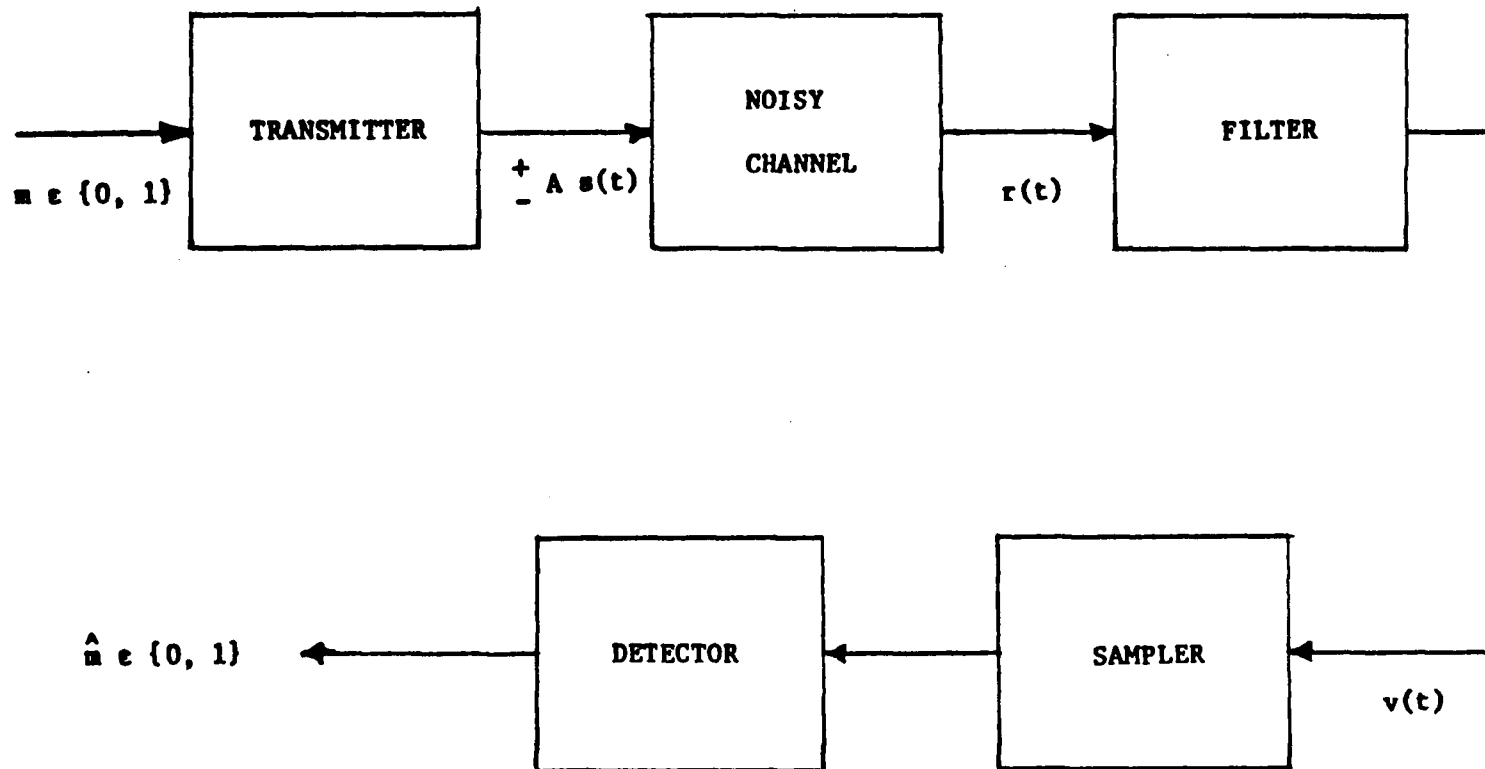
Figure 5.1. Block diagram of the data communication system.

Assume that the signal $s(t)$ is time limited to the interval $[0,T]$. If $A\ s(t)$ is sent (corresponding to $m=0$), then

$$v_i = +A\ s_i + n_i \ , \quad i=1,2,\ldots,M \tag{5.1}$$

where $\{v_i\}_{i=1}^{M}$ denote the M samples of $v(t)$, i.e. $v_i = v\left(\frac{[i-0.5]T}{M}\right)$, to be processed. The values $\{s_i\}_{i=1}^{M}$ denote the samples of $+\ s(t)$ and $\{n_i\}_{i=1}^{M}$ represent outcomes of independent Gaussian noise random variables, each with variance σ^2. If $m=1$, then $-A\ s(t)$ is sent and $v_i = -A\ s_i + n_i$, $i = 1,2,\ldots,M$. The detector bases its decision on $\{v_i\}_{i=1}^{M}$.

It is well known [1] that the optimum detector for minimizing the probability of error $P(e) \triangleq \Pr\{\hat{m} \neq m\}$ in the problem described above is the digital matched filter (DMF). The DMF computes

$$D_{OPT} \triangleq \sum_{i=1}^{M} v_i\ s_i \tag{5.2}$$

and chooses $\hat{m}=0$ if $D_{OPT} > 0$; otherwise it declares $\hat{m}=1$. The resulting probability of error is

$$P_{DMF}(e) = Q\left(\frac{A\sqrt{\sum_{i=1}^{M} s_i^2}}{\sigma}\right) \tag{5.3}$$

where $Q(\alpha) \overset{\Delta}{=} \frac{1}{\sqrt{2\pi}} \int_{\alpha}^{\infty} e^{-x^2/2} \, dx$. It is convenient to assume that $s(t)$ is

normalized so that its maximum value is equal to 1. We define the

signal-to-noise ratio (SNR) to be $20 \log_{10} \frac{A}{\sigma}$ measured in dB.

In this chapter, the penalties of the weighted partial decision detect-

ors are measured relative to the DMF detector. The penalty is defined as the

increase in signal-to-noise ratio required by a suboptimum detector in order

to achieve the same target value of probability of error as the DMF detector.

5.3. Weighted Partial Decision (WPD) Detectors

In the family of WPD detectors, the received signal samples are first

hard-limited. The decision as to which message $\hat{m}, \hat{m} \epsilon \{0,1\}$ was sent is based

on the hard-limited samples. Let the random variables representing these

samples be denoted by

$$D_i = \begin{cases} +1 \,, & \text{if} \quad \text{sgn} (v_i) = \text{sgn} (s_i) \neq 0 \\ 0 \,, & \text{if} \quad \text{sgn} (v_i) = 0 \text{ or } \text{sgn} (s_i) = 0 \\ -1 \,, & \text{otherwise} \,. \end{cases} \tag{5.4}$$

Then the general WPD detector forms the test statistic

$$D_{WPD} \overset{\Delta}{=} \sum_{i=1}^{M} D_i \, \omega_i \,, \tag{5.5}$$

where $\{\omega_i\}_{i=1}^{M}$ are the weights assigned to the different samples. The WPD

detector chooses $\hat{m}=0$ if $D_{WPD} > 0$ and $\hat{m}=1$ if $D_{WPD} < 0$. Some caution should be

exercised in choosing $\hat{m}$ if $D_{WPD} = 0$ as shown in section 4.5. The optimum (minimum P(e)) weights to be used in (5.5) are given by (4.8)

$$\omega_i^* = \ln\left(\frac{1 - p_i}{p_i}\right) , \qquad (5.6)$$

where p_i is the probability that the i-th sample has its polarity reversed, i.e. $p_i = Q(A|s_i|/\sigma)$. The weights $\omega_i = 1$, $\omega_i = |s_i|$ and $\omega_i = s_i^2$ have also been previously suggested.

Let B denote a subset of $U = \{1,2,...,M\}$ and B^c its complement. Then the probability of error for a WPD detector can be written as

$$P_{WPD}(e) = \sum_{\text{all } B} I(B) \prod_{i \varepsilon B} p_i \prod_{i \varepsilon B^c} (1-p_i) \qquad (5.7)$$

where

$$I(B) = \begin{cases} 1 , & \text{if } \sum_{i \varepsilon B} \omega_i > \sum_{i \varepsilon B^c} \omega_i \\ \frac{1}{2} , & \text{if } \sum_{i \varepsilon B} \omega_i = \sum_{i \varepsilon B^c} \omega_i \\ 0 , & \text{if } \sum_{i \varepsilon B} \omega_i < \sum_{i \varepsilon B^c} \omega_i . \end{cases}$$

In (5.7), it is assumed that if $D_{WPD} = 0$, $\hat{m}$ is chosen according to the outcome of a fair coin toss. The probability of error $P_{WPD}(e)$ can be directly computed from equation (5.7). This, however, may involve considerable computational effort. In some cases, more computationally efficient methods

can be used to compute $P_{WPD}(e)$ as described in Appendix C. An expression for the penalty at high SNR values is derived in Appendix H, namely

$$\Gamma_{WPD}(\underline{s},M,\infty) = \frac{\sum\limits_{i=1}^{M} s_i^2}{\sum\limits_{i\in B^*} s_i^2} \qquad (5.8)$$

where $B^* \subseteq U$ and B^* has the properties that $I(B^*) > 0$ and $\sum\limits_{i\in B^*} s_i^2 < \sum\limits_{i\in B} s_i^2$ for all $B \subseteq U$ for which $I(B) > 0$. The penalty for low SNR values is given by

$$\Gamma_{WPD}(\underline{s},M,0) = \frac{2^{2M-2}\sum\limits_{i=1}^{M} s_i^2}{\left[\sum\limits_{all\ B} I(B)\left\{\sum\limits_{i\in B}|s_i| - \sum\limits_{i\in B^c}|s_i|\right\}\right]^2}. \qquad (5.9)$$

This result may be derived by applying the procedure of Appendix K to $P_{WPD}(e)$ as given in (5.7).

5.4. The WPD Detector for a Piecewise Constant Amplitude Signalling Waveform

For a piecewise constant amplitude signalling waveform, the weights $\omega_i = 1$, $\omega_i = |s_i|$, $\omega_i = s_i^2$ and $\omega_i = \omega_i^*$ WPD detectors are equivalent. With $|s_i| = 1$, the penalty relative to the DMF detector is defined implicitly by

$$Q\left(\sqrt{M}\frac{A}{\sigma}\right) = \begin{cases} \sum\limits_{i=\frac{M+1}{2}}^{M} \binom{M}{i} p^i (1-p)^{M-i} & ,\ M\ odd \\[4mm] \sum\limits_{i=\frac{M+2}{2}}^{M} \binom{M}{i} p^i (1-p)^{M-i} + \frac{1}{2}\binom{M}{\frac{M}{2}}\left[p(1-p)\right]^{\frac{M}{2}} & ,\ M\ even \end{cases} \qquad (5.10)$$

where $p = Q(\sqrt{\Gamma_{WPD}(\underline{1},M,\frac{A}{\sigma})}\,\frac{A}{\sigma})$ and the notation $\Gamma_{WPD}(\underline{s},M,\frac{A}{\sigma})$ is used to explicitly indicate the dependence of the penalty Γ_{WPD} on $\underline{s} \triangleq (s_1,s_2,\ldots,s_M)$, M and $\frac{A}{\sigma}$. Equation (5.10) can be used to compute $\Gamma_{WPD}(\underline{1},M,\frac{A}{\sigma})$ as follows. Defining $y \triangleq \sqrt{\Gamma_{WPD}(\underline{1},M,\frac{A}{\sigma})}\,\frac{A}{\sigma}$, one can rewrite (5.10) as

$$Q\left(\sqrt{M}\frac{y}{\sqrt{\Gamma_{WPD}(\underline{1},M,\frac{A}{\sigma})}}\right) = T(M,y) \tag{5.11}$$

where

$$T(M,y) = \begin{cases} \sum\limits_{i=\frac{M+1}{2}}^{M} \binom{M}{i} p^i (1-p)^{M-i} & , M \text{ odd} \\[3ex] \sum\limits_{i=\frac{M+2}{2}}^{M} \binom{M}{i} p^i (1-p)^{M-i} + \frac{1}{2}\binom{M}{\frac{M}{2}} [p(1-p)]^{M/2} & , M \text{ even} \end{cases}$$

and $p = Q(y)$. From (5.11), one has

$$\Gamma_{WPD}(\underline{1},M,\frac{A}{\sigma}) = \frac{M\,y^2}{[Q^{-1}\{T(M,y)\}]^2} . \tag{5.12}$$

Figure 5.2 shows a plot of $\Gamma_{WPD}(\underline{1},M,\frac{A}{\sigma})$ against $\frac{A}{\sigma}$ for M=1, 2, 3, 4, 10 and 11 obtained by plotting $\dfrac{M\,y^2}{[Q^{-1}\{T(M,y)\}]^2}$ as a function of $y + \dfrac{\sqrt{M}\,y}{Q^{-1}\{T(M,y)\}}$. It can be observed that the penalty is a non-decreasing function of $\frac{A}{\sigma}$ and is upperbounded by 2 (3.01 dB). Explicit expressions for the penalty for small and large SNR values are now examined. In Appendix I, it is shown that
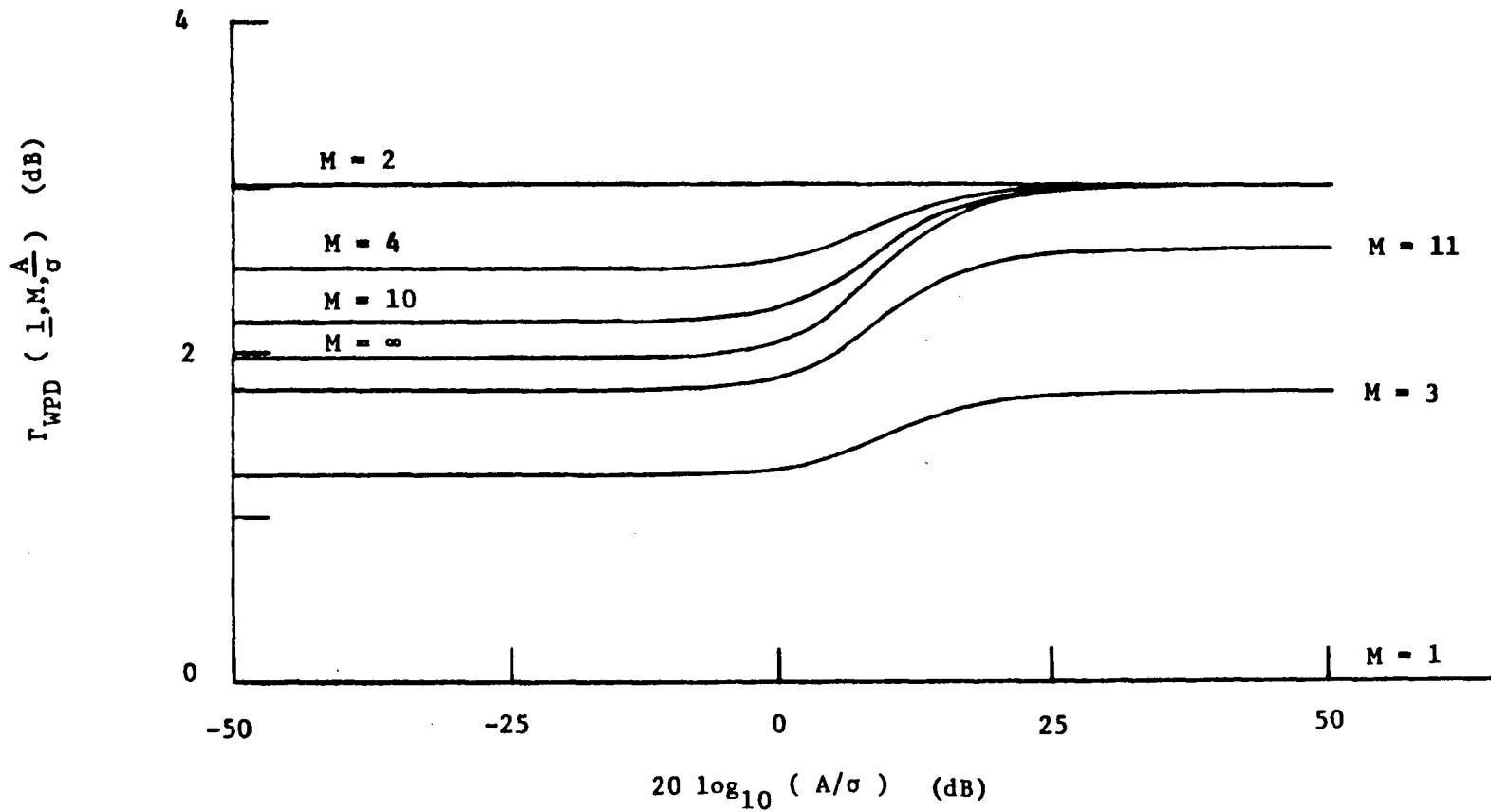
Figure 5.2. The penalty Γ_{WPD} ($\underline{1}$,M,$\frac{A}{\sigma}$) as a function of the signal-to-noise ratio for seven values of sample size M.

$$\Gamma_{WPD}(\underline{1},M,0) = \begin{cases} \dfrac{2^{2M-2}}{M \left(\dfrac{M-1}{\dfrac{M-1}{2}} \right)^2} & , \text{ M odd} \\[3em] \dfrac{2^{2M}}{M \left(\dfrac{M}{\dfrac{M}{2}} \right)^2} & , \text{ M even} . \end{cases} \tag{5.13}$$

Using Stirling's formula it follows that $\lim\limits_{M\to\infty} \Gamma_{WPD}(\underline{1},M,0) = \dfrac{\pi}{2}$. Equation

(5.13) also shows that

$$\Gamma_{WPD}(\underline{1},1,0) < \Gamma_{WPD}(\underline{1},3,0) < \cdots < \Gamma_{WPD}(\underline{1},4,0) < \Gamma_{WPD}(\underline{1},2,0) . \tag{5.14}$$

By using the approximation $Q(\alpha) \approx \dfrac{e^{-\alpha^2/2}}{\sqrt{2\pi}\,\alpha}$, $\alpha \gg 1$, in (5.10) it can be

shown that

$$\Gamma_{WPD}(\underline{1},M,\infty) = \begin{cases} 2 & , \text{ M even} \\[1em] 2 - \dfrac{2}{M+1} & , \text{ M odd} . \end{cases} \tag{5.15}$$

It is also possible to determine the penalty $\Gamma_{WPD}(\underline{1},M,\frac{A}{\sigma})$ for large values

of M. The basic approach is to derive an upper bound $\Gamma_{WPD}^{UB}(\underline{1},\infty,\frac{A}{\sigma})$ using the

Chernoff bound [28,29] and to show then that $\Gamma_{WPD}^{UB}(\underline{1},\infty,\frac{A}{\sigma})$ is also a lower

bound on $\Gamma_{WPD}(\underline{1},\infty,\frac{A}{\sigma})$. The details appear in Appendix J. The curve

$\Gamma_{WPD}(\underline{1}, \infty, \frac{A}{\sigma})$ is plotted in figure 5.2.

5.5. The Optimum WPD Detector for Arbitrary Signalling Waveforms

In the case of an arbitrary signalling waveform, the penalty $\Gamma^*_{WPD}(\underline{s}, M, \frac{A}{\sigma})$ for the optimum WPD detector can be evaluated numerically by

equating $Q\left(\sqrt{\sum_{i=1}^{M} s_i^2} \frac{A}{\sigma}\right)$ to the right side of (5.7) with

$P_i = Q\left(\sqrt{\Gamma^*_{WPD}(\underline{s}, M, \frac{A}{\sigma})} \frac{A}{\sigma} |s_i|\right)$ and $\omega_i = \ln\left(\frac{1-P_i}{P_i}\right)$. The procedure is

analogous to that followed in (5.10) to (5.12). The results for a raised

cosine and a half sinusoid signalling waveform are plotted in figures 5.3 and

5.4 respectively. In both figures, for a fixed value of M, the penalty

increases with $\frac{A}{\sigma}$ even though it is essentially constant for small and large

values of $\frac{A}{\sigma}$.

It is shown in Appendix J that, for large values of M, the penalty is

upper bounded by

$$\Gamma^{UB}_{WPD}(\underline{s}, \infty, \frac{A}{\sigma}) = \frac{-y^2 < s^2(t) >}{< \ln\{4Q(y|s(t)|)[1-Q(y|s(t)|)]\} >} \tag{5.16}$$

where $y = \sqrt{\Gamma^{UB}_{WPD}(\underline{s}, \infty, \frac{A}{\sigma})} \frac{A}{\sigma}$ and $< f(t) > \triangleq \frac{1}{T} \int_0^T f(t)dt$ is the average of $f(t)$

$f(t)$ on the interval $t \in [0,T]$. This bound is plotted in figures 5.3 and 5.4.

For the examples considered here $\Gamma^*_{WPD}(\underline{s}, M, \frac{A}{\sigma})$ was close to $\Gamma^{UB}_{WPD}(\underline{s}, \infty, \frac{A}{\sigma})$ when

$M > 10$. As an example, $|\Gamma^{UB}_{WPD}(\underline{s}, \infty, \frac{A}{\sigma}) - \Gamma^*_{WPD}(\underline{s}, 10, \frac{A}{\sigma})| < 0.14$ dB for both
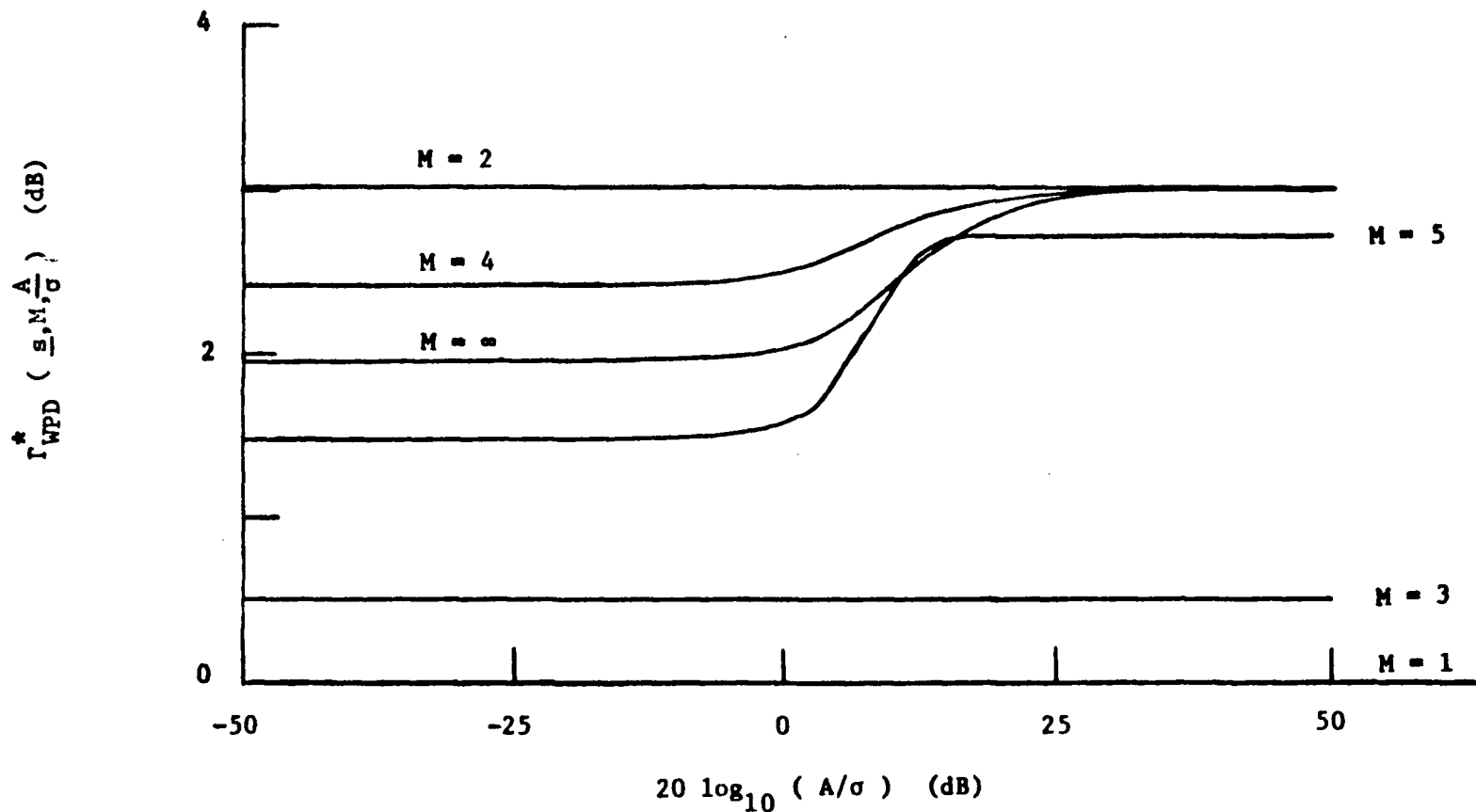
Figure 5.3. The penalty Γ^*_{WPD} ($\underline{s}$,M,$\frac{A}{\sigma}$) of the optimum WPD detector as a function of signal-to-noise ratio for a raised cosine signalling waveform. Six values of sample size M are illustrated. The curve for M = ∞ is an upper bound.
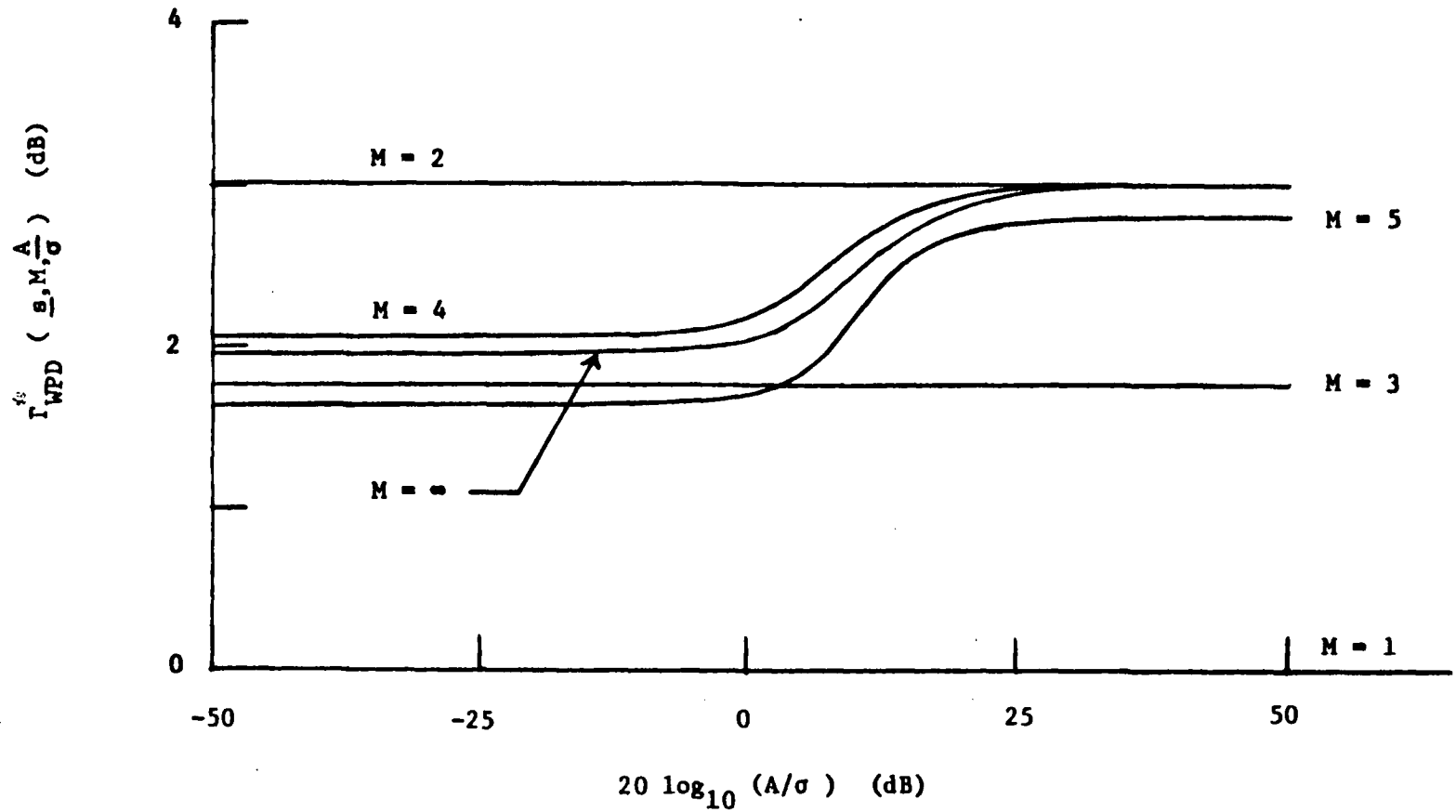
Figure 5.4. The penalty Γ_{WPD}^{*} ($\underline{s}$,M,$\frac{A}{\sigma}$) of the optimum WPD detector as a function of signal-to-noise ratio for a half sinusoid signalling waveform. Six values of sample size M are illustrated. The curve for M = ∞ is an upper bound.

the half sinusoid and raised cosine. For large values of $\frac{A}{\sigma}$, (5.16) becomes

$$\Gamma_{WPD}^{UB}(\underline{s},\infty,\infty) = \frac{-y^2 < s^2(t) >}{< -y^2 s^2(t)/2 >} = 2.$$

5.6. The Weights $\omega_i = |s_i|$ and $\omega_i = s_i^2$ WPD Detectors

The weights $\omega_i = |s_i|$ and $\omega_i = s_i^2$ WPD detectors have been previously examined for low signal-to-noise ratio conditions. It has also been shown that the optimum WPD detector is equivalent to the $|s_i|$ and s_i^2 weights detectors for low and high SNR conditions respectively. In this section, the performance of these weighting choices for other values of SNR is investigated. The penalty $\Gamma_{WPD}(\underline{s},M,\frac{A}{\sigma})$ for the $|s_i|$ weights and the s_i^2 weights WPD detectors may be evaluated using the technique of the previous section. Figures 5.5 and 5.6 show $\Gamma_{WPD}(\underline{s},M,\frac{A}{\sigma})$ as a function of signal-to-noise ratio for a raised cosine and a half sinusoid signalling waveform respectively. In both figures the $\omega_i = |s_i|$ weights are used. There are plots for the cases of M = 1, 2, 3, 4, 5, 10 and 11 samples. Figures 5.7 and 5.8 show $\Gamma_{WPD}(\underline{s},M,\frac{A}{\sigma})$ versus SNR for a raised cosine and a half sinusoid respectively, for the same values of sample size with weights $\omega_i = s_i^2$. In all cases, for fixed M, the penalty increases with $\frac{A}{\sigma}$ but is approximately constant for small and large values of $\frac{A}{\sigma}$.

5.7. Discussion

The performance losses for WPD detectors in Gaussian noise have been
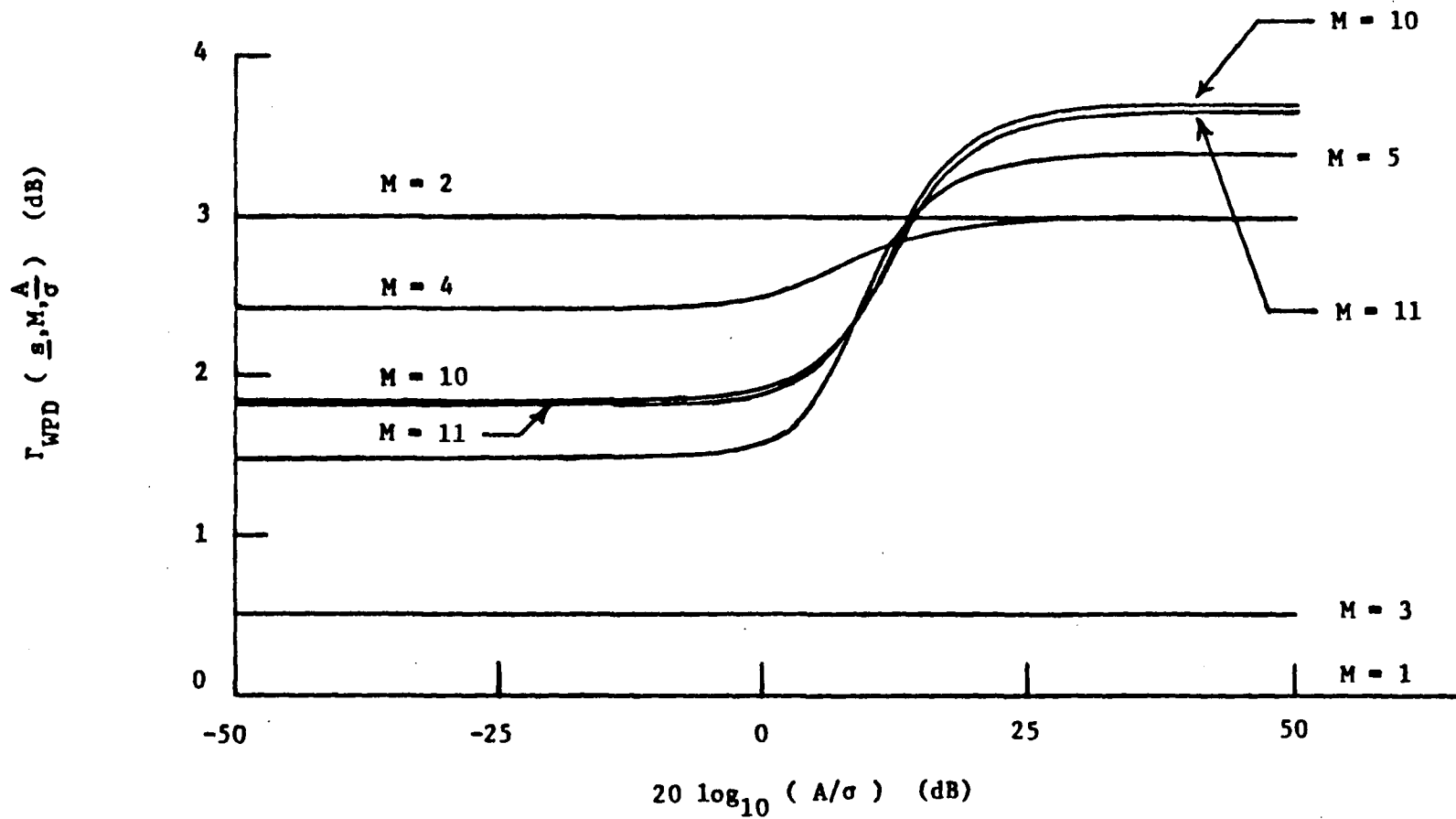
Figure 5.5. The penalty Γ_{WPD} ($\underline{s}$,M,$\frac{A}{\sigma}$) of the $\omega_i = |s_i|$ weights WPD detector as a function of signal-to-noise ratio for a raised cosine signalling waveform. Seven values of sample size M are illustrated.
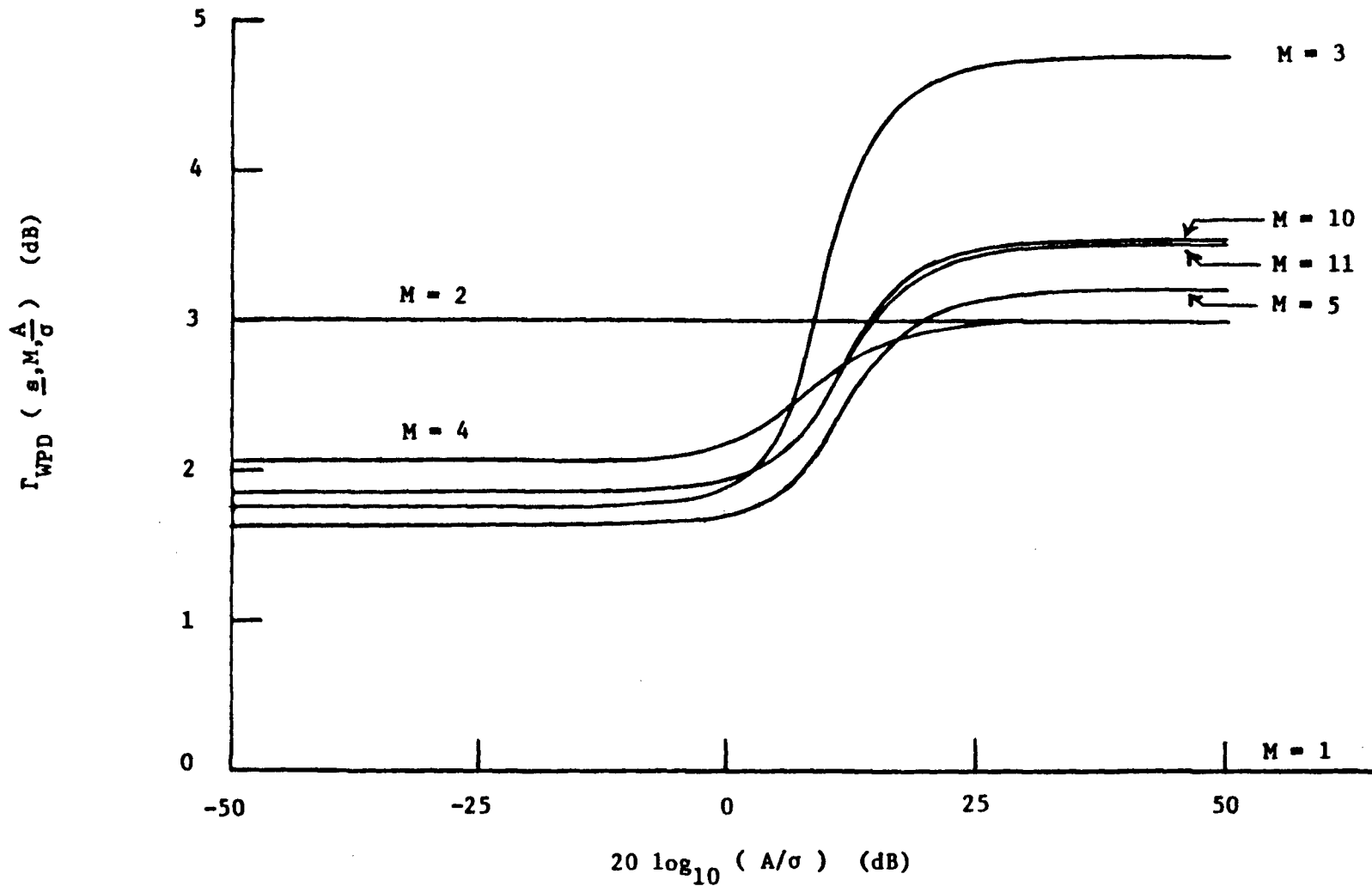
Figure 5.6. The penalty Γ_{WPD} ($\underline{s}$,M,$\frac{A}{\sigma}$) of the ω_i = $|s_i|$ weights WPD detector as a function of signal-to-noise ratio for a half sinusoid signalling waveform. Seven values of sample size M are illustrated.
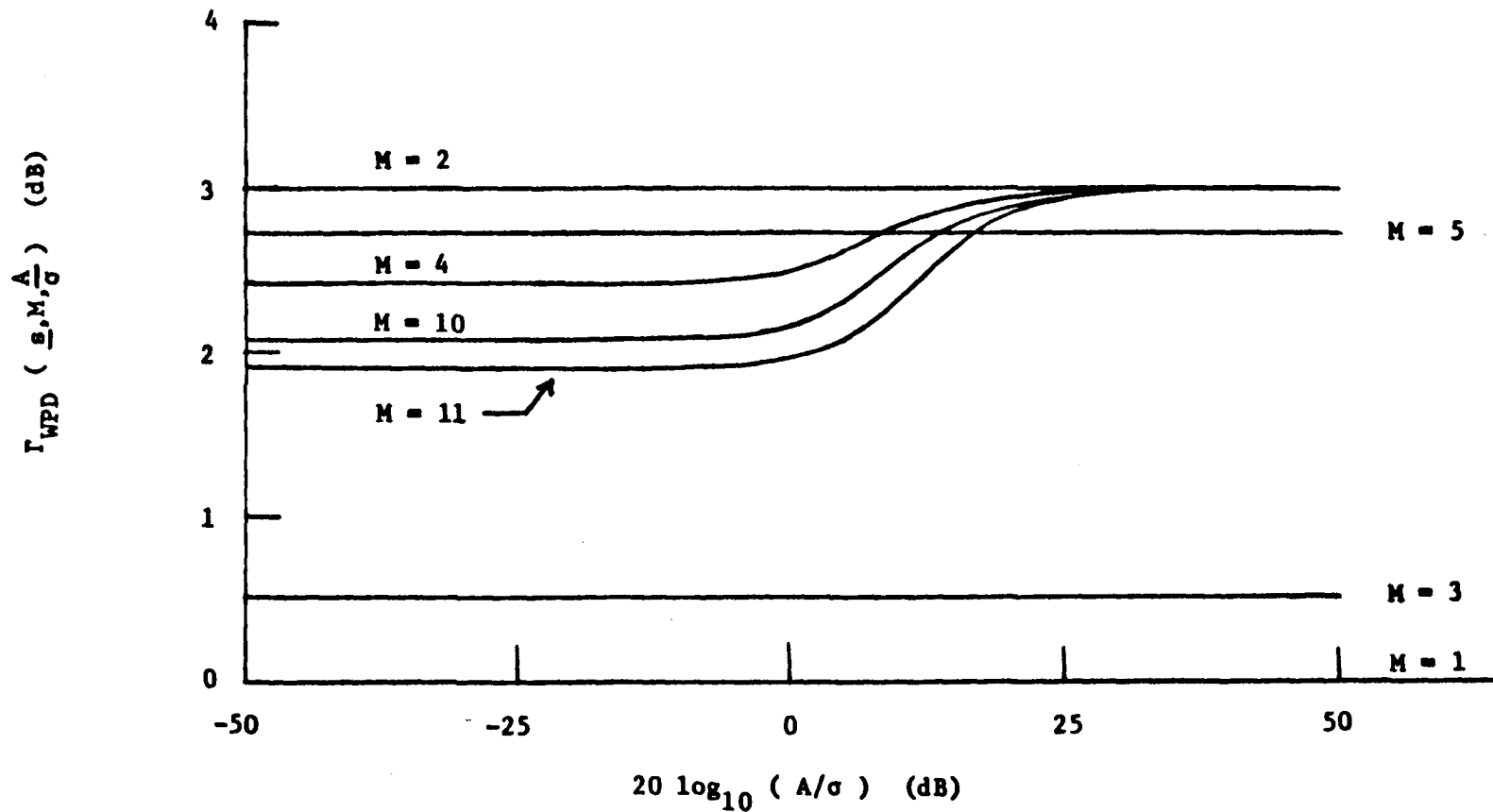
Figure 5.7. The penalty Γ_{WPD} ($\underline{s}$,M,$\frac{A}{\sigma}$) of the $\omega_i = s_i^2$ weights WPD detector as a function of signal-to-noise ratio for a raised cosine signalling waveform. Seven values of sample size M are illustrated.
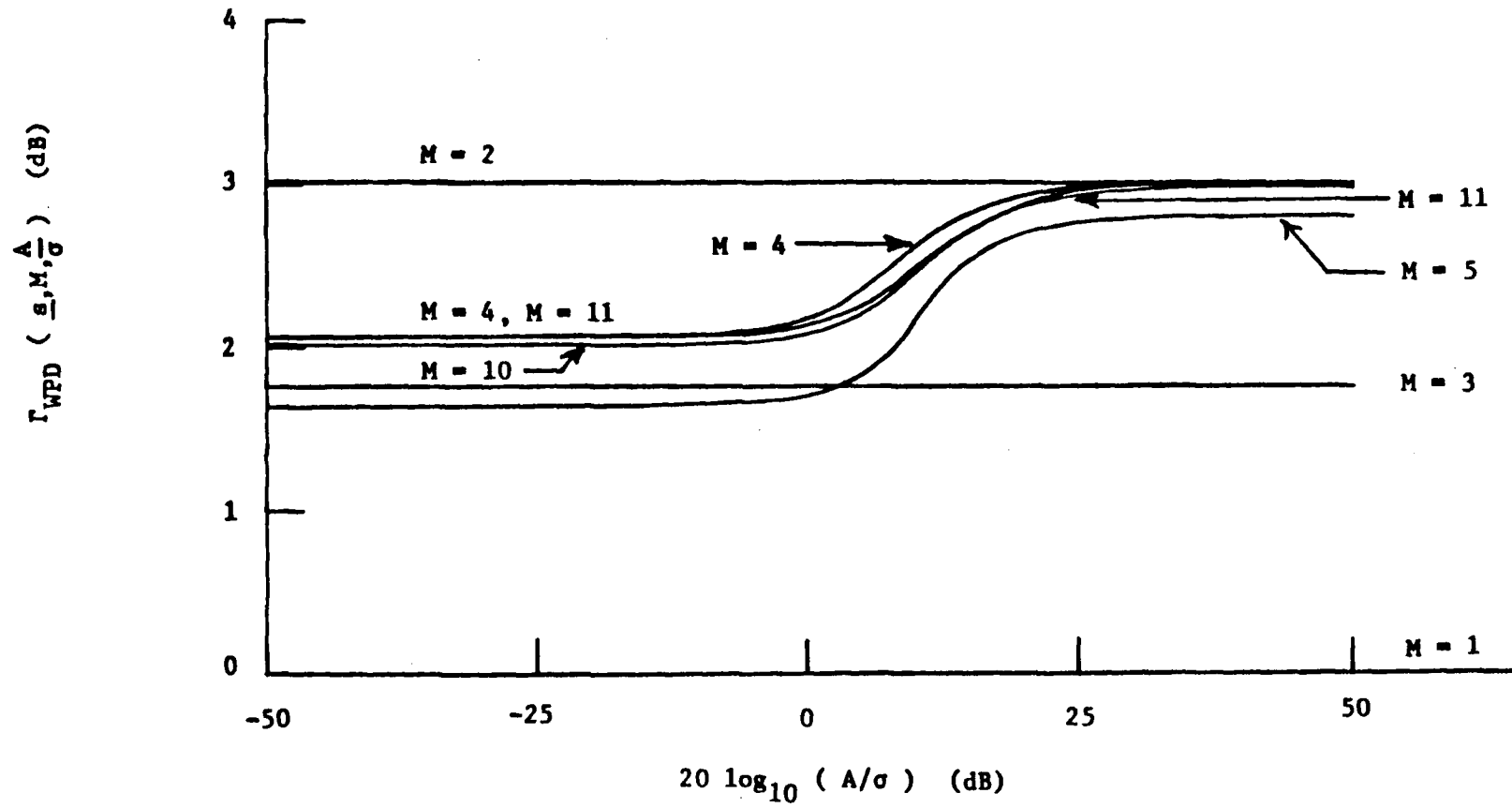
Figure 5.8. The penalty Γ_{WPD} ($\underline{s}, M, \frac{A}{\sigma}$) of the $\omega_i = s_i^2$ weights WPD detector as a function of signal-to-noise ratio for a half sinusoid signalling waveform. Seven values of sample size M are illustrated.

investigated. Three choices of weights have been considered. Previous analyses of these suboptimal schemes have been confined to low signal-to-noise ratio conditions. In general, the penalty depends on the choice of weights, the samples of the signalling waveform (and their number) as well as on the signal-to-noise ratio. In all of the examples considered, the penalties of the WPD detectors are approximately constant for low SNR values, increase in a transition region, and are approximately constant for high SNR values. Since equations (5.8) and (5.9) are independent of the signal-to-noise ratio, the losses for the general WPD detector will be approximately constant for low and high SNR values.

Since the $\omega^* = \ln \frac{1-p_i}{p_i}$ weights WPD detector is the optimum detector for hard-limited samples and the DMF detector is the optimum processor for continuous amplitude samples, the penalties of figures 5.2 - 5.4 represent the fundamental losses due to hard-limiting of independent samples. In all cases, this loss is a non-decreasing function of signal-to-noise ratio and is upper bounded by 2(3.01 dB).

The value of $\pi/2 = 1.96$ dB is often cited as the loss due to hard-limiting [25,31,37]. This result applies to an infinite number of independent samples and a vanishingly small SNR. The work of this chapter has shown that the loss is a function of the signal-to-noise ratio and of the number of samples. Independent samples are assumed in this work and the results are shown to agree with the previous result when the number of samples is infinite and the SNR is vanishingly small. However, the well known result of 1.96 dB as it applies to an infinite number of independent samples does not represent a physically realistic system. The results derived here deal with finite numbers of

independent samples. This is representative of real systems.

The $\omega_i = |s_i|$ detector is optimal for low SNR conditions. Figures 5.5 - 5.8 show that the penalty for this detector may exceed 2(3.01 dB) for high SNR values and is greater than the penalty incurred by the s_i^2 weights detector. Similarly, the s_i^2 weights detector which is optimal for high SNR's has greater loss at low SNR values than the $|s_i|$ weights detector.

VI PENALTIES OF SAMPLE-AND-SUM AND BINARY PARTIAL DECISION DETECTORS

IN GAUSSIAN NOISE

6.1. Introduction

The performances of the SAS and BPD detectors were analyzed for

low signal-to-noise (SNR) conditions in chapters 2 and 3. In this chapter,

the performances of SAS and BPD detectors are analyzed for arbitrary

signal-to-noise ratios. The effects on the penalties of the signalling

waveform employed, the number of samples processed, and the SNR are

considered in detail. The SAS detector is examined first because its

loss constitutes a part of the BPD detector's loss. The losses are

compared to those of some WPD detectors and a relationship between the

losses of the SAS, BPD and WPD detectors for low SNR and finite sample

sizes is derived.

The model considered here is the same as in section 5.2.

Antipodal signals are used to communicate a message $m \in \{0,1\}$

over an additive white Gaussian noise (AWGN) channel. The signals +A s(t)

and -A s(t) are sent corresponding to m = 0 and m = 1 respectively. The

receiver processes M samples $\{v_i\}_{i=1}^{M}$, $v_i = \pm A s_i + n_i$ where $\{s_i\}_{i=1}^{M}$ and

$\{n_i\}_{i=1}^{M}$ denote the samples of the signal s(t) (normalized so that its maximum

amplitude is equal one) and outcomes of independent Gaussian noise random

variables respectively. Signal-to-noise ratio (SNR) is defined to be

$20 \log_{10} \frac{A}{\sigma}$ measured in dB.   The penalty is defined as the increase in

signal-to-noise ratio required by the suboptimum detector in order to

achieve the same target value of probability of error as the DMF

detector.

6.2. The Sample-and-Sum (SAS) Detector Loss

In this section, the penalty incurred in using the SAS detector is analyzed. This detector [5,6,13] forms the statistic

$$D_{SAS} \triangleq \sum_{i=1}^{M} v_i \; sgn \; (s_i) \tag{6.1}$$

where $sgn(x) = \begin{cases} +1, & \text{if } x > 0 \\ 0, & \text{if } x = 0 \text{ and chooses } \hat{m}=0 \text{ if } D_{SAS} > 0. \text{ Otherwise, } \hat{m}=1 \\ -1, & \text{if } x < 0 \end{cases}$

is chosen.

Given that $m=0$, i.e. $+A \; s(t)$ is transmitted, the mean of D_{SAS} is

$$\overline{D}_{SAS} = A \sum_{i=0}^{M} |s_i| \tag{6.2}$$

and its variance is given by

$$\sigma^2_{D_{SAS}} = M \; \sigma^2 . \tag{6.3}$$

An error occurs if $D_{SAS} < 0$. To compute the probability of error, $P_{SAS}(e)$, we observe that D_{SAS} is a Gaussian random variable(r.v.) since it is the sum

of independent Gaussian r.v.'s. Also, because of the symmetry, $P_{SAS}(e|m=1) = P_{SAS}(e|m=0)$. Hence,

$$P_{SAS}(e) = Q\left(\frac{A \sum_{i=1}^{M} |s_i|}{\sqrt{M} \, \sigma}\right) \tag{6.4}$$

where $Q(\alpha) = \frac{1}{\sqrt{2\pi}} \int_{\alpha}^{\infty} e^{-x^2/2} \, dx$. The penalty Γ_{SAS} incurred by the SAS

detector relative to the DMF detector is implicitly defined by comparing $P_{SAS}(e)$ with $P_{DMF}(e)$ as given by (5.3) namely,

$$Q\left(\frac{A\sqrt{\sum_{i=1}^{M} s_i^2}}{\sigma}\right) = Q\left(\frac{A \sum_{i=1}^{M} \sqrt{\Gamma_{SAS}} \, |s_i|}{\sqrt{M} \, \sigma}\right). \tag{6.5}$$

From (6.5), it follows that

$$\Gamma_{SAS} = \frac{M \sum_{i=1}^{M} s_i^2}{(\sum_{i=1}^{M} |s_i|)^2}. \tag{6.6}$$

Note that Γ_{SAS} is independent of the channel noise power, but does depend on the samples $\{s_i\}_{i=1}^{M}$ and the number of samples M. Where necessary, we will use $\Gamma_{SAS}(\underline{s}, M)$ to indicate this dependence explicitly. For large values of

M,

$$\sum_{i=1}^{M} s_i^2 = \frac{M}{T} \int_0^T |s(t)|^2 \, dt \tag{6.7a}$$

and

$$\sum_{i=1}^{M} |s_i| = \frac{M}{T} \int_0^T |s(t)| \, dt \ . \tag{6.7b}$$

Consequently, equation (6.6) can be rewritten as

$$\Gamma_{SAS} = \frac{T \int_0^T s^2(t) \, dt}{[\int_0^T |s(t)| \, dt]^2} = \frac{E_s}{T[< |s(t)| >]^2} \tag{6.8}$$

where $E_s \triangleq \int_0^T s^2(t) \, dt$ is the energy of the signalling waveform $s(t)$ and

$< |s(t)| > \triangleq \frac{1}{T} \int_0^T |s(t)| \, dt$ is its average magnitude. Equation (6.8) has

been previously derived (2.10) for a particular filtering scheme with a large

number of samples in a low SNR environment. The present derivation

shows that it is valid for any SNR.

We now use equation (6.6) to illustrate how Γ_{SAS} varies with M for a

few commonly encountered signalling waveforms. For a constant (or piecewise

constant) amplitude signalling waveform, $\Gamma_{SAS} = 1$, i.e. 0 dB as expected.

For a half sinusoid signalling waveform, the samples are

$$s_i = \sin \frac{\pi}{M} (i - 0.5), \quad i = 1,2,\ldots,M. \quad \text{In this case, } \sum_{i=1}^{M} |s_i| = \text{cosec} \frac{\pi}{2M}$$

[30,1·341·1] and $\sum_{i=1}^{M} s_i^2 = \begin{cases} 1, & M=1 \\ \dfrac{M}{2}, & M > 2 \end{cases}$. From (6.6)

$$\Gamma_{SAS} = \begin{cases} 1 & , \ M = 1 \\ \dfrac{M^2}{2} \sin^2 \left(\dfrac{\pi}{2M}\right) , & M > 2 \end{cases} , \text{ half sinusoid.} \tag{6.9}$$

The penalty Γ_{SAS} given by (6.9) is plotted as a function of M in figure 6.1. The asymptotic value of Γ_{SAS} for large M is $\dfrac{\pi^2}{8}$ or 0.912 dB.

The penalties for a full sinusoid ($s_i = \sin [\frac{2\pi}{M} (i-0.5)]$) and a raised cosine ($s_i = [1-\cos \frac{2\pi}{M} (i-0.5)]/2$) signalling waveform are given respectively by

$$\Gamma_{SAS} = \begin{cases} 1 , \ M = 1 \text{ or } 2 \\ \dfrac{M^2}{8} \sin^2 \left(\dfrac{\pi}{M}\right) , & M = 4,6,8\ldots \\ \dfrac{M^2}{8} \left[\dfrac{\sin(\pi/M)}{1 + \cos(\pi/M)}\right]^2 , \ M = 3,5,7\ldots \end{cases} , \text{ full sinusoid} \tag{6.10}$$

and

$$\Gamma_{SAS} = \begin{cases} 1, \ M = 1, 2 \\ \dfrac{3}{2} , \ M > 3 \end{cases} , \text{ raised cosine .} \tag{6.11}$$
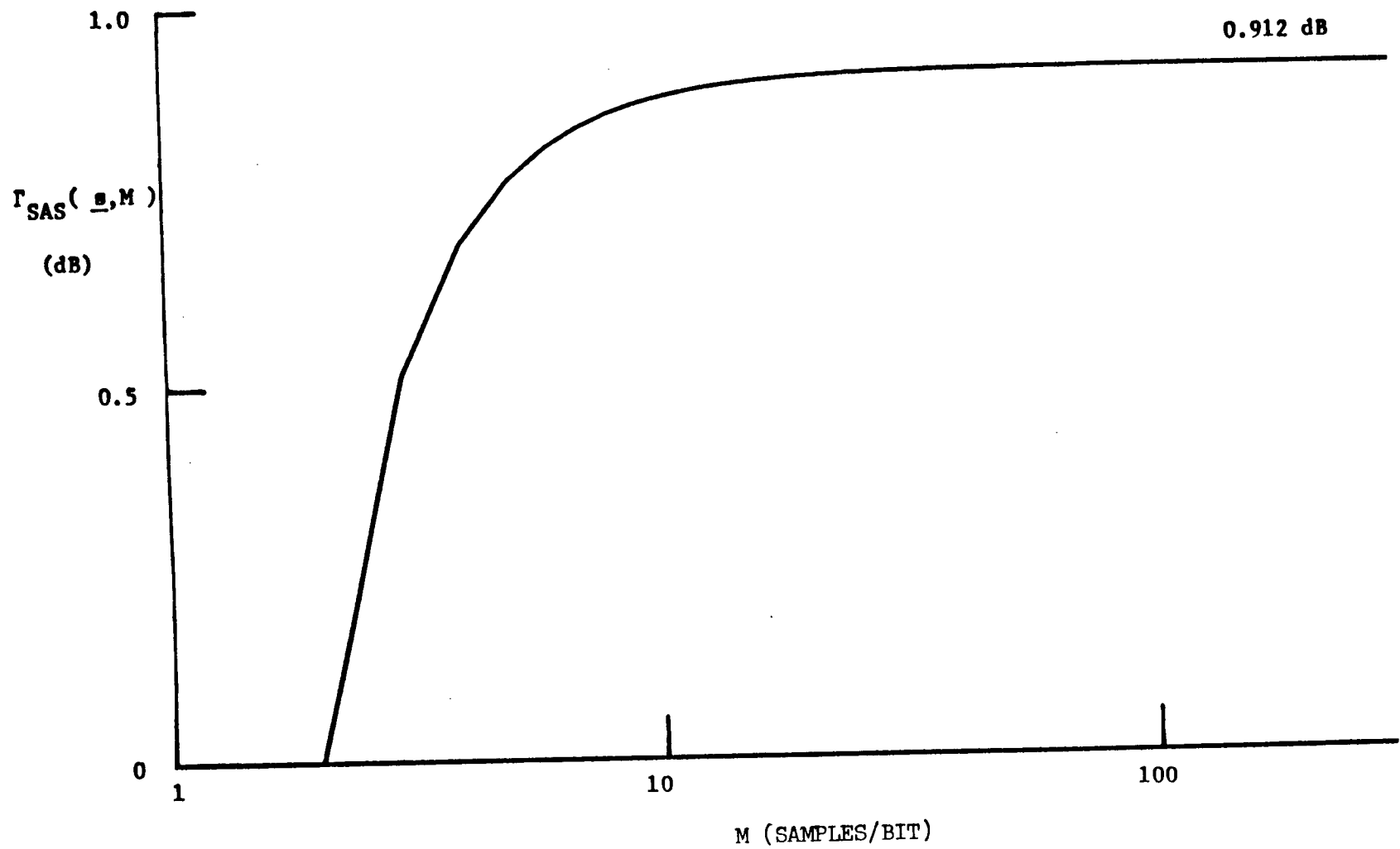
Figure 6.1. The penalty $\Gamma_{SAS}(\underline{s},M)$ as a function of the number of bit samples for a half sinusoid.

The asymptotic values of Γ_{SAS} as given by (6.10) and (6.11) are $\frac{\pi^2}{8}$ or 0.912 dB and $\frac{3}{2}$ or 1.76 dB. A plot of Γ_{SAS} for a full sinusoid signalling waveform is shown in figure 6.2.

In all these examples, the asymptotic value of Γ_{SAS} is reached rapidly. The magnitude of the difference $|\Gamma_{SAS}(\underline{s},M) - \Gamma_{SAS}(\underline{s},\infty)|$ is less than 0.1 dB for $M > 11$.

6.3. The Binary Partial Decision (BPD) Detector Loss

The BPD detector forms the test statistic [2,3]

$$D_{BPD} \triangleq \sum_{i=1}^{M} D_i$$

where the partial decision random variable D_i is defined by

$$D_i = \begin{cases} +1 \ , & \text{if } sgn(v_i) = sgn(s_i) \neq 0 \\ 0 \ , & \text{if } sgn(v_i) = 0 \text{ or } sgn(s_i) = 0 \\ -1 \ , & \text{otherwise} \ . \end{cases} \tag{6.12}$$

The BPD detector chooses $\hat{m} = 0$ if $D_{BPD} > 0$ and $\hat{m} = 1$ if $D_{BPD} < 0$. Some caution should be exercised (section 4.5) in choosing $\hat{m}$ if $D_{BPD} = 0$. This detector may be thought of as the special case of the WPD detector for which the weights all equal one ($\omega_i = 1$). It can be easily implemented using a counter which is incremented or decremented by 1 depending on the polarties of v_i and s_i.
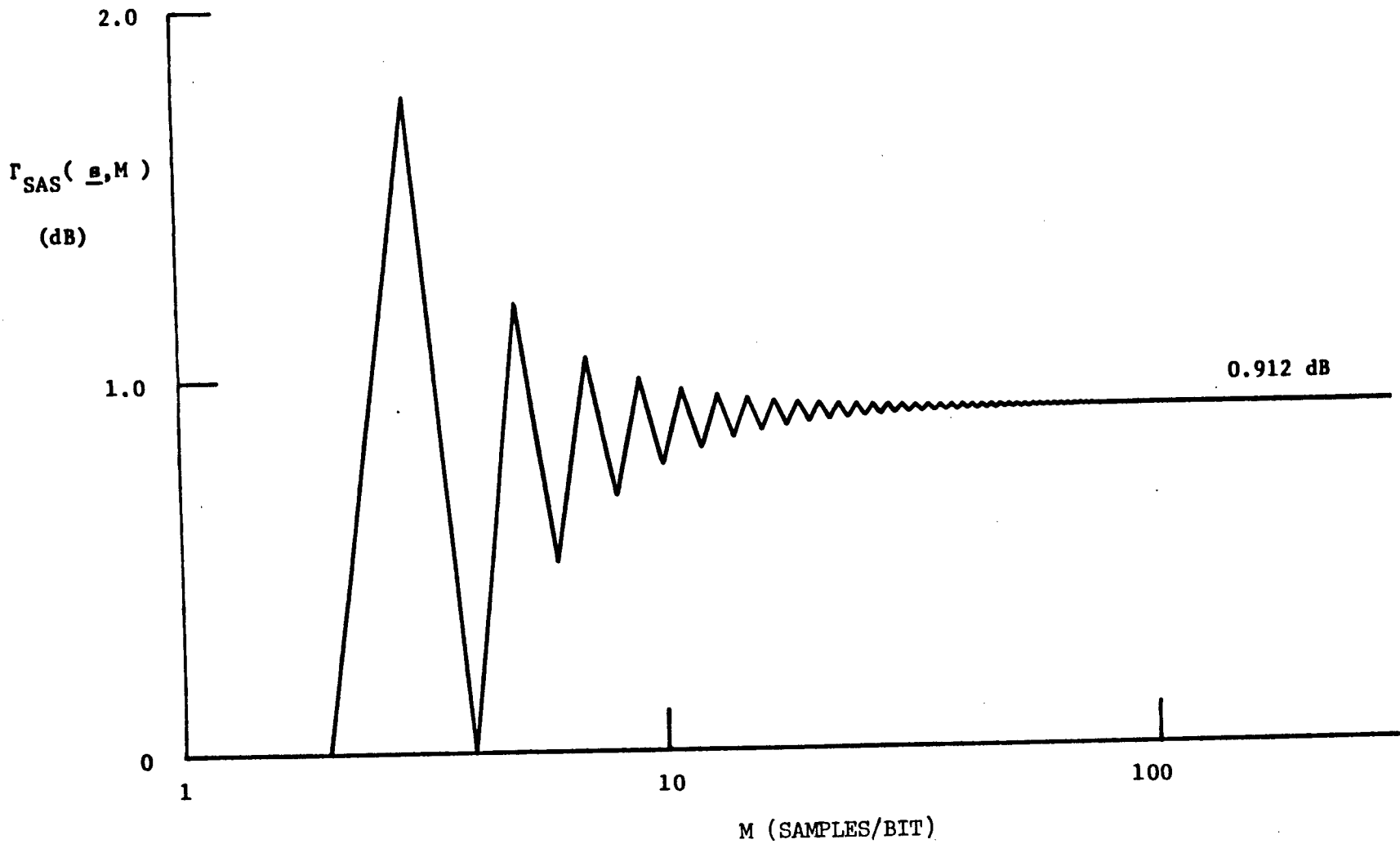
Figure 6.2. The penalty $\Gamma_{SAS}(\underline{s}, M)$ as a function of the number of bit samples for a sinusoid.

The probability of error is the probability that a majority of the transmitted samples are received with their polarities reversed, i.e.

$$
P_{BPD}(e) = \begin{cases} \displaystyle\sum_{i=\frac{M+1}{2}}^{M} P_i^M \,, & M \text{ odd} \\[3em] \displaystyle\sum_{i=\frac{M+2}{2}}^{M} P_i^M + \frac{1}{2} P_{\frac{M}{2}}^M \,, & M \text{ even} \end{cases}
$$

(6.13)

where $P_i^M \triangleq Pr\{$exactly i polarity errors in the M samples$\}$.

By equating the right hand side of (6.13) with $P_{DMF}(e)$ as in section 5.4 the penalties $\Gamma_{BPD}(\underline{s}, M, \frac{A}{\sigma})$ can be numerically evaluated. Plots of $\Gamma_{BPD}(\cdot, \cdot, \cdot)$ as a function of $\frac{A}{\sigma}$ for the raised cosine and half sinusoid signalling waveforms are shown in figures 6.3 and 6.4. The values of sample size illustrated are M = 1 - 5, 10 and 11 for both waveforms. For high SNR, it follows from (5.8) that

$$
\Gamma_{BPD}(\underline{s}, M, \infty) = \frac{\displaystyle\sum_{i=1}^{M} s_i^2}{\text{sum of the } \left\lceil \frac{M}{2} \right\rceil \text{ smallest terms in } \{s_i^2\}_{i=1}^M}
$$

(6.14)

where $\lceil x \rceil$ denotes the smallest integer $> x$. Equation (6.14) holds for an arbitrary signalling waveform.

For large values of M, one has
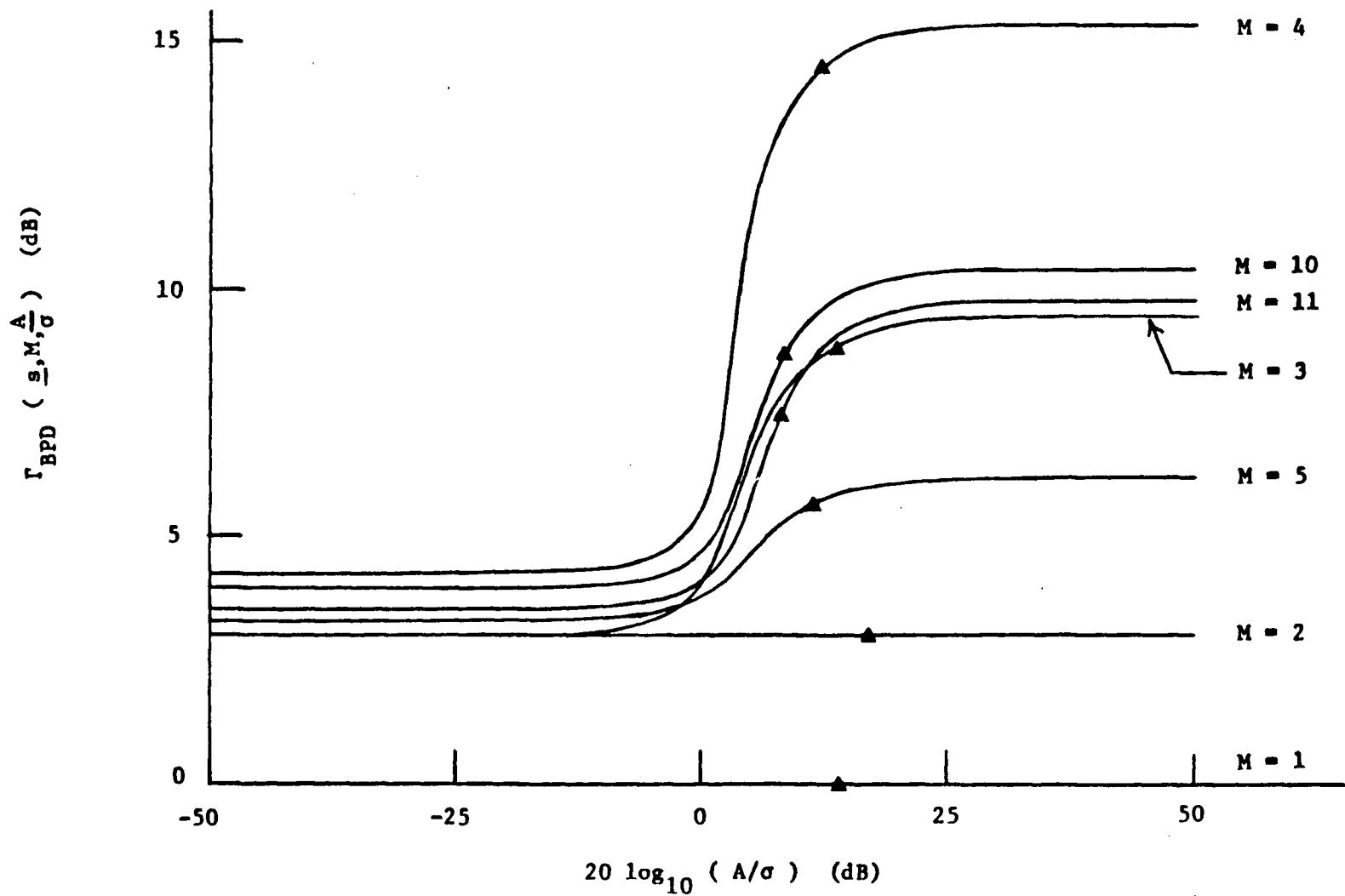
Figure 6.3. The penalty Γ_{BPD} ($\underline{s}$,M,$\frac{A}{\sigma}$) as a function of the signal-to-noise ratio for a raised cosine signalling waveform. Seven values of sample size M are illustrated. The solid triangles indicate points for which $P_{BPD}(e) = 10^{-7}$.
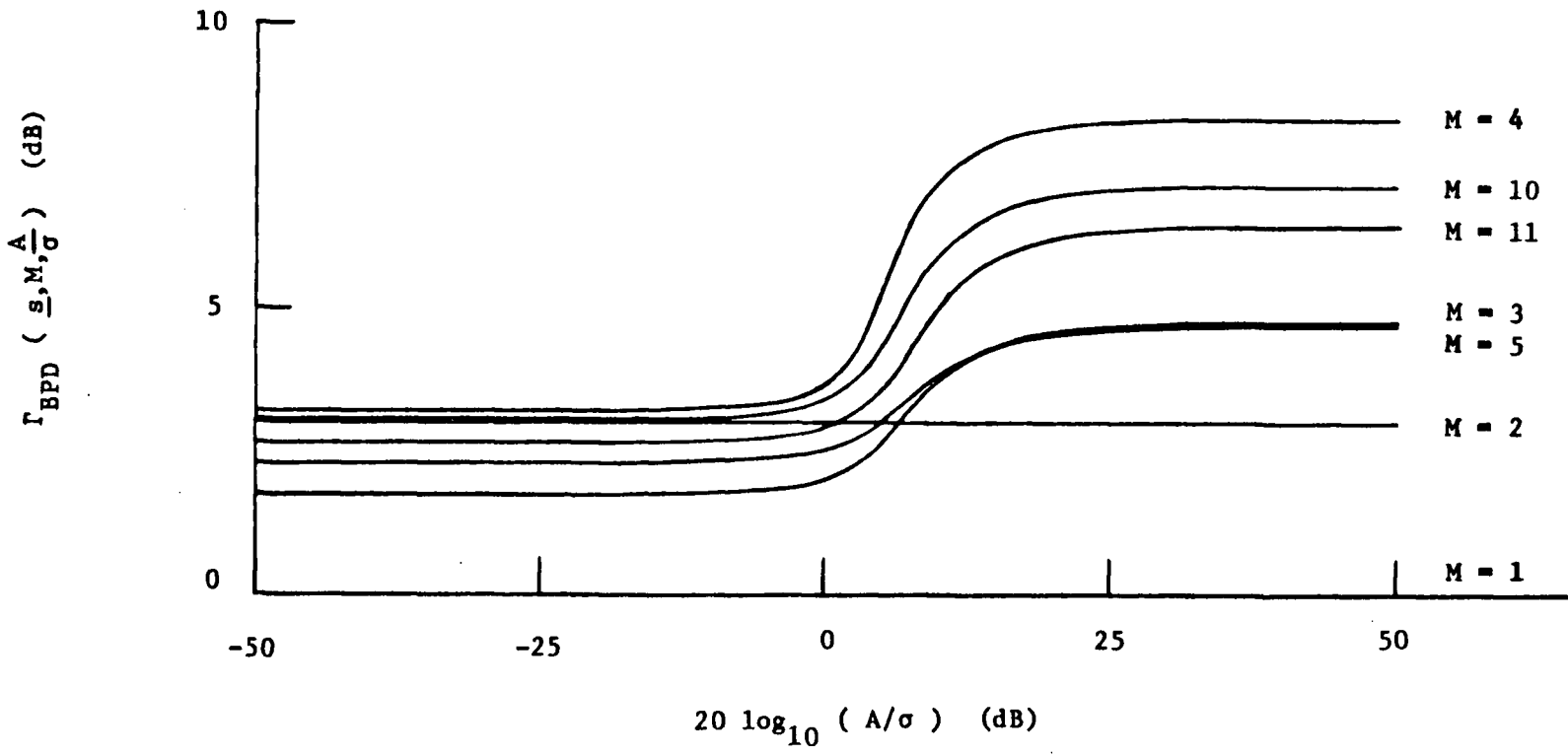
Figure 6.4. The penalty Γ_{BPD} ($\underline{s},M,\frac{A}{\sigma}$) as a function of the signal-to-noise ratio for a half sinusoid signalling waveform. Seven values of sample size M are illustrated.

$$\Gamma_{BPD}(\underline{s},\infty,\infty) = \frac{\int_0^T s^2(t)\ dt}{\int_W s^2(t)\ dt} \qquad (6.15)$$

where W is a union of intervals in $[0,T]$ with a total width of $\frac{T}{2}$ which

minimizes $\int_W s^2(t)\ dt$.

For a raised cosine signalling waveform, (6.15) becomes

$$\Gamma_{BPD}(\text{raised cosine},\infty,\infty) = \frac{\int_0^{2\pi}[\frac{1}{2}(1-\cos t)]^2\ dt}{2\int_0^{\pi/2}[\frac{1}{2}(1-\cos t)]^2\ dt} = \frac{6\pi}{3\pi - 8}$$

$$\text{or } 11.22 \text{ dB.} \qquad (6.16)$$

For a half sinusoid waveform, we have

$$\Gamma_{BPD}(\text{half sinusoid},\infty,\infty) = \frac{\int_0^\pi \sin^2 t\ dt}{2\int_0^{\pi/4} \sin^2 t\ dt} = \frac{2\pi}{\pi - 2} \text{ or } 7.41 \text{ dB .} \qquad (6.17)$$

In the case of a piecewise constant signalling waveform, (6.14)

reduces to $\Gamma_{BPD}(\underline{1},M,\infty) = \begin{cases} 2, & M \text{ even} \\ 2 - \frac{2}{M+1}, & M \text{ odd} \end{cases}$ in agreement with (5.15).

The asymptotic values for low SNR's will now be considered. In

Appendix K, it is shown that for an arbitrary signalling waveform,

$$\Gamma_{BPD}(\ \underline{s},M,0\ ) = \Gamma_{WPD}(\ \underline{1},M,0\ ) \cdot \Gamma_{SAS}(\ \underline{s},M\ ) \qquad (6.18)$$

Equation (6.18) can be interpreted as follows: suppose the penalties are measured in dB; then for low SNR values, the penalty incurred by the BPD detector is the sum of the penalty incurred by the SAS detector and the penalty incurred by the WPD (or BPD) detector operating with a piecewise constant signalling waveform (as given by (5.13)). Strictly speaking, this relation is only valid for $\frac{A}{\sigma} = 0$. It is however, nearly exact over a wide range of signal-to-noise ratio because of the flat nature of the penalty curves in that range.

From (6.18) and the fact that $\lim_{M \to \infty} \Gamma_{WPD}(\ \underline{1},M,0) = \pi/2$ (section 2.3), it follows that for large M,

$$\Gamma_{BPD}(\ \underline{s},\infty,0\ ) = \frac{\pi}{2}\ \Gamma_{SAS}(\ \underline{s},\infty\ ) \ . \qquad (6.19)$$

This result was previously derived for a particular filtering scheme in section 2.4.

6.4. Discussion of Results

The penalties associated with the use of the SAS and BPD detectors have been analyzed. The loss incurred by the SAS detector depends on the samples of the signalling waveform used but is independent of the signal-to-noise ratio. In contrast, the losses associated with the BPD

detector (and the WPD detectors) depend on the signal-to-noise ratio as well as on the signal samples.

While the BPD detector is easier to implement than the WPD detectors analyzed in chapter V, the penalty of the BPD detector was more sensitive to the choice of the signalling waveform and in some cases was much greater than the penalty of the WPD detectors. Also shown in figure 6.3 are the points corresponding to $P_{BPD}(e) = 10^{-7}$. It can be seen from figure 6.3 that for the raised cosine waveform, the penalty using a BPD detector with M = 4 and $P_{BPD}(e) = 10^{-7}$ is about 14.5 dB. The corresponding penalty for the optimum WPD detector is only ~ 2.8 dB.

VII   CONCLUSION

7.1. Summary of Results

In this section, the highlights of the thesis research are summarized.

Three suboptimum detectors which find application in practical digital systems have been described. The penalties of each have been analysed and identified. The relationships between the losses of the systems have been derived. Previous work in this area was mainly numerical and example specific. The present work treats the topic theoretically and gives some results that are fairly general and can be applied to systems other than those examined in the examples.

The effects of dependence among the signal samples on the penalties have been examined. It has been shown that, in some cases, the penalties can be reduced by processing more, dependent, samples. It has been found that the amount of loss recoverable depends on the prefilter characteristic and the sampling rate.

The optimal detector which bases its decision on a number of hard-limited samples has been presented. This detector is optimal in the sense that it minimizes the bit error probability. The detector is simple and inexpensive since it is essentially a one-bit analog-to-digital converter (ADC) and does not require an automatic gain control (AGC). This result is general in that it applies to arbitrary SNR values, arbitrary numbers of samples, and most practical noise environment models.

The generalization of the optimum hard-limiting detector for binary signals to higher quantization and signalling levels has also been derived.

That is, the minimum bit error probability detector for M-ary signalling with received signal samples quantized to an arbitrary number of levels has been found. Again, these results have been obtained using theoretical analysis whereas previous related work, in many cases, has been numerical and example specific.

The fundamental loss due to hard-limiting in Gaussian noise has been investigated in depth. This loss is measured in the signal detectability sense. That is, the loss is expressed as the increase in SNR required to maintain a target value of error probability. Much attention has been paid to the loss due to hard-limiting in the past. The result most often quoted is that the loss is $\pi/2 = 1.96$ dB. This result applies to an infinite number of independent samples and a vanishingly small signal-to-noise ratio. The present work shows that the loss is a function of the signal-to-noise ratio and of the number of samples. Independent samples are assumed in our work and the results agree with the previous result when the number of samples is infinite and the SNR is vanishingly small. The results are important because they apply to real world system conditions. The well known result of 1.96 dB as it applies to an infinite number of independent samples does not represent a physically realistic system. The work done here which deals with a finite number of independent samples is representative of real systems.

In addition to the investigation of the fundamental loss due to hard-limiting, the losses incurred by some ad hoc schemes that hard-limit the received samples have been examined. Some of the results of

this work are of considerable interest for practical design. It is shown, for example, that one common ad hoc procedure has very large losses at high SNRs and is therefore unsuitable for application in a strong signal environment.

7.2. Suggestions for Further Research

There are a number of issues arising from the thesis work that provide interesting topics for further research. Some of these are presented and briefly discussed in this section.

The effects of dependence among the signal samples on the detector penalties was investigated for large time-bandwidth product conditions and low SNRs. The generalization of these results to arbitrary time-bandwidth products and arbitrary SNRs has not been treated in this thesis.

The optimum detector for M-ary signalling with an arbitrary, given, quantizer was derived. The optimum quantizer thresholds that minimize the bit error probability were not specified. A related question is the sensitivity of the detector performance to variations in threshold settings.

The performance of the optimum detector for M-ary signalling may be evaluated. Hereunder, one can consider different quantization levels and modulation formats.

The losses of the suboptimum detectors under bandlimited conditions with appreciable ISI are of interest. Performance evaluation in these cases is probably best done by the application of tight bounds for the error probabilities.

APPENDIX A

In this appendix, we show that as $M\to\infty$, the probability of error for the WPD detector is

$$P(e) = Q\left(\sqrt{\frac{4E_s}{\pi N_o}}\right). \tag{A.1}$$

Recall that $Q(\alpha)$ can be represented by the infinite series [15,16]

$$Q(\alpha) = \frac{1}{2} - \frac{1}{\sqrt{2\pi}}\left\{\alpha - \frac{\alpha^3}{6} + \frac{\alpha^5}{40} - \ldots + \frac{(-1)^n \alpha^{2n+1}}{(2n+1)2^n n!} + \ldots\right\}. \tag{A.2}$$

Thus, from (2.15), for large values of M (small signal-to-noise ratio),

$$P_i = \frac{1}{2} - \sqrt{\frac{T}{\pi M N_o}}\, |s_i|\, . \tag{A.3}$$

As $M\to\infty$, the mean of D_{WPD}, i.e $\sum_{i=1}^{M} (1-2P_i)|s_i|$, is given by (see page 14)

$$\sqrt{\frac{4M}{\pi N_o T}} \int_0^T s^2(t)\, dt = \sqrt{\frac{4M}{\pi N_o T}}\, E_s \tag{A.4}$$

and the variance of D_{WPD}, i.e. $\sum_{i=1}^{M} 4P_i(1-P_i)|s_i|^2$, is given by

$$\frac{M}{T} \int_0^T s^2(t)dt = \frac{ME_s}{T} \tag{A.5}$$

But
$$P(e) = Q\left(\frac{\text{Mean of } D_{WPD}}{\sqrt{\text{variance of } D_{WPD}}}\right)$$

$$= Q\left(\sqrt{\frac{4E_s}{\pi N_o}}\right).$$

APPENDIX B

It is to be shown that the probability of error for the BPD detector is

$$P(e) = Q \left(\sqrt{\frac{4E_s}{\pi N_o \alpha}} \right). \tag{B.1}$$

Using (A.3), it can be determined that as $M \to \infty$, the mean of D_{BPD}, i.e. $\sum_{i=1}^{M} (1-2p_i)$, is given by

$$\sqrt{\frac{4M}{\pi T N_o}} \int_0^T |s(t)| dt \tag{B.2}$$

and its variance, i.e. $\sum_{i=1}^{M} 4p_i(1-p_i)$, is given by M. Hence

$$P(e) = Q \left(\frac{\text{mean of } D_{BPD}}{\sqrt{\text{variance of } D_{BPD}}} \right)$$

$$= Q \left(\sqrt{\frac{4E_s}{\pi N_o \alpha}} \right)$$

APPENDIX C

In this appendix the calculation of P(e) for the SAS, BPD and WPD detectors for small values of M is briefly described. Let us denote the noiseless received waveform by $f(t)$. Thus $f(t)$ results from passing the transmitted waveform $s(t)$ through the lowpass filter. Then, for the SAS detector,

$$P(e) = Q \left(\frac{\sum\limits_{i=1}^{M} |f_i|}{M\sqrt{N_o/2T}} \right) \tag{C.1}$$

where f_i, $i=1,2,3,\ldots,M$ denotes the ith sample of $f(t)$.

The calculation of P(e) for the BPD and WPD detector is computationally more involved. Let p_i denote the probability that the channel causes a reversal in the polarity of f_i, i.e.,

$$p_i = Q \left(\frac{|f_i|}{\sigma_n} \right) \tag{C.2}$$

where $\sigma_n = \sqrt{MN_o/2T}$. Also define $q_i = 1 - p_i$.

Suppose A is some subset of $U = \{1,2,3,\ldots,M\}$. Then the probability that the samples $\{f_i\}_{i \in A}$ have their polarities reversed by the noise and the remaining samples $\{f_i\}_{i \in A^c}$ retain their original polarities is given by

$$P_A = \left(\prod_{i \in A} p_i \right) \left(\prod_{i \in A^c} q_i \right) . \tag{C.3}$$

Hence,

$$P(e) = \sum_A P_A \quad \text{where the sum is taken over all subsets A which would}$$

lead to a wrong decision. This brute-force method of calculating P(e) is

time consuming. A more efficient way of evaluating P(e) for the BPD detector can be obtained by noting that it is just the probability that a majority of the samples have their polarities reversed, i.e.,

$$P(e) = \sum_{n=0}^{\lfloor M/2 \rfloor} P_{n,M} \qquad \text{(C.4)}$$

where $P_{n,M}$ = Pr {exactly n of the M samples are correct}. In (C.4) it is assumed for simplicity that M is odd. If M is even, then

$$P(e) = \sum_{n=0}^{M/2} P_{n,M} - \frac{1}{2} P_{M/2,M}.$$

In any case, $P_{n,M}$ represents the generalized binomial distribution and can be recursively evaluated [17] using

$$P_{n,m} = q_m P_{n-1,m-1} + P_m P_{n,m-1}$$

$$P_{0,0} = 1, \quad P_{0,m} = P_1 P_2 \cdots P_m, \quad \text{and} \quad P_{n,m} = 0 \text{ if } n > m. \qquad \text{(C.5)}$$

APPENDIX D

It is to be shown that as $M \to \infty$

$$E[D_i D_j] - \bar{D}_i \bar{D}_j = 2/\pi \arcsin \{r_n(j-i)\}. \tag{D.1}$$

One has that

$$E[D_i D_j] = E[\text{sgn}(v_i s_i) \text{sgn}(v_j s_j)] = \Pr(n_i > -|s_i|, \, n_j > -|s_j|)$$

$$+ P_r(n_i < -|s_i|, \, n_j < -|s_j|) - P_r(n_i > -|s_i|, \, n_j < -|s_j|)$$

$$- P(n_i < -|s_i|, \, n_j > -|s_j|). \tag{D.2}$$

Let

$$B_1(\zeta, \, \beta, \, \rho) = \int_\zeta^\infty \int_\beta^\infty \frac{1}{2\pi\sqrt{1-\rho^2}} \exp\left\{ \frac{-(x_1^2 - 2\rho x_1 x_2 + x_2^2)}{2(1-\rho^2)} \right\} dx_2 dx_1 \tag{D.3}$$

denote the bivariate Gaussian distribution [15]. Then (D.2) becomes

$$E[D_i D_j] = 2[B_1(-|s_i|/\sigma_n, \, -|s_j|/\sigma_n, \, r_n(j-i))$$

$$+ B_1(|s_i|/\sigma_n, \, |s_j|/\sigma_n, \, r_n(j-i))] - 1 \tag{D.4}$$

where $\sigma_n^2 = \dfrac{MN_o \gamma_n}{2cT}$ and the noise is assumed to be stationary. The two dimen-

sional Taylor series, centred at the origin, for $f(x,y)$ is

$$f(x,y) = \sum_{m=0}^{\infty} \frac{1}{m!} \left[x \frac{\partial}{\partial x} + y \frac{\partial}{\partial y} \right]^m f(x,y) \Bigg|_{\substack{x=0 \\ y=0}} . \tag{D.5}$$

Combining (D.5) with (D.3) gives

$$B_i(\zeta,\beta,\rho) = \frac{1}{4} + \frac{1}{2\pi} \arcsin \rho - \frac{\zeta+\beta}{2\sqrt{2\pi}} + \frac{\zeta\beta}{2\pi\sqrt{1-\rho^2}} - \frac{\rho(\zeta^2+\beta^2)}{4\pi\sqrt{1-\rho^2}} + \epsilon(\zeta,\beta) \tag{D.6}$$

where $\epsilon(\zeta,\beta) \to 0$ as ζ^3, β^3, $\zeta\beta^2$ and $\zeta^2\beta$. Using (D.6) in (D.4) gives for large M,

$$E[D_i D_j] = 2/\pi \arcsin \{r_n(j-1)\} - \frac{2cT(|s_i|-|s_j|)^2}{\pi M N_o \gamma_n \sqrt{1-r_n^2(j-1)}} \tag{D.7}$$

By proceeding as in Appendix A it may be shown that as $M \to \infty$

$$\overline{D_i} = \sqrt{\frac{4cT}{\pi M N_o \gamma_n}} |s_i| . \tag{D.8}$$

Combining (D.8) with (D.7) results in (D.1).

APPENDIX E

In this appendix it will be shown that as $M \to \infty$ (3.23)

$$\frac{T}{ME_s} \sum_{\substack{i=1 \\ j \neq i}}^{M} \sum_{j=1}^{M} |s_i||s_j|\arcsin\{r_n(j-i)\} \approx 2 \sum_{j=1}^{\infty} \arcsin\{r_n(i)\} \quad . \qquad (E.1)$$

One has that

$$\sum_{\substack{i=1 \\ j \neq i}}^{M} \sum_{j=1}^{M} |s_i||s_j|\arcsin\{r_n(j-i)\} = 2\{\sum_{k=2}^{M} |s_k||s_{k-1}|\arcsin\{r_n(1)\}$$

$$+ \sum_{k=3}^{M} |s_k||s_{k-2}|\arcsin\{r_n(2)\} + \dots$$

$$+ \sum_{k=N}^{M} |s_k||s_{k-N+1}|\arcsin\{r_n(N-1)\} + \dots \}$$

$$= 2\{\arcsin\{r_n(1)\} \sum_{k=2}^{M} |s_k||s_{k-1}| + \arcsin\{r_n(2)\} \sum_{k=3}^{M} |s_k||s_{k-2}| + \dots$$

$$+ \arcsin\{r_n(N-1)\} \sum_{k=N}^{M} |s_k||s_{k-N+1}| + \dots \} \quad . \qquad (E.2)$$

Note that, for fixed N,

$$\lim_{M \to \infty} \frac{T}{M} \sum_{k=N}^{M} |s_k||s_{k-N+1}| = \lim_{M \to \infty} \frac{T}{M} \sum_{k=N}^{M} |s_k||s_{k-N+1}| + \lim_{M \to \infty} \frac{T}{M} \sum_{k=1}^{N-1} |s_k|^2$$

$$\doteq \lim_{M \to \infty} \frac{T}{M} \sum_{k=1}^{M} \left| s\left(\frac{[k-0.5]T}{M}\right) \right|^2 = \int_0^T s^2(t)dt = E_s \quad\quad\quad\quad (E.3)$$

where, without loss of generality, it has been assumed that $s_i = s([i-0.5]T/M)$. Using the result of (E.3) with (E.2) gives (E.1).

APPENDIX F

It is to be shown that when the channel noise has a Cauchy distribution the optimum weights for high SNR's are given by $\omega_i^* = 1$. In a Cauchy noise environment the probability that a sample has its polarity reversed is $p_i = \Pr(N_i > |s_i|) = \int_{|s_i|}^{\infty} \frac{b/\pi}{b^2 + \alpha^2} \, d\alpha$. Making use of the series

$\frac{1}{1+x} = 1 - x + x^2 - \ldots$ yields

$$p_i = \int_{|s_i|}^{\infty} \frac{b}{\pi \alpha^2} \left[1 - \left(\frac{b}{\alpha}\right)^2 + \left(\frac{b}{\alpha}\right)^4 - \left(\frac{b}{\alpha}\right)^6 + \ldots \right] d\alpha$$

$$= -\frac{1}{\pi} \left[\frac{b}{\alpha} - \frac{1}{3} \left(\frac{b}{\alpha}\right)^3 + \frac{1}{5} \left(\frac{b}{\alpha}\right)^5 + \ldots \right] \Big|_{\alpha = |s_i|}^{\infty}$$

$$= \frac{1}{\pi} \left[\frac{b}{|s_i|} - \frac{1}{3} \left(\frac{b}{|s_i|}\right)^3 + \frac{1}{5} \left(\frac{b}{|s_i|}\right)^5 + \ldots \right] .$$

For large signal-to-noise ratios, $\frac{|s_i|}{b} \gg 1$ and $\omega_i^* = \ln\left(\frac{\pi |s_i|}{b}\right)$.

Assume that $s(t) = C \, \tilde{s}(t)$ where $\tilde{s}(t)$ is a waveform with unit amplitude and C is a constant. Then,

$$\omega_i^* = \ln\left(\frac{\pi |C| |\tilde{s}_i|}{b}\right) = \ln(|C|) + \ln\left(\frac{\pi}{b} |\tilde{s}_i|\right) .$$

For large values of $|C|$ and hence large SNR's, $\omega_i^* = \ln(|C|)$. Since the optimum decision rule is not changed by scaling the weights, one may use $\omega_i^* = 1$ for large SNR's.

APPENDIX G

In this appendix it is shown that the optimal weights for the case of
a raised cosine pulse in Cauchy noise sampled 3 times are

$$\omega_1^* = \begin{cases} |s_1| & \text{if SNR} < 15.1 \text{ dB} \\ 1 & \text{if SNR} > 15.1 \text{ dB} \end{cases}$$

Note that there are 8 possible combinations of the 3 received signal
samples and that $\omega_1^* = \omega_3^*$. Therefore, the sample vectors $\underline{v} = (+,+,+)$, $(+,+,-)$
and $(-,+,+)$ will be assigned message $\hat{m} = 0$ and the vectors $\underline{v} = (-,-,-)$,
$(-,-,+)$ and $(+,-,-)$ will be assigned $\hat{m} = 1$. This is true for any
signal-to-noise ratio and any choice of weights provided that $\omega_1 = \omega_3$.
According to the $|s_1|$ weights, the detector chooses $\hat{m}=0$ for $\underline{v}=(-,+,-)$ and $\hat{m}=1$
for $\underline{v}=(+,-,+)$. But for p_1 specified by the Cauchy distribution and $\frac{A}{b} < 15.1$
dB, $\ell n[\frac{1-p_1}{p_1}] + \ell n[\frac{1-p_3}{p_3}] < \ell n[\frac{1-p_2}{p_2}]$. Thus, the optimum weights are equivalent
to the $|s_1|$ weights in this SNR region. When $\frac{A}{b} > 15.1$ dB,

$$\ell n[\frac{1-p_1}{p_1}] + \ell n[\frac{1-p_3}{p_3}] > \ell n[\frac{1-p_2}{p_2}]$$ and $\hat{m} = 0,1$ are chosen corresponding to
$\underline{v}=(+,-,+)$, $(-,+,-)$ respectively by both the optimum and unity weights
detectors.

APPENDIX H

In this appendix it is shown that the penalty for the general WPD detector at high SNR values is given by (5.8)

From (5.7), for high SNR values, the probability of error becomes

$$P_{WPD}(e) = \sum_{B \subseteq \{1,2,\ldots M\}} I(B) \prod_{i \in B} P_i \qquad \text{(H.1)}$$

where

$$I(B) = \begin{cases} 1 & , \text{ if } \sum_{i \in B} \omega_i > \sum_{i \in B^c} \omega_i \\ \frac{1}{2} & , \text{ if } \sum_{i \in B} \omega_i = \sum_{i \in B^c} \omega_i \\ 0 & , \text{ if } \sum_{i \in B} \omega_i < \sum_{i \in B^c} \omega_i \end{cases}$$

Also, for large $\frac{A}{\sigma}$,

$$P_i = Q\left(\sqrt{\Gamma_{WPD}(\underline{s},M,\frac{A}{\sigma})} \frac{A}{\sigma} |s_i|\right) \approx \frac{e^{-\Gamma_{WPD}(\underline{s},M,\frac{A}{\sigma})[\frac{A}{\sigma} s_i]^2/2}}{\sqrt{2\pi \Gamma_{WPD}(\underline{s},M,\frac{A}{\sigma})} \frac{A}{\sigma} |s_i|} . \qquad \text{(H.2)}$$

Hence,

$$\prod_{i \in B} P_i \approx \frac{e^{-\Gamma_{WPD}(\underline{s},M,\frac{A}{\sigma})\,[\frac{A}{\sigma}]^2\,\frac{1}{2}\sum_{i \in B} s_i^2}}{\prod_{i \in B} \sqrt{2\pi\,\Gamma_{WPD}(\underline{s},M,\frac{A}{\sigma})}\,\frac{A}{\sigma}\,|s_i|}\,. \tag{H.3}$$

From (H.3), it can be seen that $P_{WPD}(e)$ as given by (H.1) will be dominated (for high SNR) by the set (or sets) B for which $I(B) > 0$ and $\sum_{i \in B} s_i^2$ is minimum. Let B^* denote one such set, that is, $B^* \subseteq U \triangleq \{1,2,\ldots,M\}$ and $I(B^*) > 0$ and $\sum_{i \in B^*} s_i^2 < \sum_{i \in B} s_i^2$ for all $B \subseteq U$ for which $I(B) > 0$. Since $\Gamma_{WPD}(\underline{s},M,\frac{A}{\sigma}) > 1$, it follows from (H.1) that as $\frac{A}{\sigma}$ increases

$$\ell n\{P_{WPD}(e)\} \approx -\Gamma_{WPD}(\underline{s},M,\frac{A}{\sigma})\,[\frac{A}{\sigma}]^2 \cdot \frac{1}{2}\sum_{i \in B^*} s_i^2\,. \tag{H.4}$$

Recall that

$$P_{DMF}(e) = Q\left(\frac{A\sqrt{\sum_{i=1}^{M} s_i^2}}{\sigma}\right) \approx \frac{e^{-[\frac{A}{\sigma}]^2\,\frac{1}{2}\sum_{i=1}^{M} s_i^2}}{\sqrt{2\pi\sum_{i=1}^{M} s_i^2}\,\frac{A}{\sigma}}\,, \quad \text{for large } \frac{A}{\sigma}\,,$$

so that

$$\ln\{P_{DMF}(e)\} \approx - \left[\frac{A}{\sigma}\right]^2 \frac{1}{2} \sum_{i=1}^{M} s_i^2, \text{ for large } \frac{A}{\sigma} . \tag{H.5}$$

Equating (H.4) with (H.5) yields

$$\Gamma_{WPD}(\underline{s}, M, \frac{A}{\sigma}) \approx \frac{\sum\limits_{i=1}^{M} s_i^2}{\sum\limits_{i \in B^*} s_i^2}, \text{ for large } \frac{A}{\sigma} .$$

APPENDIX I

It is to be shown that the penalty for the WPD detector with a piecewise constant amplitude signalling waveform and low SNR is given by (5.13). We consider first the derivation for odd values of M.

Differentiating (5.10) with respect to $\frac{A}{\sigma}$ and then letting $\frac{A}{\sigma} = 0$ yields

$$\Gamma_{WPD}(\underline{1}, M, 0) = \frac{M \, 2^{2M-2}}{\left[\displaystyle\sum_{i=\frac{M+1}{2}}^{M} \binom{M}{i}(2i-M) \right]^2} \quad , \text{ M odd .} \tag{I.1}$$

One has

$$\sum_{i=\frac{M+1}{2}}^{M} i \binom{M}{i} = \sum_{i=\frac{M+1}{2}}^{M} M \binom{M-1}{i-1} = M \sum_{i=\frac{M-1}{2}}^{M-1} \binom{M-1}{i}$$

$$= M \left[\frac{2^{M-1} + \binom{M-1}{\frac{M-1}{2}}}{2} \right] \quad , \text{ M odd.} \tag{I.2}$$

Also,

$$\sum_{i=\frac{M+1}{2}}^{M} M \binom{M}{i} = M 2^{M-1} \quad , \text{ M odd .} \tag{I.3}$$

Using (I.2) and (I.3) in (I.1) one obtains

$$\Gamma_{WPD}(\underline{1},M,0) = \frac{2^{2M-2}}{M \left(\frac{M-1}{2} \right)^2} \quad , \text{ M odd.} \tag{I.4}$$

In a similar way, it can be shown that

$$\Gamma_{WPD}(\underline{1},M,0) = \frac{2^{2M}}{M \left(\frac{M}{2} \right)^2} \quad , \text{ M even .} \tag{I.5}$$

It might be noted from (I.4) and (I.5) that

$$\Gamma_{WPD}(\underline{1},2k+1,0) = \frac{2k}{2k+1} \Gamma_{WPD}(1,2k,0) \quad , \text{ k=1,2,3,... .}$$

APPENDIX J

It is to be shown that for a large number M of samples the penalty for the optimum WPD detector is upper bounded by (5.16).

Let $\{X_i\}_{i=1}^M$ be M independent random variables defined by

$$X_i = \begin{cases} \ln\left(\frac{1-p_i}{p_i}\right) & \text{with probability } p_i \\ -\ln\left(\frac{1-p_i}{p_i}\right) & \text{with probability } (1-p_i) \end{cases}$$

where $p_i = Q\left(\sqrt{\Gamma_{WPD}(\underline{s},M,\frac{A}{\sigma})}\,\frac{A}{\sigma}\,|s_i|\right)$. Then

$$P_{WPD}^*(e) = \Pr\left\{\sum_{i=1}^M X_i > 0\right\} . \tag{J.1}$$

One can use the Chernoff bound [29: Eq. (5.4.15)] to upperbound the right hand side of (J.1)

$$P_{WPD}^*(e) < \prod_{i=1}^M E[e^{\lambda X_i}] \tag{J.2}$$

where λ is a positive number which can be chosen to optimize the bound. For the present problem, the best value to use is $\lambda = \frac{1}{2}$. Then (J.2) becomes

$$P_{WPD}^*(e) < \prod_{i=1}^M 2\sqrt{p_i(1-p_i)} . \tag{J.3}$$

An upper bound $\Gamma_{WPD}^{UB}(\underline{s}, M, \frac{A}{\sigma})$ is obtained by equating the right hand side of (J.3) to $P_{DMF}(e)$, namely

$$Q\left(\frac{A}{\sigma}\sqrt{\sum_{i=1}^{M} s_i^2}\right) = \prod_{i=1}^{M} 2\sqrt{p_i(1-p_i)} \tag{J.4}$$

where $p_i \triangleq Q\left(\sqrt{\Gamma_{WPD}^{UB}(\underline{s}, M, \frac{A}{\sigma})}\,\frac{A}{\sigma}\,|s_i|\right)$. For large M,

$$Q\left(\frac{A}{\sigma}\sqrt{\sum_{i=1}^{M} s_i^2}\right) \approx \frac{e^{-\frac{1}{2}\left(\frac{A}{\sigma}\right)^2 \sum_{i=1}^{M} s_i^2}}{\sqrt{2\pi \sum_{i=1}^{M} s_i^2}\,\frac{A}{\sigma}} . \tag{J.5}$$

Using (J.5) in (J.4) yields for large M,

$$\left(\frac{A}{\sigma}\right)^2 \int_0^T s^2(t)dt = -\int_0^T \ln\left\{4Q\left(\sqrt{\Gamma_{WPD}^{UB}(\underline{s}, \infty, \frac{A}{\sigma})}\,\frac{A}{\sigma}\,|s(t)|\right)\right.$$

$$\left[1-Q\left(\sqrt{\Gamma_{WPD}^{UB}(\underline{s}, \infty, \frac{A}{\sigma})}\,\frac{A}{\sigma}\,|s(t)|\right)\right]\right\} dt . \tag{J.6}$$

Letting $\sqrt{\Gamma_{WPD}^{UB}(\underline{s}, \infty, \frac{A}{\sigma})}\,\frac{A}{\sigma} = y$, we can rewrite (J.6) as

$$\Gamma_{WPD}^{UB}(\underline{s}, \infty, \frac{A}{\sigma}) = \frac{-y^2 \int_0^T s^2(t)dt}{\int_0^T \ln\{4Q(y|s(t)|)[1-Q(y|s(t)|)]\}dt} . \tag{J.7}$$

Equation (J.7) can be used to plot $\Gamma_{WPD}^{UB}(\underline{s}, \infty, \frac{A}{\sigma})$ as a function of $\frac{A}{\sigma}$.

For a piecewise constant amplitude waveform the upper bound is also a lower bound. This is now shown. One has (5.10)

$$P_{WPD}(e) = \begin{cases} 1 - \sum_{i=\frac{M+1}{2}}^{M} \binom{M}{i} p^i (1-p)^{M-i} & , M \text{ odd} \\ \\ 1 - \sum_{i=\frac{M+2}{2}}^{M} \binom{M}{i} p^i (1-p)^{M-i} + \frac{1}{2} \binom{M}{\frac{M}{2}} [p(1-p)]^{\frac{M}{2}} & , M \text{ even} \end{cases} \qquad (J.8)$$

where $p = Q(\sqrt{\Gamma_{WPD}(\underline{1}, M, \frac{A}{\sigma})} \; (\frac{A}{\sigma})$. Therefore

$$P_{WPD}(e) > \begin{cases} \binom{M}{\frac{M+1}{2}} [p(1-p)]^{\frac{M}{2}} (\frac{p}{1-p})^{\frac{1}{2}} & , M \text{ odd} \\ \\ \frac{1}{2} \binom{M}{\frac{M}{2}} [p(1-p)]^{\frac{M}{2}} & , M \text{ even} . \end{cases} \qquad (J.9)$$

Since $\binom{M}{\frac{M+1}{2}} = \frac{2^{\frac{M+1}{2}}}{M+1} \prod_{i=1}^{\frac{M-1}{2}} (2 + \frac{1}{i}) > \frac{2^M}{M+1}$ when M is odd and

$\binom{M}{\frac{M}{2}} = 2 \binom{M-1}{\frac{M}{2}} > \frac{2^M}{M}$ when M is even (J.9) yields

$$P_{WPD}(e) > \begin{cases} \frac{1}{M+1} (\frac{p}{1-p})^{1/2} [4p(1-p)]^{\frac{M}{2}} & , M \text{ odd} \\ \\ \frac{1}{2M} [4p(1-p)]^{\frac{M}{2}} & , M \text{ even} . \end{cases} \qquad (J.10)$$

Using (J.3) (with $p_i = p$ for all i), (J.5) and (J.10) one obtains for large M

$$\left(\frac{A}{\sigma}\right)^2 = - \ln \left\{ 4Q\left(\sqrt{\Gamma_{WPD}(\underline{1},\infty,\frac{A}{\sigma})} \frac{A}{\sigma}\right) \cdot \right.$$

$$\left. \left[1 - Q\left(\sqrt{\Gamma_{WPD}(\underline{1},\infty,\frac{A}{\sigma})} \frac{A}{\sigma}\right)\right] \right\} .$$

(J.11)

Letting $\sqrt{\Gamma_{WPD}(\underline{1},\infty,\frac{A}{\sigma})} \frac{A}{\sigma} = y$, (J.11) may be rewritten as

$$\Gamma_{WPD}(\underline{1},\infty,\frac{A}{\sigma}) = \frac{-y^2}{\ln\{4Q(y)[1-Q(y)]\}} .$$

(J.12)

Equation (J.12) is used to plot $\Gamma_{WPD}(\underline{1},\infty,\frac{A}{\sigma})$ as a function of $\frac{A}{\sigma}$.

APPENDIX K

In this appendix, it is proved that

$$\Gamma_{BPD}(\underline{s},M,0) = \Gamma_{WPD}(\underline{1},M,0) \cdot \Gamma_{SAS}(\underline{s},M) . \qquad (K.1)$$

From equations (5.3) and (6.13), $\Gamma_{BPD}(\underline{s},M,\frac{A}{\sigma})$ is implicitly defined by

$$Q\left(\sqrt{\sum_{i=1}^{M} s_i^2} \; \frac{A}{\sigma}\right) = \begin{cases} \displaystyle\sum_{j=\frac{M+1}{2}}^{M} P_j^M & \text{, M odd} \\[4ex] \displaystyle\sum_{j=\frac{M+2}{2}}^{M} P_j^M + \frac{1}{2} P_{\frac{M}{2}}^M & \text{, M even} \end{cases} \qquad (K.2)$$

where $P_j^M \triangleq \Pr\{\text{exactly } j \text{ (polarity) errors in the M samples}\}$

$$= \sum_{k_1=1}^{M} \sum_{k_2=k_1+1}^{M} \cdots \sum_{k_j=k_{j-1}+1}^{M} \prod_{\ell \in \{k_1,k_2,\ldots,k_j\}} P_\ell \prod_{k \in U-\{k_1,\ldots,k_j\}} (1-P_k)$$

and $P_\ell = Q\left(\sqrt{\Gamma_{BPD}(\underline{s},M,\frac{A}{\sigma})} \; |s_\ell| \frac{A}{\sigma}\right)$. Differentiating with respect to $\frac{A}{\sigma}$ and then letting $\frac{A}{\sigma} = 0$ in (K.2), we obtain

$$\sqrt{\sum_{i=1}^{M} s_i^2} = \left(\tfrac{1}{2}\right)^{M-1} \sqrt{\Gamma_{BPD}(\underline{s},M,0)} \sum_{j=\frac{M+1}{2}} \sum_{k_1=1}^{M} \sum_{k_2=k_1+1}^{M} \cdots \sum_{k_j=k_{j-1}+1}^{M}$$

$$\left[\sum_{\ell \epsilon \{k_1,\ldots,k_j\}} |s_\ell| \; - \sum_{k \epsilon U-\{k_1,\ldots,k_j\}} |s_k| \right], \; M \text{ odd} \tag{K.3}$$

$$= \left(\tfrac{1}{2}\right)^{M-1} \sqrt{\Gamma_{BPD}(\underline{s},M,0)} \sum_{j=\frac{M+1}{2}}^{M} \{2\binom{M-1}{j-1} - \binom{M}{j}\} \sum_{i=1}^{M} |s_i| \; . \tag{K.4}$$

Similarly, for M even, one has

$$\sqrt{\sum_{i=1}^{M} s_i^2} = \left(\tfrac{1}{2}\right)^{M-1} \sqrt{\Gamma_{BPD}(\underline{s},M,0)} \sum_{j=\frac{M+2}{2}}^{M} \{2\binom{M-1}{j-1} - \binom{M}{j}\} \sum_{i=1}^{M} |s_i| \; . \tag{K.5}$$

From (K.4) and (K.5) one has

$$\Gamma_{BPD}(\underline{s},M,0) = C_M \frac{\sum_{i=1}^{M} s_i^2}{(\sum_{i=1}^{M} |s_i|)^2} \; , \; M=1,2,3,\ldots \tag{K.6}$$

for some constant C_M. In particular,

$$\Gamma_{WPD}(\underline{1},M,0) = \Gamma_{BPD}(\underline{1},M,0) = \frac{C_M}{M} \; . \tag{K.7}$$

Using (6.6) and (K.7) in (K.6), we have

$$\Gamma_{BPD}(\underline{s},M,0) = \Gamma_{WPD}(\underline{1},M,0) \cdot \Gamma_{SAS}(\underline{s},M) \; .$$

REFERENCES

[1]   T.C. Tozer and J. Kollerstrom, "Penalties of hard decision in signal detection," _Electron. Lett._, vol. 16, pp.199-200, Feb. 1980.

[2]   V.M. Milutinovic, "Suboptimum detection procedure based on the weighting of partial decisions," _Electron. Lett._, vol. 16, pp.237-238, Mar. 1980.

[3]   V.M. Milutinovic, "Comparison of three suboptimum detection procedures," _Electron. Lett._, vol. 16, pp.681-683, Aug. 1980.

[4]   G.B. Lockhart, "Implementation of digital matched filters in data receivers," _Electron. Lett._, vol. 10, pp.311-312, July 1974.

[5]   C.M. Chie, "Performance analysis of digital integrate-and-dump filters," _IEEE Trans. Commun._, vol. COM-30, pp.1979-1983, Aug. 1982.

[6]   H. Chang, "Presampling filtering, sampling and quantization effects on the digital matched filter performance," in _Proc. International Telemetering Conference_, San Diego,CA, USA, Sept. 28-30, 1982, pp.889-915.

[7]   N.C. Beaulieu and C. Leung, "On the performance of three suboptimum detection schemes for binary signalling," _IEEE Trans. Commun._, vol. COM-33, pp.241-245, Mar. 1985.

[8]   N.C. Beaulieu and C. Leung, "Optimal detection of hard-limited data signals in different noise environments," _IEEE Trans. Commun._, vol. COM-34, pp.619-622, June 1986.

[9] N.C. Beaulieu, "Penalties of Sample-and-Sum and Weighted Partial Decision Detectors in Gaussian Noise," under review.

[10] N.C. Beaulieu and C. Leung, "The Optimal Hard-Limiting Detector for Data Signals in Different Noise Environments," in Proc. IEEE ICC, Toronto, Canada, June 23-25, 1986, pp.32.6.1-32.6.5.

[11] M. Schwartz and L. Shaw, Signal Processing: Discrete Spectral Analysis, Detection and Estimation. New York: McGraw-Hill, 1975.

[12] R.W. Stroh, "An experimental microprocessor-implemented 4800 bit/s limited distance voice band PSK modem," IEEE Trans. Commun., vol. COM-26, pp.507-512, May 1978.

[13] V.C. Hamacher, "Analysis of a simplified sampled signal detector," Queen's university Research Report 65-1, Mar. 1965.

[14] M. Fisz, Probability Theory and Mathematical Statistics. New York: J. Wiley, 1963, pp.202-211.

[15] J. Patel and C. Read, Handbook of the Normal Distribution. New York: Marcel Dekker, 1982, p.50.

[16] M. Abramowitz and I.A. Stegun, Handbook of Mathematical Functions. New York: Dover, 1972, pp.931-932.

[17] G.P. Wadsworth and J.G. Bryan, Applications of Probability and Random Variables. New York: McGraw-Hill, 1974, pp.89-91.

[18] C. Cherry, Pulses and Transients in Communication Circuits. London: Dover, 1950.

[19] A.I. Zverev, Handbook of Filter Synthesis. New York: J. Wiley, 1967, pp.67-71.

[20]   W. Rudin, Principles of Mathematical Analysis. New York: McGraw-Hill, 1964.

[21]   R.V. Churchill and J.W. Brown, Fourier Series and Boundary Value Problems. New York: McGraw-Hill, 1978, p.84.

[22]   R.E. Ziemer and W.H. Tranter, Systems, Modulation, and Noise. Boston: Houghton Mifflin, 1976.

[23]   M. Rosenblatt, "A Central limit theorem and a strong mixing condition," Proc. Nat. Acad. Sci., vol. 42, pp.42-47, 1956.

[24]   R. Deutsch, Nonlinear Transformations of Random Processes. Englewood Cliffs, N.J. :   Prentice-Hall, 1962.

[25]   M. Kanefsky, "Detection of weak signals with polarity coincidence arrays," IEEE Trans. Inform. Theory, vol. IT-12, pp.260-268, Apr. 1966.

[26]   M.J. Levin, "Generation of a sampled gaussian time series having a specified correlation function," IRE Trans. Inform. Theory, vol. IT-6, pp.545-548, Dec. 1960.

[27]   J.H. Miller and J.B. Thomas, "Detectors for discrete-time signals in non-gaussian noise," IEEE Trans. Inform. Theory, vol. IT-18, pp. 241-250, Mar. 1972.

[28]   H. Chernoff, "A measure of asymptotic efficiency for tests of a hypothesis based on the sum of observations," Annals Math. Stat., vol. 23, pp. 493-507, 1952.

[29]   R.G. Gallager, Information Theory and Reliable Communication. New York: J. Wiley, 1968.

[30]   I.S. Gradshteyn and I.M. Ryzhik, <u>Table of Integrals, Series and</u>
        <u>Products</u>. New York: Academic Press, 1980.

[31]   J.M. Wozencraft and I.M. Jacobs, <u>Principles of Communication</u>
        <u>Engineering</u>. New York: J. Wiley, 1968.

[32]   N.C. Beaulieu and C. Leung, "A comparison of three suboptimum
        detectors for binary signalling," in <u>Proc. IEEE ICC</u>, Chicago, USA,
        June 23-26, 1985, pp.18.4.1-18.4.6.

[33]   N.C. Beaulieu and C. Leung, "On hard-limiting in sampled binary
        data systems," <u>North American Radio Science Meeting (URSI)</u>,
        Vancouver, Canada, June 17-21, 1985, p.330.

[34]   N.C. Beaulieu, "Penalties of Weighted Partial Decision Detectors in
        Gaussian Noise," in <u>Proc. IEEE International Montech Conference on</u>
        <u>Antennas and Communications</u>, Montreal, Canada, Sept. 29-Oct. 1, 1986.

[35]   V. Milutinovic, "Performance comparison of two suboptimum detection
        procedures in real environment," <u>IEE Proc.</u>, vol. 131, Pt. F, pp.341-
        344, July 1984.

[36]   V.M. Milutinovic, "Generalised WPD procedure for microprocessor-
        based signal detection," <u>IEE Proc.</u>, vol. 132, Pt. F, pp.27-35,
        Feb. 1985.

[37]   P.M. Schultheiss and F.B. Tuteur, "Optimum and Suboptimum Detection of
        Directional Gaussian Signals in an Isotropic Gaussian Noise Field
        Part II: Degradation of Detectability Due to Clipping," <u>IEEE Trans.</u>
        <u>on Military Electronics</u>, vol.MIL-9, pp.208-211, July-Oct. 1965.

GLOSSARY

binary antipodal signals

    two signals, each of which is the negative of the other

binary partial decision

    a decision based on a single signal sample which has two possible

    outcomes

digital matched filter

    the optimum detector which bases its decision on a number of

    independent signal samples

hard decision

    a decision which has two possible outcomes

hard-limiting

    a transformation that assigns one value to all positive arguments

    and a second value to all negative arguments

M-ary signalling

    the transmitter sends one of M signals depending on the message

    sequence

maximum aposteriori probability (MAP) rule

    the receiver chooses as its estimate of the transmitted signal

    that signal which is most likely given the received signal

penalty

    the deterioration in performance of a suboptimum detector measured

    relative to an optimum detector; the increase in signal-to-noise

    ratio required by a suboptimum detector in order to maintain the

    same error probability as an optimum detector

sample-and-sum detector

the received signal is sampled and the samples are summed

signalling element

one of the signal waveforms sent by the transmitter

weighted partial decision

a decision based on a single signal sample which may have one

of several outcomes, the larger the outcome the more heavily

the decision is weighted

PUBLICATIONS

N.C. Beaulieu and C. Leung, "Optimal Detection of Hard-Limited Data Signals in Different Noise Environments", IEEE Trans. Commun., vol. COM-34, no.6, pp.619-622, June 1986.

N.C. Beaulieu and C. Leung, "On the Performance of Three Suboptimum Detection Schemes for Binary Signalling", IEEE Trans. Commun., vol.COM-33, no.3, pp.241-245, March 1985.

N.C. Beaulieu, "Comment on 'Calculating Binomial Probabilities When the Trial Probabilities are Unequal'", J. of Statistical Computation and Simulation, vol.20, no.4, pp.327-328, 1985.

E.V. Jull, N.C. Beaulieu and D.C.W. Hui, "Perfectly Blazed Triangular Groove Reflection Gratings", J. of the Optical Society of America, vol.1, no.2, Feb. 1984.

N.C. Beaulieu, "Penalties of Sample-and-Sum and Weighted Partial Decision Detectors in Gaussian Noise", submitted.

N.C. Beaulieu, "Penalties of Weighted Partial Decision Detectors in Gaussian Noise", IEEE International Montech Conference on Antennas and Communications, Montréal, Sept. 1986.

N.C. Beaulieu and C. Leung, "The Optimum Hard-Limiting Detector for Data Signals in Different Noise Environments", IEEE International Conference on Communications, Toronto, pp.32.6.1-32.6.5, June 1986.

PUBLICATIONS

N.C. Beaulieu and C. Leung, "A Comparison of Three Suboptimum Detectors for Binary Signalling", IEEE International Conference on Communications, Chicago, pp.18.4.1-18.4.6, June 1985.

N.C. Beaulieu and C. Leung, "On Hard-Limiting in Sampled Binary Data Systems", North American Radio Science Meeting (URSI), Vancouver, Canada, June 1985.

E.V. Jull, N.C. Beaulieu and D.C.W. Hui, "Dual Blazed Triangular Groove Reflection Gratings", IEEE Antennas and Propagation Society International Symposium, Houston, Texas, May 1983.

E.V. Jull and N.C. Beaulieu, "An Unusual Reflection Grating Behaviour Suitable for Efficient Frequency Scanning", IEEE Antennas and Propagation Society International Symposium, Québec, June 1980.